1992

A kinematic study of the Summit Valley Plutonic Complex, Klamath Mountains, California

Nancy E. Griesau
University at Albany, State University of New York

A kinematic study of the Summit Valley Plutonic Complex, Klamath Mountains, California

A thesis presented to the Faculty
of the State University of New York
at Albany
in partial fulfillment of the requirements
for the degree of
Master of Science
College of Science and Mathematics
Department of Geological Sciences

Nancy E. Griesau

1992

A kinematic study of the Summit Valley Plutonic Complex, Klamath Mountains, California

Abstract of
a thesis presented to the Faculty
of the State University of New York
at Albany
in partial fulfillment of the requirements
for the degree of
Master of Science

School of Science and Mathematics
Department of Geological Sciences

Nancy E.Griesau

1992

Abstract

The Summit Valley plutonic complex (SVPC) is a multi-phase intrusive body of Late Jurassic age. Crystallization age for a zircon of 150+1 Ma and a cooling age for a hornblende of 144+1 Ma indicate a protracted period of high temperature. The SVPC is irregularly shaped, covers < 15 km^2, and is believed to be in the western limb of a post-Nevadan syncline, with an easterly dip estimated at about 45^0. The SVPC penetrated the Orleans Fault and intruded and contact metamorphosed the upper and lower plates of the thrust. The Orleans Fault is a major tectonic boundary separating the Western Paleozoic and Triassic Belt (upper) from the Western Jurassic Belt (lower). Ductile shear zones at the contact of the plutonic complex and in the interior suggest that the plutonic complex was sheared either during or soon after intrusion; movement along the Orleans Fault may have been the cause.

Igneous rocks range from ultramafic to dioritic composition, with the most abundant rock type being hornblende gabbro. Many of the shear zone rocks are in granulite facies containing neoblasts of clinopyroxene; amphibolites are also found, and locally, shear zones are retrograded to greenshcist facies (both statically and dynamically). Exposed rocks of the lower plate in contact with the plutonic complex include the pebbly mudstone of the LRO which is metamorphosed to biotite hornfels within the contact aureole; the slatey mudstone of the Galice Fm is in fault contact with the plutonic complex and only exhibits greenschist facies assemblages; an intrusive contact has not been found. Upper plate rocks of the RCT are primarily serpentinized harzburgite which is found in screens and pendants within

the plutonic complex; there is a pronounced contact aureole in RCT rocks at the southeastern margin of the plutonic complex.

Ductile shear zones found within and at the edge of the plutonic complex vary in thickness from centimeters to tens of meters. Dikes are found throughout the plutonic complex and in the country rocks, generally measure from 6cm to 60cm, and occasionally are seen to cross-cut ductile shear zones. Vein-filled fractures cross-cut both ductile shear zones and dikes and are considered to be the latest of the three types of structures.

Several shear zones in the SVPC were analysed to determine sense of shear. The data from the shear zones and from veins, many with slickenfibers to indicate slip sense, were used to determine the paleostress field of the deformation which caused them. These structures were analysed graphically with the use of stereographic projection plots, and mathematically with the use of two computer programs for stress inversion, Hardcastle's (based on Reches' method) and Lisle's method (called ROMSA). Dikes in the SVPC and in the adjacent LRO were also used to constrain σ_3 .

After rotation to remove post-Nevadan dip, the stress field during deformation of the SVPC was found to have σ_1 almost vertical, and σ_2 and σ_3 subhorizontal and switching places with each other in positions trending approximately 180^0 and 270^0. Stress ratio (Phi) values for fractures were low (about 0.22) suggesting that σ_2 and σ_3 were very close in magnitude of stress and may appear to flip with each other. Direction of transport of material in the hanging wall was west-northwest, with some indication that this progressively changed through time to a more north-northwesterly direction.

The Nevadan Orogeny is believed to have been a compressive event with crustal slices telescoped beneath each other, possibly achieving tens of kilometers of crustal shortening along the Orleans Fault alone. Such a tectonic regime would have required that σ_1 was horizontal, with the intermediate stress also horizontal and a minimum stress that was vertical. Tectonic burial may have been responsible for the stress field configuration seen in the SVPC if the vertical stress became the maximum stress through underthrusting to greater and greater depths.

ACKNOWLEDGEMENTS

My thesis advisor, Greg Harper, deserves many thanks for his guidance and support, materially and academically, on this project. He taught me how to be a scientist, to look at my work critically, and he showed me how to think creatively to develop models and to recreate the "paleopicture" that is the essence of Geology, especially Tectonics. I also thank him for enabling me to spend some time in the magnificent Six Rivers National Forest in northern California, the site of my field work.

I wish to thank my other committee members, William S. F. Kidd and Winthrop D. Means, for their academic support throughout my studies and for helpful criticism in their review of this work.

My Mom and Dad, my husband Frank, my daughter Genevieve, and my whole family have been a driving force in the completion of my thesis, always maintaining high expectations of me. My field assistant, Susan DeLay, gave me five weeks of her life to be a fastidious helper as well as providing companionship and stimulating conversation. And finally, I want to mention with pride, everyone in the geology department at SUNY Albany, especially my officemates and our supersecretaty, Diana Paton.

Everyone mentioned above has an enthusiasm for learning and a love of Nature and life which has inspired me and enhanced the quality of my life.

TABLE OF CONTENTS

List of Figures

List of Tables

CHAPTER 1. INTRODUCTION

1.1 PURPOSE OF STUDY

Field evidence indicates that the Late Jurassic Summit Valley Plutonic Complex (SVPC) was deformed either continuously during intrusion, or between episodes of intrusion during the time of the Nevaden orogeny [this study; Harper, in review] using criteria described by Vernon et al [1989], Paterson et al [1989a], Hollister and Crawford [1986], and Paterson et al [1989b]. The SVPC penetrates two terranes juxtaposed by a thrust fault (the Orleans fault), and movement along this fault during emplacement is credited with the high-temperature shearing in the SVPC. It was hoped that a kinematic study of the deformation direction in the SVPC would reveal the direction of movement along the Orleans fault. This information could also contribute to understanding the direction of relative plate motion for western North America during the Nevadan orogeny. A field and petrographic study of this pluton was undertaken to ascertain the local kinematics at the time of intrusion.

1.2 DESCRIPTION OF FIELD AREA

1.2.1 Geographic Location

The Summit Valley Plutonic Complex is located about 45 km south of the Oregon border and about 20 km east of Crescent City, California and is in the Six Rivers National Forest, Del Norte County, California (see Attachments: Geologic Map). The study area covers the north half of the Summit Valley 7 1/2' Quadrangle (the

SE quarter of the Ship Mountain 15' Quadrangle). Forest Service road 15N01, also known as the Gasquet-Orleans (GO) Road, cuts through the southern portion of the plutonic complex.

1.2.2 Terrain and Climate

The Summit Valley Plutonic Complex is part of a deeply dissected peneplain, and the terrain is rugged with many rock slides. Elevation at the peak of Summit Valley is 4924 ft.. The climate is variable with the season, with more than 200cm of precipitation in the winter (snow at higher elevations) and very dry in the summer. Access to the mountain by the GO Road in winter is impossible, due to heavy snow accumulation.

1.2.3 Outcrop

The Summit Valley Plutonic Complex has a surface exposure of about 15 sq.km. Foliage cover is extensive, consisting mostly of various evergreens (including Douglas Fir) and deciduous trees (tan oak, manzanita, salal, rhododendron, and huckleberry). Thick manzanita growth makes off-trail hiking extremely difficult. Outcrop is afforded mostly by roadcuts along the GO Road and logging roads. Creek exposure is available, but difficult to reach because of steep terrain. The Summit Valley hiking trail provides access to the central part of the plutonic complex.

1.3 PREVIOUS WORK

Early reconnaissance mapping of the study area had been done by Hershey [1911]. On the old Weed sheet of the California geologic map series [Strand, 1963], the area is shown as mapped but no mention is made of the geologist who performed the mapping. Harper [1980a], Harper and others [1983], and Norman [1984] were the first workers to do more detailed mapping in the study area. Norman [1984] did extensive field work in the study area, including the mapping of the Summit Valley plutonic complex and the Lems Ridge Olistostrome, as part of her M.S. thesis. She mapped lithologic units and structural features, and used microprobe, petrography, and various other techniques for compositional analyses. Harper [1980] mapped areas to the north of the study area, and the area to the north and east of the study area has been mapped by several workers including Snoke [1972, 1977], Norman and others [1983], and Gorman [1985]. Since Norman's work, the Lems Ridge Olistostrome to the west of the study area has been studied in detail by Ohr [1987]. Most recently, Harper and others [in review] did $^{40}Ar/^{39}Ar$ and Pb/U age dating of the SVPC to constrain age and cooling history of the plutonic complex.

CHAPTER 2. REGIONAL GEOLOGY

Due to continued east-directed subduction since mid-Paleozoic time to present occurring at the western continental margin, various terranes have been accreted to North America in what is today the Klamath Mountains Province [Burchfiel and Davis, 1981]. The terranes and thrusts are seen to generally have younger ages proceeding westward. Rock types in the various terranes are of similar origin: volcaniclastic rocks, intact and dismembered ophiolites, and marine sediments. There is strong evidence that during the Jurassic period, these terranes were volanic arcs and ocean crust that formed in proximity to the continental margin [Harper and Wright, 1984] before being accreted to western North America.

The Klamath Mountains Province was divided by Irwin [1960, 1966] into four lithotectonic units bounded by east-dipping thrust faults, with a pronounced arcuate geometry. These four belts are, from east to west: the eastern Klamath belt, the central metamorphic belt, the western Paleozoic and Triassic belt, and the western Jurassic belt (see fig. 2.1). Ages of rocks in the eastern Klamath belt range from the Ordovician to Jurassic, as indicated mostly by fossil dating of limestones and cherts. The central metamorphic belt consists of schists which yield a Devonian age of metamorphism from Rb-Sr ages of the schists and K-Ar ages of amphibolite [Irwin, 1981]. Collision and accretion of these two belts to the paleomargin of North America occurred by Early Triassic time [Burchfiel and Davis, 1981].

The western Paleozoic and Triassic belt is composed mostly of dismembered and incomplete ophiolites, melange of volcanic arc origin, and associated sedimentary rocks. It has been divided by Irwin [1972] into three terranes, which are, from east to

Figure 2.1 The geology of the Klamath Mountains Province.

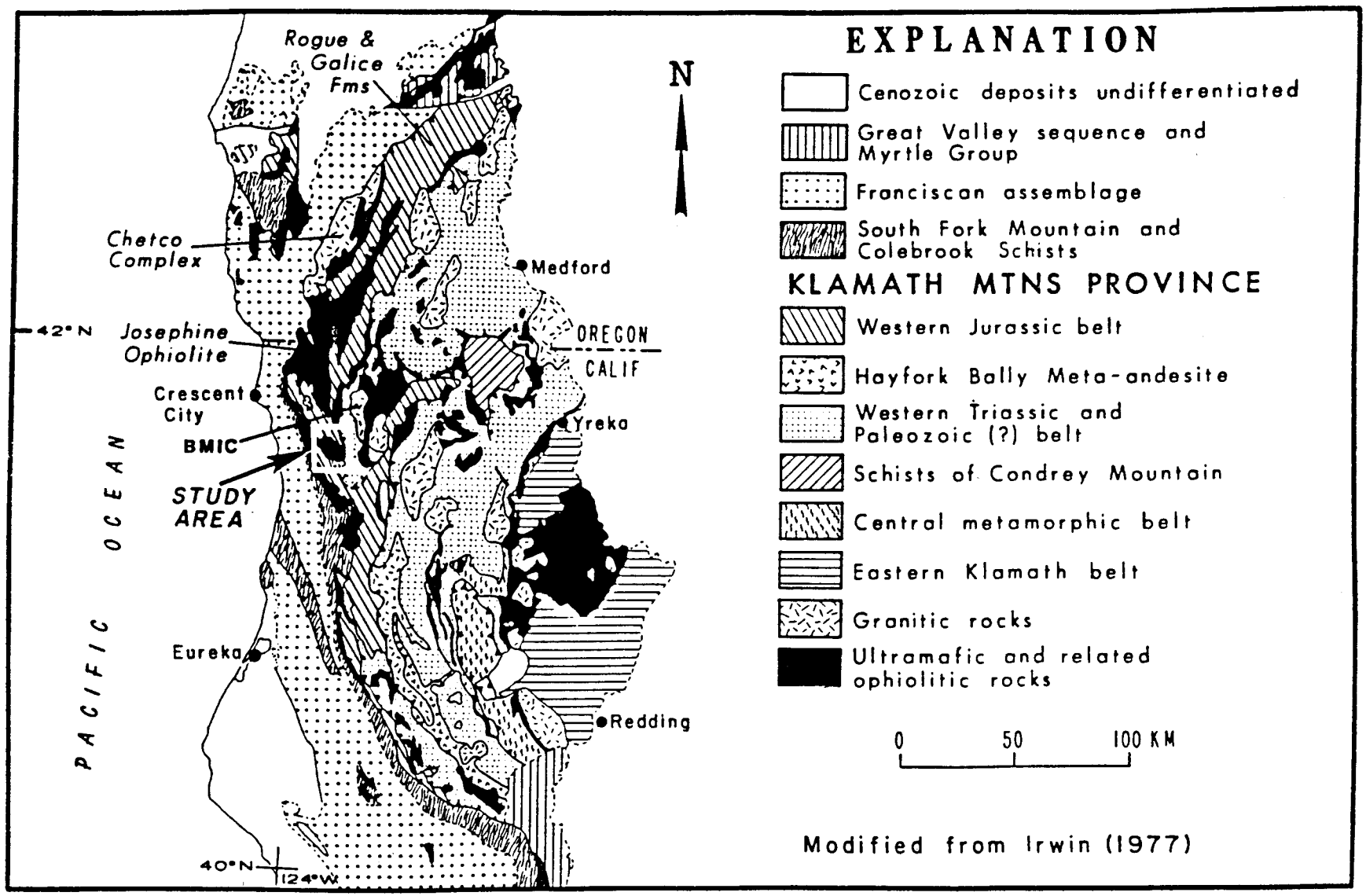
Rogue &
Galice
Fms
Chetco
Complex
Josephine
Ophiolite
42° N
Crescent
City
BMIC
STUDY
AREA
PACIFIC OCEAN
Eureka
40° N
124° W
Medford
OREGON
CALIF
Yreka
Redding
N
EXPLANATION
Cenozoic deposits undifferentiated
Great Valley sequence and
Myrtle Group
Franciscan assemblage
South Fork Mountain and
Colebrook Schists
KLAMATH MTNS PROVINCE
Western Jurassic belt
Hayfork Bally Meta-andesite
Western Triassic and
Paleozoic (?) belt
Schists of Condrey Mountain
Central metamorphic belt
Eastern Klamath belt
Granitic rocks
Ultramafic and related
ophiolitic rocks
0
50
100 KM
Modified from Irwin (1977)

west, the North Fork terrane, the Hayfork terrane, and the Rattlesnake Creek terrane. The Northfork terrane is a narrow zone found only in the southern region of the Klamath mountains [Irwin, 1972, 1981]. In the western district, the Northfork terrane contains rocks of ophiolitic association, including ultramafics, gabbro, diabase, pillow basalt, as well as red radiolarian chert. Stratigraphically above and lying to the east of the ophiolitic rocks, is a succession of tuffs, chert, mafic volcanics, phyllite, pebble conglomerate, and exotic blocks of Paleozoic limestone. Dating of the radiolarian cherts and tuffs has shown the Northfork terrane to be of Mesozoic age [Irwin, 1981]. Irwin [1981] describes the Hayfork terrane as a three-unit succession (from west to east, lower to upper) 1.) coherent volcanic rocks; 2.) chert, argillite, and limestone; and 3.) a disorganized unit of mafic volcanic rocks, siliceous volcanics and sedimentary rocks (chert, phyllite, and limestone). Wright [1982] and Wright and Fahan [1988] have subdivided the Hayfork terrane into two subterranes, combining Irwin's two lower units into the western Hayfork terrane, a volcanic sequence with associated sedimentary rocks, and naming Irwin's upper melange-type unit the eastern Hayfork terrane. Wright and Fahan [1988] cite significant lithological and age differences between the two terranes: the eastern Hayfork terrane is no younger than Triassic, while the western is Mid-Jurassic; the eastern Hayfork terrane consists primarily of broken formation and melange of radiolarian chert and argillite, while the western is a coherent section of volcaniclastic strata and associated sedimentary rocks; the two subterranes are separated by the east-dipping Wilson Point thrust fault which Wright [1982] has mapped as a regional fault which defines a basic structural division in the southwest Klamath Mountains. The Rattlesnake Creek terrane (RCT), the westernmost of the three terranes, consists of a suite of rocks characteristic of an ophiolite: ultramafic rock, gabbro, diabase, pillow basalt, chert, various mafic volcanic rocks, granitic

rocks, and lenses, pods, and blocks of limestone, phyllite, sandstone, and conglomerate (fig. 2.2. Extensive disruption of the formations and intermixing of various lithologies and rocks of widely differing ages suggests that the RCT is a melange [Irwin, 1981]. Recent work has shown that the melange unit is intruded by plutons and dikes with U/Pb zircon ages of 192-212 Ma and overlain by coherent strata of volcaniclastic rocks with minor flows and hemipelagic sediments [Gray and Wright, 1984; Wright and Wyld, 1985]. Gray and Wright [1984] propose that the plutons and dikes are the core of a ~200 Ma old volcanic arc and the volcaniclastic rocks are the extrusive equivalent. Irwin's [1972] Rattlesnake Creek terrane has been extended from the southern Klamaths into the study area and northward to include the basement complex of the Preston Peak ophiolite (mapped by Snoke [1977]) and the overlying stratified sedimentary and volcanic rocks [Gray and Petersen, 1982; Norman et al., 1983; Gorman, 1985; Gray, 1986].

The Western Jurassic Belt is composed of three thrust sheets from northwest to southeast, the Chetco Intrusive Complex (Illinois River gabbro), the Rogue and Galice Formations, the Josephine Ophiolite, and the Lem's Ridge Olistostrome (fig. 2.3). The Chetco Intrusive Complex is a gabbro to quartz diorite batholith which ranges from 153 to 160 Ma in age based on K/Ar hornblende ages [Dick, 1976]. The Chetco Intrusive Complex is believed to be the plutonic root of a volcanic arc [Dick, 1976, 1977; Harper and Wright, 1984]. Structurally above the Chetco Intrusive Complex, separated by the Pearsoll Peak thrust fault, is the Rogue Formation which is present only in Oregon in the northwest region of the Klamath Mountains Province. The Rogue Fm. consists of a thick sequence of marine andesitic pyroclastic rocks and some volcanic flows, and may represent the volcanic portion of the island arc associated with the Chetco Intrusive Complex [Dick, 1976;

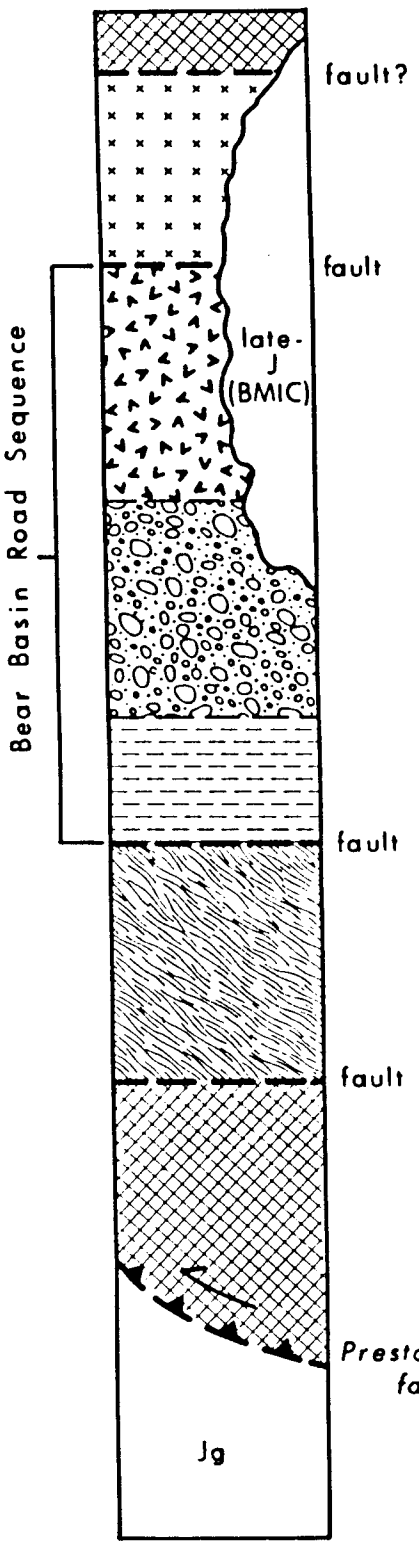

BMIC - Bear Mountain Igneous Complex
Alpine-type peridotite (mostly serpentinized).

Baldy Peak volcanic unit: metabasalt (massive and often plagioclase-phyric) with minor chert and siliceous argillite. Maybe equivalent to the mafic complex of Snoke (1977).

Metabasalt (massive and pillowed), often plagioclase-phyric, intercalated with meta-sedimentary rocks including chert, tuff, siliceous argillite, marble, sandstone, and conglomerate (clasts are derived from metamorphic, ophiolitic, and volcanic sources).

Metaconglomerate with lesser argillite: clasts are derived from metamorphic, volcanic, and ophiolitic sources. Equivalent to the conglomerate-grit unit of Snoke (1977).

Metamorphosed siliceous argillite, chert, and minor marble. Equivalent to the argillite unit of Snoke (1977).

Serpentinite-matrix melange with the following blocks (all metamorphosed): ophiolitic blocks, chert, siliceous argillite, tuff, carbonate-rich phyllite, volcanic-rich sandstone, and amphibolites that yield K/Ar dates of 193 ± 7 and 190 ± 14 m.y.

Alpine-type peridotite (partially serpentinized): mostly harzburgite with minor lherzolite and dunite (Frishman, 1980).

Galice Formation: highly deformed flysch deposit that conformably overlies the Josephine ophiolite (Harper, 1980b, 1983).

Figure 2.2 Tectono-stratigraphic sequence of the Rattlesnake Creek terrane. (From Gorman, 1985)

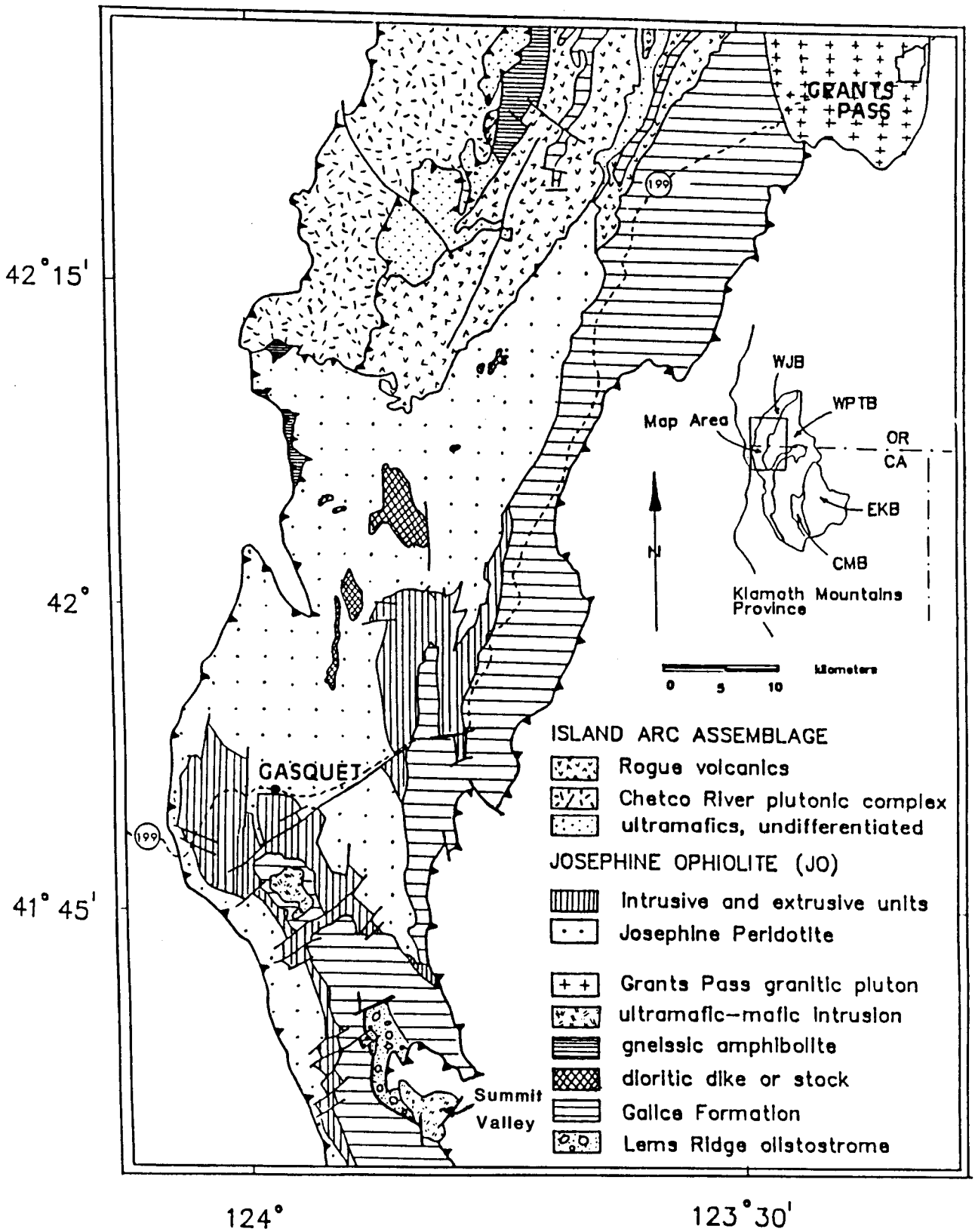

Figure 2.3 Generalized geologic map of the western Jurassic belt (from Ohr, 1987).

Garcia, 1979, 1982]. Saleeby [1984] obtained an age of ~157 Ma from a silicic tuff-breccia in the Rogue Formation, and ~150 Ma from late dacite dikes. Lying conformably above the Rogue Fm. is the Galice Formation which is a thick flysch sequence consisting of slatey argillite, metagraywacke, and some conglomerate. Radiolaria and the pelecypod Buchia concentrica (Sowerby) in the Galice Fm. indicate a late Jurassic age [Harper and Wright, 1984; Harper, 1983]. The Galice Formation lies depositionally over the Rogue Fm. but is also in depositional contact with the structurally higher Josephine ophiolite in northern California (fig. 2.4).

The Josephine ophiolite is a relatively intact and complete ophiolite, including a large basal peridotite covering more than 1000 sq.km. Zircon samples from plagiogranite dikes in a remnant of the ophiolite in the southern Klamaths yielded a 164 Ma U/Pb zircon age [Wright and Wyld, 1986; Wyld and Wright, 1988], and another from a plagiogranite body (west of Gasquet) in the high level gabbros yielded a 162 Ma age [Harper et al, in review]. Locally, the Josephine ophiolite is overlain by the Lem's Ridge Olistostrome (LRO), a melange-type sediment fill of a fracture zone [Harper et al, 1983, 1984]. It is now believed that the fracture was a transform fault between the oceanic crust from which the Josephine ophiolite was derived and older Klamath basement (RCT) [Ohr, 1987].

The Josephine ophiolite is believed to have been a short-lived back-arc spreading basin with a transform-dominated geometry (similar to the Gulf of California), with spreading parallel to the terrane boundary (fig.2.5). The remnant arc was to the east in the ~200 Ma RCT [Gray and Wright, 1984; Wright and Wyld, 1985], and the younger island arc was off to the west (Chetco Complex) dated at between ~151 Ma [Harper et al, in review] to ~155 Ma [Dick, 1976]. Spreading in the back-arc basin

was terminated with the onset of the Nevaden Orogeny (late Jurassic) during which there was intense shortening, folding and deformation, and underthrusting of the western Klamath terrane towards the east. Crustal segments were underthrust and stacked as imbricate slices along the east-dipping thrust faults, with greenschist facies conditions imposed over much of the region, while locally amphibolite facies conditions were attained (for example, the Chetco Complex [Grady, 1990] and the Summit Valley Plutonic Complex [Norman. 1984].

The Summit Valley Plutonic Complex intrudes the Orleans fault, the boundary between the Western Paleozoic and Triassic belt (WPTB) and the Western Jurassic belt (WJB). The lithological units of the upper and lower plates are the Rattlesnake Creek terrane (RCT) and the Lems Ridge Olistostrome (LRO) respectively (fig. 2.6). Norman [1984] made a structure contour map of the Orleans fault based on outcrop patterns and dip orientations of the lithological contact between the upper WPTB and the lower WJB in the study area (and beyond) and found it generally to be striking north-south, and dipping gently ($0\text{-}20^0$) to the east, but locally dipping much more steeply (60^0) due to post-Nevadan folding. This study proposes that movement on the Orleans Fault during intrusion of the SVPC caused shear zones and fractures to develop. It is these structures along with dikes that have been used to try to determine the slip direction along the Orleans Fault as well as the stress field during the Nevadan Orogeny.

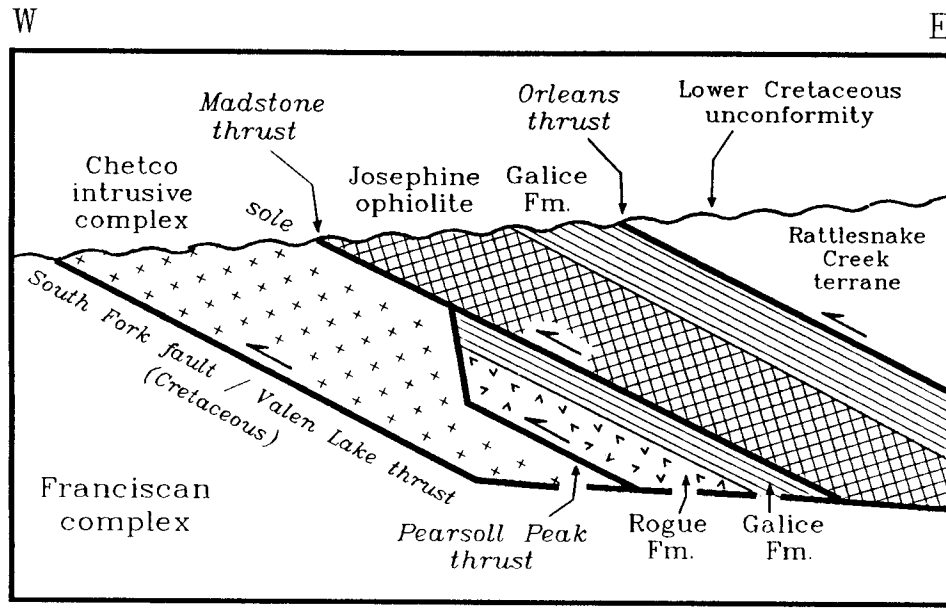

Figure 2.4 Cross-section showing contact relationships in the western Jurassic belt. (From Harper et al, (in review))

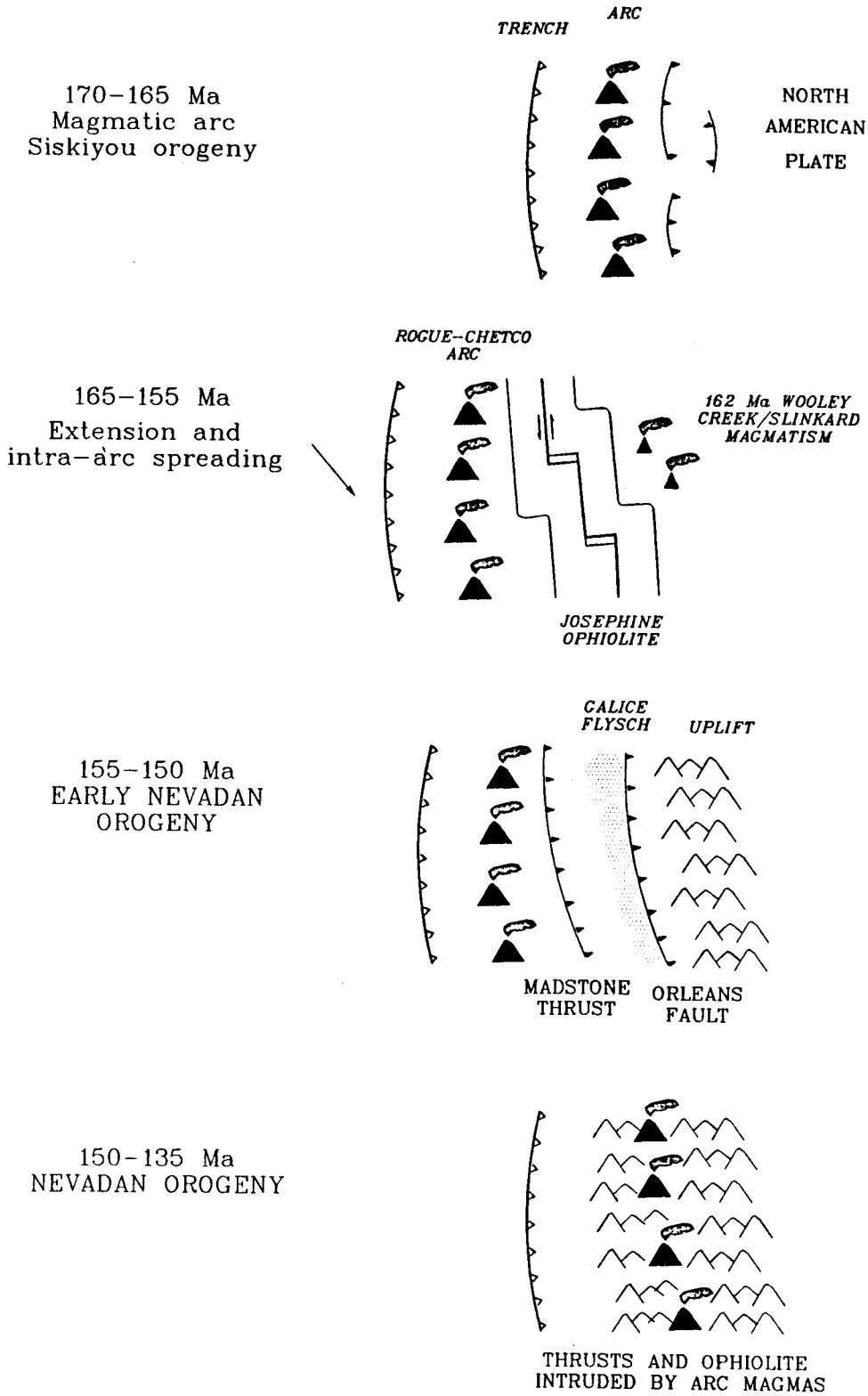

Figure 2.5 Tectonic model for the development of the Josephine ophiolite. Note that spreading axis strikes approximately east-west. (Modified from Harper and Wright [1984], and Harper et al [1990])

Figure 2.6 Cross-section of SVPC showing terranes of the upper and lower plates and the Orleans fault. (From Norman, 1984)

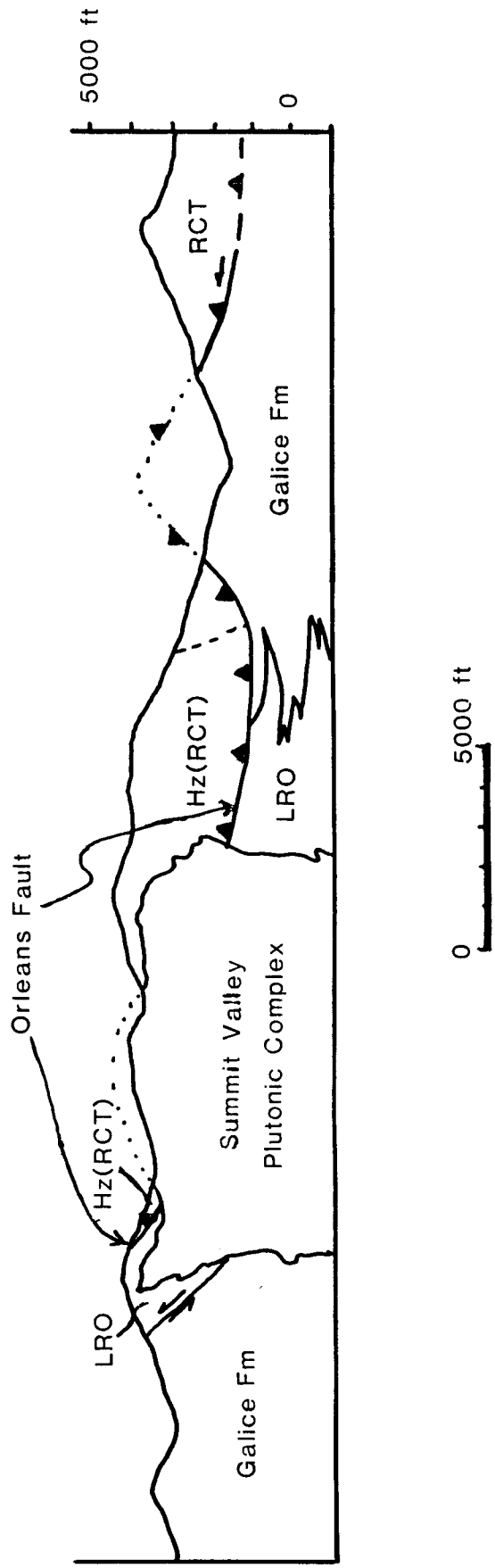
5000 ft
0
RCT
Galice Fm
Hz(RCT)
LRO
Orleans Fault
Hz(RCT)
Summit Valley
Plutonic Complex
LRO
Galice Fm
0
5000 ft

CHAPTER 3. GEOLOGY OF THE PLUTONIC COMPLEX

3.1 LITHOLOGY

3.1.1 Igneous Complex

The SVPC is a collection of magmatic bodies resulting from multiple intrusive pulses (see Attachments: Geologic Map; fig. 3.1). The composition of the magmatic bodies varies from early mafic intrusions of olivine pyroxenite all the way up to rare late quartz pegmatites [Norman, 1984]. From Norman's [1984] description, the igneous rock types exposed in the SVPC, in order of abundance from greatest to least, are gabbroic rocks, clinopyroxene-rich rocks, dioritic rocks, hornblendite, and leucocratic rocks. Secondary minerals such as chlorite, epidote, and clinozoisite are widespread, but are most abundant in shear zones and fractures. This alteration is thought to be from circulating hydrothermal fluids and occurred at about the same time as intrusion and shearing of the plutonic complex, rather than as a separate, later regional thermal event.

3.1.2 Shear Zones

The shear zone rocks generally consist of banded mylonite, with dark mineral layers alternating with light-colored mineral layers (figs. 3.2 and 3.3). The darker layers consist of hornblende-rich layers and clinopyroxene-rich layers with some plagioclase, while the light-colored layers consist mostly of plagioclase. The hornblende is typically dark brown pargasitic hornblende (fig. 3.4) but ranges to

Figure 3.1 Megabreccia along the GO Road, showing at least three progressive phases of injection ranging from darker to lighter colored rocks.

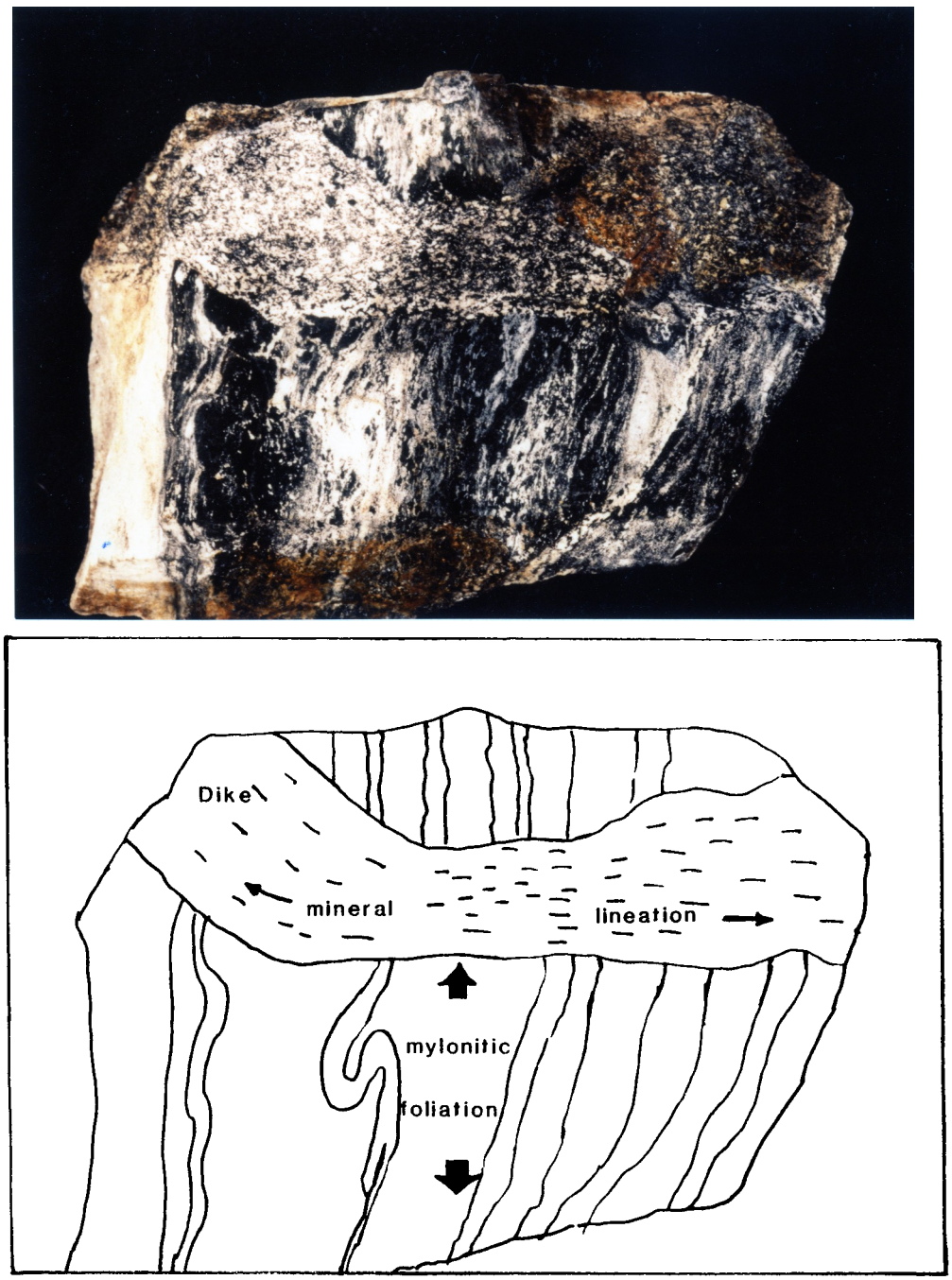

Figure 3.2 Mylonite crosscut by hornblendite dike. The plane of the dike goes down into the page, and is normal to the stretching lineation in the mylonite which it crosscuts. Long dimension of rock sample is 150mm.

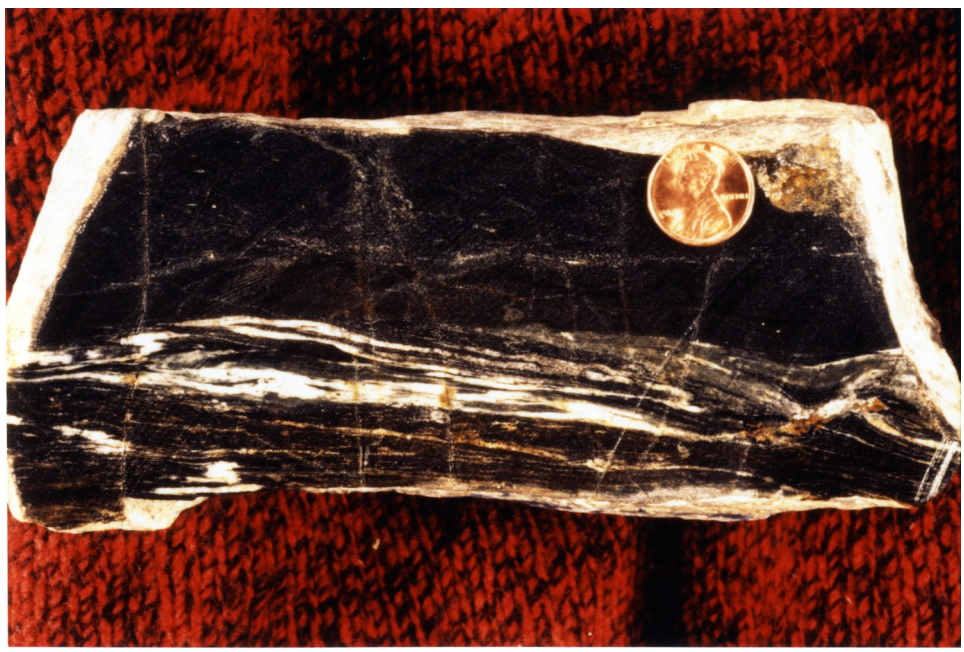

Figure 3.3 Rock sample CS 8a is a hornblendite mylonite containing hbld, plag, cpx, and opaques. Note folded plag-rich layers.

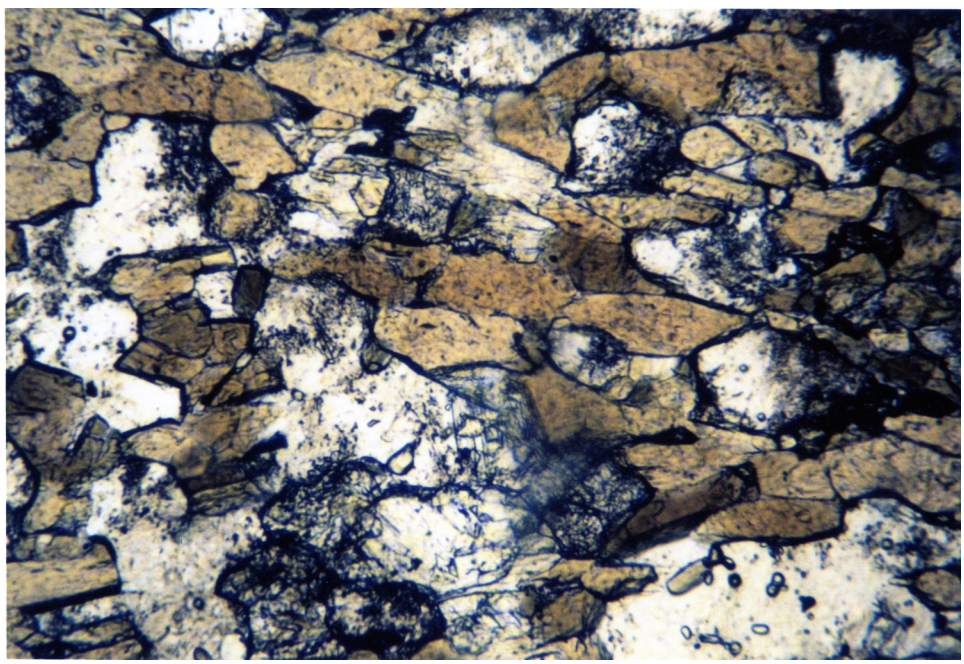

Figure 3.4 Rock sample SV 19-1 is an amphibolite containing brown amphibole, plag(An_{55}), and opaques. Field of view is about 1.5mm long. (Plane light)

green actinolite (fig. 3.5) [Norman, 1984]; these are sometimes seen in the same rock with actinolitic hornblende replacing brown hornblende, other times as two distinct phases in the same rock. The clinopyroxene is diopside (salite) (fig. 3.6) [Norman, 1984]. Plagioclase, which is found in both the lighter layers and in the darker layers, can vary in composition from andesine [An_{39}] in the hornblende layers to bytownite [An_{82}] in the clinopyroxene layers in the same rock [Norman, 1984]. Norman interpreted this as due to the reaction of

$$CPX + An_{80} <-> Hbld + An_{40}.$$

Plagioclase is both twinned and untwinned, and there are rare zoned grains. Clinopyroxene is also found in the plagioclase-rich layers. Some mylonites are overprinted by lower amphibolite - greenschist mineral assemblages with actinolite, clinozoisite, prehnite, sericite, and sphene [Norman, 1984]. These rocks are discussed in more detail below (Chap.5 Shear Zones -Ductile Deformation).

3.1.3 Country Rocks

The SVPC intrudes both the lower and upper plates of the Orleans fault. Exposed rocks of the lower plate are the Lems Ridge olistostrome (LRO) and the Galice Fm. The Galice Fm. is in fault contact with the plutonic complex at the southwestern margin, but an intrusive contact has not been found, nor is there evidence of contact metamorphism [Norman,1984].

The LRO is a 13 km-long (in outcrop) belt of olistostromal debris flows in sedimentary contact with pillow lavas below and the Galice Fm. above (at a northern location). It contains abundant clasts and exotic blocks of older rocks.

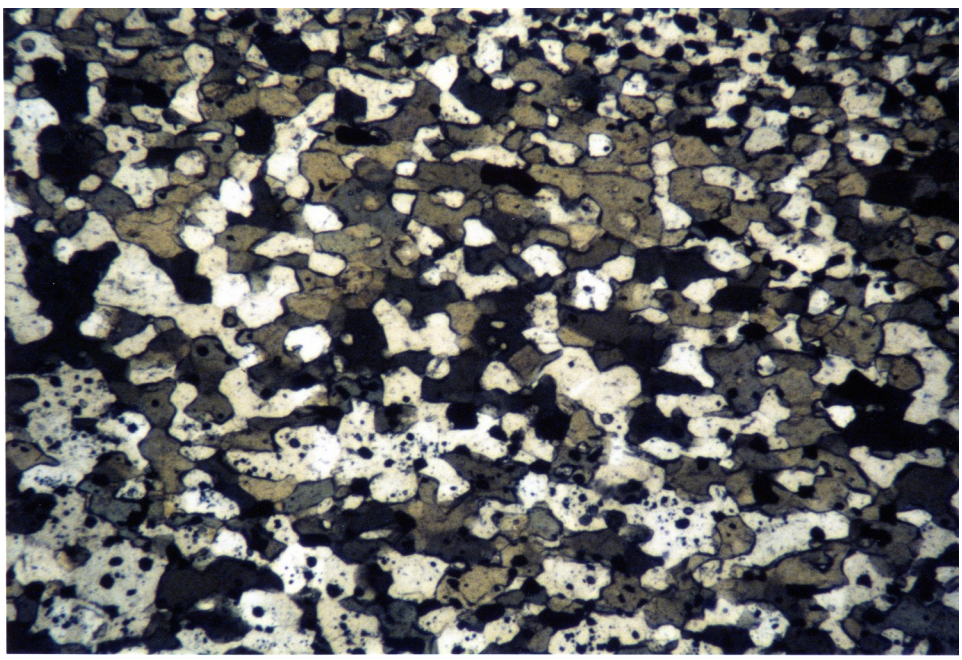

Figure 3.5 Thin section of sample CS 16-3 contains green amphibole, plag(An_{55}), and opaques. Note granoblastic texture. Field of view is about 3mm long. (Plane light)

A.

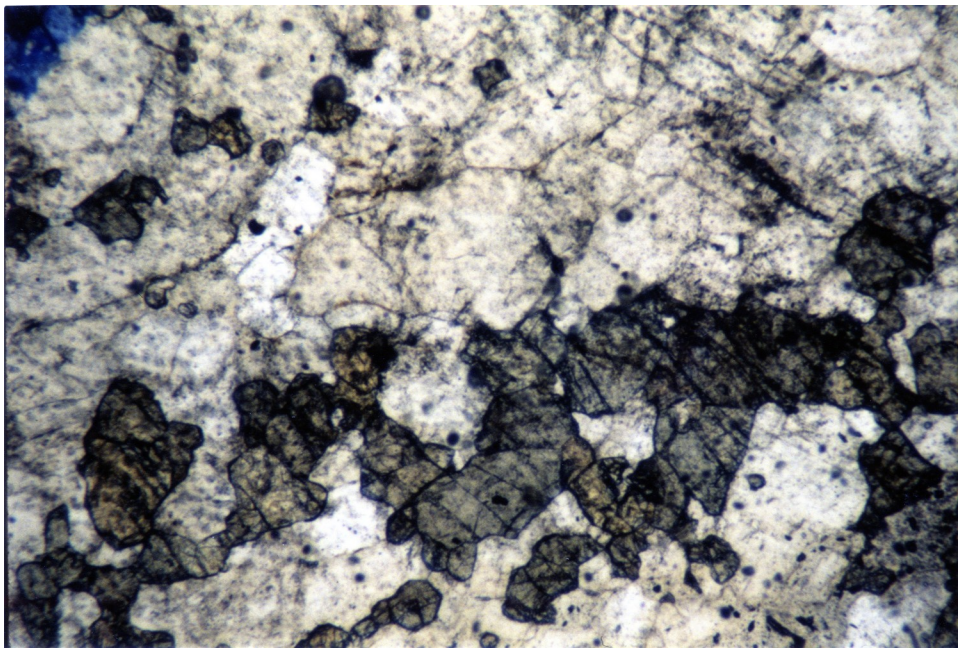

B.

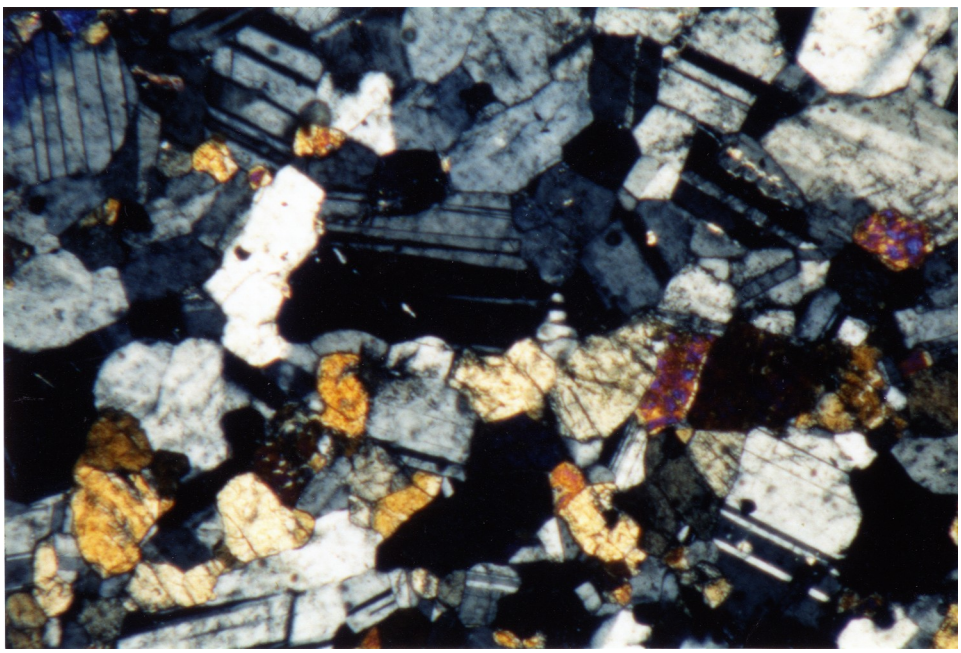

Figure 3.6 Thin section of Sample CS 8a (see fig.3.3), containing cpx, plag(An_{50}), hbld (not in this view), and opaques. View A - plane light. View B - crossed polars. Field of view is about 3mm long.

The LRO is composed mainly of black pebbly mudstone of continental affinity, and massive tuffaceous greenstones [Ohr, 1987]. It is contact metamorphosed to biotite hornfels adjacent to the plutonic complex [Norman,1984].

The upper plate rocks belong to the Rattlesnake Creek terrane (RCT) which is primarily harzburgite tectonite with three distinct lithologic units: alpine-type peridotite, a serpentine-matrix melange with ophiolitic blocks, and metavolcanic rocks with hemipelagic and clastic metasedimentaty rocks interposed [Gorman,1985]. The serpentinized harzburgite of the RCT is in contact with the plutonic complex along the eastern and northern margin, and screens and pendants of varying sizes are found within the plutonic complex. The protolith was composed of serpentine + talc + magnetite $\pm$ chlorite $\pm$ magnesite $\pm$ dolomite. A contact aureole is pronounced at the southeastern contact of the pluton with the RCT, where a prograde metamorphic assemblage of forsterite + tremolite + enstatite + chlorite + magnetite + trace of talc and dolomite can be found within 30m of the pluton [Norman,1984].

3.2 STRUCTURE OF PLUTONIC COMPLEX

3.2.1 General Structure

The Summit Valley Plutonic Complex is irregularly shaped and forms a mountain with a "saddle" at its crest (hence the name Summit "Valley"). The plutonic complex is incompletely unroofed, and screens and pendants of serpentinized harzburgite from the upper plate (RCT) are found in the study area.

The SVPC is located along a structural trend with a large post-Nevadan syncline that has been mapped in the Galice Fm. to the north of the plutonic complex and which is also evident from the outcrop pattern of the Preston Peak (Orleans) thrust near the study area (see Attachments: Geologic Map) [Norman, 1984]. The SVPC is located on the east dipping limb and is estimated to dip 20^0-60^0 based on bedding orientations collected in the Galice Fm. just to the north of the plutonic complex [Norman, 1984]. The SVPC has also been modified by late faulting. Landslides are common where serpentinized harzburgite has been sheared during this late faulting.

3.2.2 Contacts

The contact between the plutonic complex and the country rock appears to be generally very steep in most cases, and the contact varies from intrusive to sheared (see Attachments: Geologic Map) [Norman, 1984]. The SVPC is composed of pods and sections of different lithological suites representing numerous magmatic pulses. The contacts between these suites are complex: some are sharp, others are gradational, but sheared contacts are common.

3.2.3 Mylonite Zones

There are several mylonitic shear zones running through the SVPC, varying in thickness from centimeters to tens of meters (see fig. 5.15 for locations). The rocks in the shear zones are characterized by foliations, lineations, fine grain size, and mineral segregation or layering, and were referred to as "gneissic gabbros" by Norman [1984]. Orientations of the different shear zones vary from one to another,

and the kinematics appear to be complex. The saddle in the summit of the mountain may be a result of an extensive shear zone which is more easily eroded.

3.2.4 Dikes

Dikes are found in many outcrops within the SVPC and in the surrounding country rocks. Most dikes are fine-grained microdiorites, but some in the SVPC are hornblende-plagioclase pegmatites . The microdiorites were the last intrusive pulse, and are found cross-cutting all types of rocks in the plutonic complex including other dikes [Norman, 1984]. Width of the dikes usually ranges from 6cm to 60cm (fig. 6.2).

CHAPTER 4. METHODS OF STUDY

4.1 DATA COLLECTION

4.1.1 Field Work

Three types of structures have been studied for this analysis: ductile shear zones, vein-filled fractures, and dikes. Orientations of shear zones were measured in the field, recording orientations of shear zone walls (where possible), foliation planes, lineations, and sense of shear where evident. Dike orientations were also measured, recording orientation of dike walls and dike steps. Cross-cutting relationships were also noted to establish a sequence of dike intrusions to check for any progressive change in the stress field through time. Fracture planes were measured, along with slickenstriae where present. Only fractures with mineral vein fill were recorded in this study, and several different minerals (prehnite, epidote, and serpentine) were noted as fracture filling. Rock samples were marked in the field according to the method described by Prior et al [1987], so that fabric information from the samples could contribute to the reconstruction of the regional geology.

4.1.2 Laboratory Work

The petrofabrics of selected samples were investigated to determine sense of shear. For mylonites, thin section slabs were cut on a plane parallel to the lineation and perpendicular to the foliation, as suggested by Simpson [1986] (fig. 4.1). In the case of mylonite fabrics, the orientation that affords the best vantage point for detection

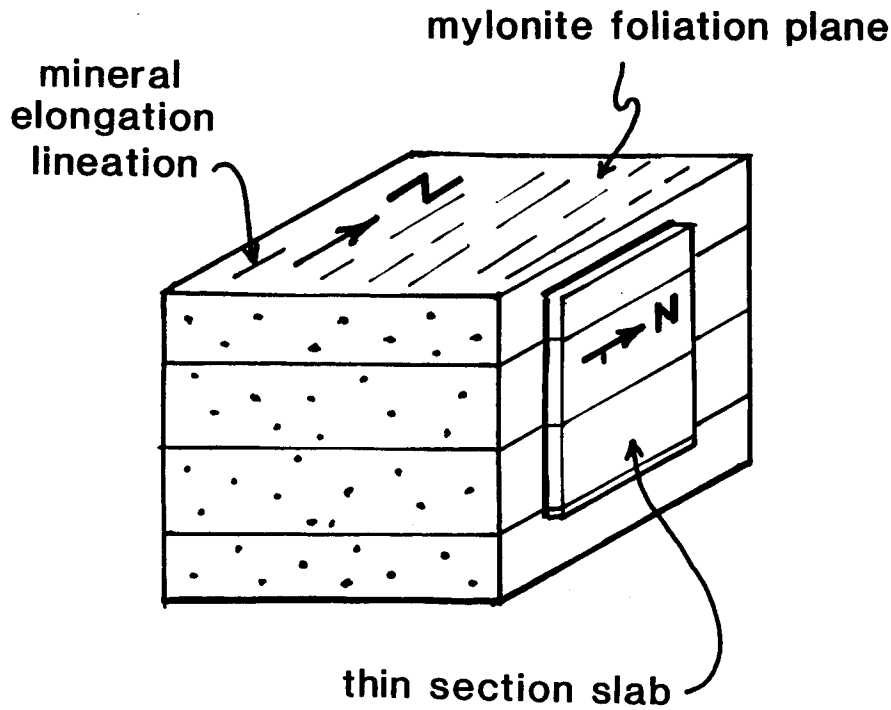

Figure 4.1 Recommended orientation for hand specimen and thin section. The section is cut perpendicular to the foliation and parallel to the mineral elongation lineation in the mylonite. (From Simpson, 1980).

of shear sense is normal to a plane that contains the maximum principal stretch direction and is perpendicular to the foliation [Simpson, 1986]. This perspective permits the best view of the rotational features of simple shear.

As is generally the case in the study of strained rocks, the available data from mylonites discloses little about the deformation history of the rock, only the final step or steps in the process. Evidence of previous increments of finite strain will have been obliterated by later deformation. The assumption must be made that the whole deformation history was consistent with the latest deformation unless otherwise indicated.

4.2 DATA PROCESSING

4.2.1 Stereographic Projection Plots

Structural data for shear zones, dikes and veins are plotted using a Schmidt equal area net (lower hemisphere projection) as follows: dikes are plotted as the poles to the plane (wall) of the dike, and cusps and steps are plotted as linear features; veins are plotted as poles to the fracture planes; mylonites are represented by plotting the poles to the foliation planes and the elongation direction as a linear feature. Veins and shear zones are plotted with an added embellishment, a slip vector which is an arrow added to the pole to the fault plane (fig. 4.2), according to the slip linear plot technique of Aleksandrowski (1985) as described by Marshak and Mitra [1988]. The slip linear plot illustrates the direction and sense of offset and allows the paleostress field for the deformation to be inferred. The efficacy of this method is also due to the fact that it accommodates the variations in orientations of fault data

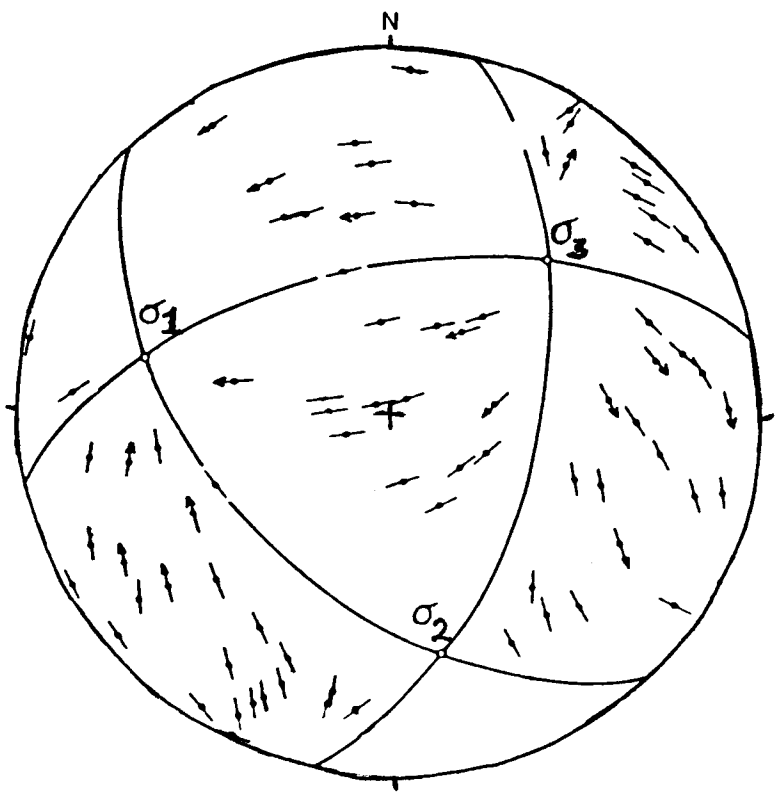

Figure 4.2 The slip-linear plot of Aleksandrowski (1985). Arrows (slip-linears) indicate direction of movement of hanging wall. Slip-linears point toward σ_1 and away from σ_3 . (From Marshak and Mitra, 1988)

due to preexisting anisotropies in rocks that dispose them to fail on planes other than those predicted by theoretical models. With this method, the pole to the vein (fault) plane is plotted as well as the lineation (slickenstriae) orientation. The slip direction is indicated by an arrow through the pole to the fault plane which is a trace of the "M" plane (fig. 4.3). The M-plane, or "movement" plane, is a plane containing the pole to the fault plane and the lineation. The direction the arrow (slip vector) points is the direction of movement of the hanging wall. Arrows that are radial and point toward the primitive circle are dip-slip faults, and arrows that are parallel to the primitive circle are strike-slip. Ideally, the slip vectors from a fault array that is plotted in this manner will all point towards one point on the net (which is σ_1) (fig. 4.2) and away from another point (which is σ_3), or the M-planes will intersect at σ_1 and σ_3. The conditions under which this technique is useful are the following: a constant stress field (the axes of principal stress must have remained in the same orientation during the deformation), and no fault plane rotation during the deformation [Aleksandrowski, 1985].

The slip linear plot was designed for use in solving the kinematics of complex fault arrays involving brittle fractures with slickenstriae. This plot is used in this study to illustrate the direction of slip in ductile shear zones in the SVPC. However, as a tool to derive the principal axes of stress, the slip linear plot is not as accurate with ductile shear zone data as it is for fractures. A fracture is generally a small strain experienced by the rock, whereas a ductile shear zone is an accumulation of significant finite strain, and earlier deformation fabrics are overprinted by later strain. A change in the stress field through time, for example, would not be discernible with this technique.

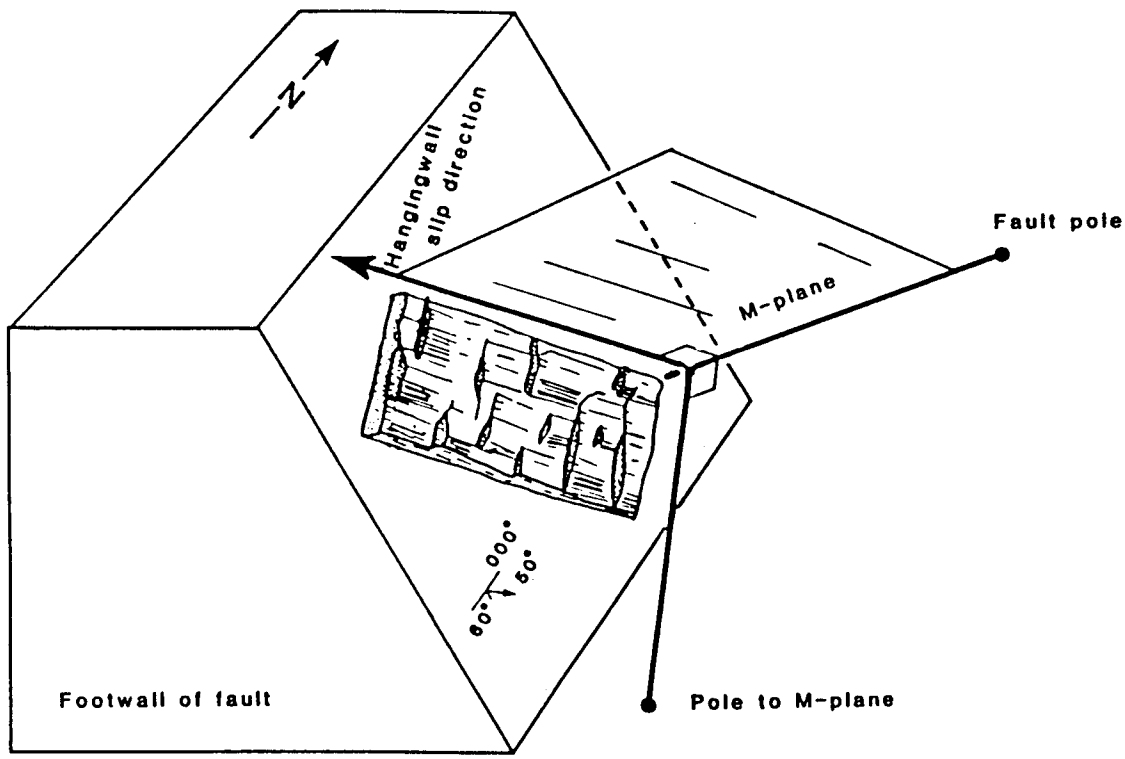

Figure 4.3 The M-plane contains the pole-to-fault and the lineation or slickenstriae. (from Marshak and Mitra, 1988)

4.2.2 Rotation of Data to Paleohorizontal

The SVPC is located in the east-dipping limb of a post-Nevadan syncline [Norman, 1984] (see Attachments: Geologic Map), and it was decided to rotate the orientations of structural data in the SVPC to conform with the best estimate of the paleohorizontal considering that there are no primary indicators of paleohorizontal within the plutonic complex itself. The dip is estimated to be about 45^0 towards the East from data from G.H. Harper [unpublished data], and was derived in the following manner: slatey cleavage of Nevadan age in the Galice Fm just outside the plutonic complex to the northwest was rotated back to paleohorizontal based on a cross-cutting dike (also of Nevadan age) which exhibits cumulate layering (assumed to be an indicator of paleohorizontal) [Harper, unpublished data]. The (rotated) orientation of the Galice Fm slatey cleavage was compared to cleavage found in the LRO immediately adjacent to the SVPC on the western margin ["D1" deformation of Norman, 1984; and this study] by graphical means using an equal area lower hemisphere stereonet projection (fig. 4.4), using the pole-to-cleavage to illustrate the difference between the mean cleavage orientations. The axis of rotation was taken from Norman's [1984] data of post-Nevadan ("F2" folding) (fig. 4.5) which indicates a mean fold axis striking about 336^0 and nearly horizontal.

To summarize then, the SVPC shear zone data (Chap.5) and vein data (Chap. 7) has been rotated 45^0 about a 336^0 axis, which is to say that all poles-to planes (fault, shear zone wall, foliation) and lineations have been rotated towards the East by 45^0 on a stereonet projection about an axis with azimuth 336^0. Looking down-axis towards 336^0, that would be a counter-clockwise rotation of poles about that axis.

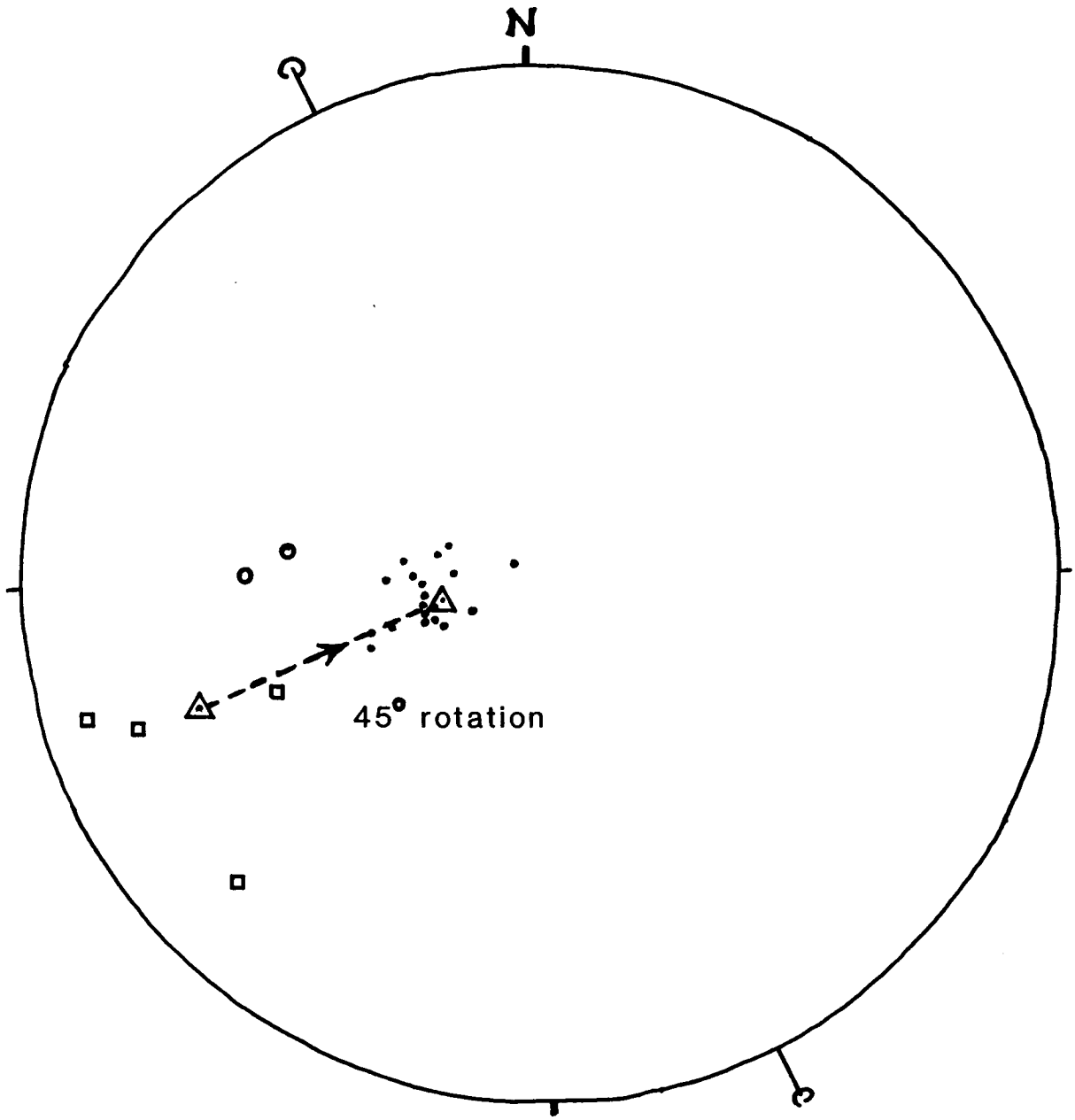

Figure 4.4 Determination of the rotation path of cleavage in the LRO for paleohorizontal by comparison with slatey cleavage in the Galice Fm just outside of the plutonic complex. Dotted line is rotation path.

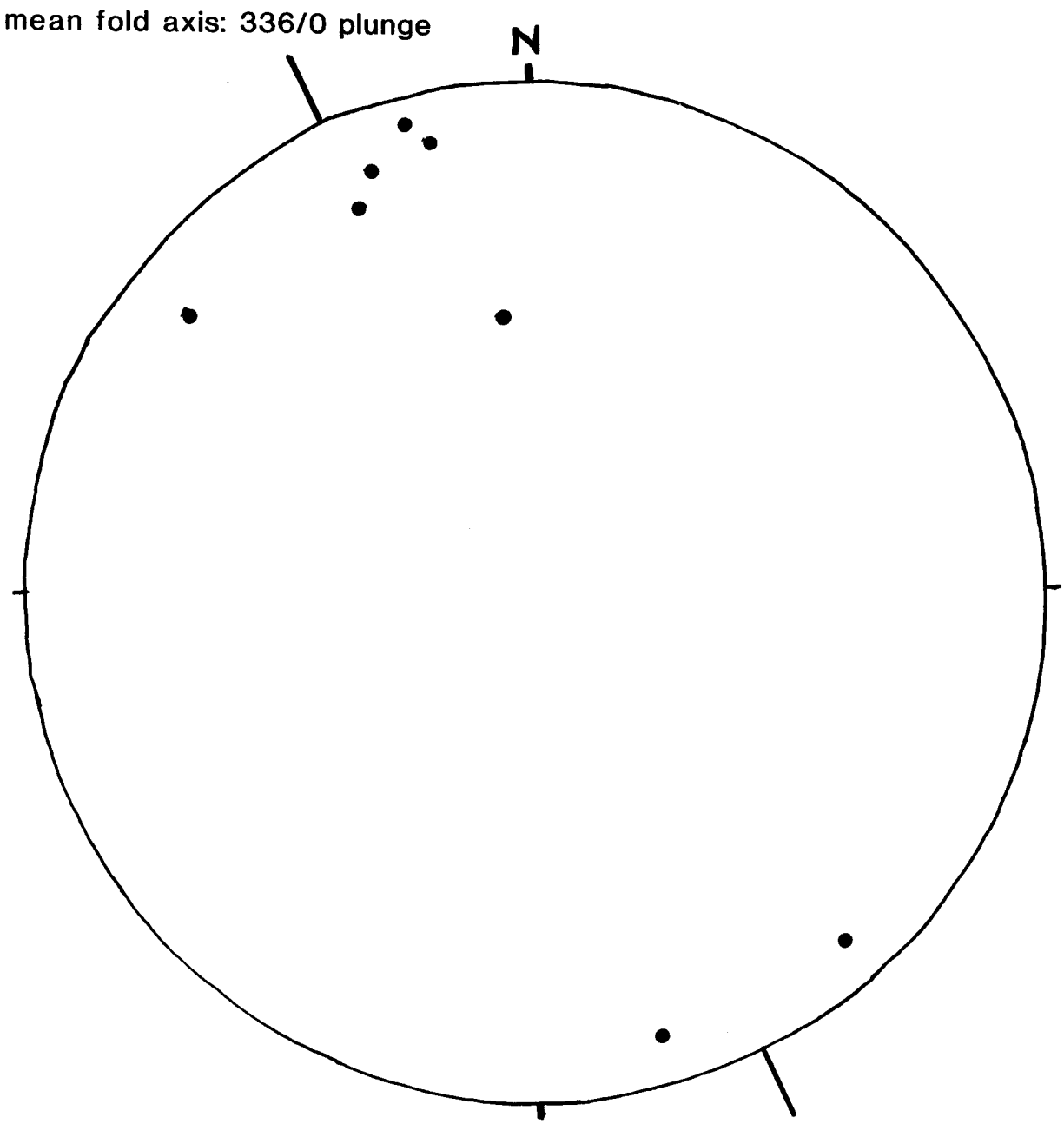

Figure 4.5 Post-Nevadan F_2 fold axes from Domain 2 [Norman,1984].

4.2.3 Stress Analyses

Two computer stress analysis programs were utilized in an effort to determine the orientations of the principal stresses in the paleostress field during the deformation of the SVPC using structural data from the shear zones and veins. The first program is one based on the work of Reches [1987] and Bott [1959], and written by Hardcastle [1989] and Hardcastle and Hills [1991]. The second, called ROMSA, was written by Lisle [1988] and is based on a graphical technique of paleostress analysis by Angelier and Mechler. Fault information was input into the computer programs according to the format specified for each program, including strike and dip of fault, azimuth and plunge of lineations, and sense of slip or fault type. The same set of data was input into the two different programs.

The Reches method performs a least squares regression on the matrix of data to best fit a general stress tensor satisfying as best it can, the following assumptions: 1)slip in the fault plane occurs normal to the direction of zero shear stress, and 2)the magnitudes of shear and normal stresses on the fault satisfy the Coulomb failure criterion:

$$\text{Shear Stress} > \text{Cohesion} + \text{Friction} * (\text{Normal Stress} - PH_2O).$$

The eigenvalues and eigenvectors of this general stress tensor are solved for, and this gives the magnitudes and directions of the principal stresses. Values of fluid pressure, coefficient of friction, and cohesion can be varied to obtain different possible orientations and magnitudes for the principal stresses. The following ranges were used:

Fluid pressure:	-Shear Zones: 0.5 to 0.7
	-Veins: 0.0 to 0.5
	-(0.5 recommended for upper crustal rocks)
Coefficient of friction:	-Shear Zones: 0.25 to .85
	-Veins: 0.25 0.85
	-(.85 recommended for upper crustal rocks)
Cohesion:	-0 to 1 for shear zones and veins (1 recommended for upper crustal rocks).

Lisle's method uses the fault plane orientation and slip direction much the way a fault plane solution interprets the first motion of an earthquake, and relies on the following assumptions:

- that slip takes place along the direction of maximum resolved shear stress on the fault plane.
- that similar to fault plane solutions (with the compressional and dilational quadrantal arrangement of potential σ_1 and σ_3 directions), the maximum compressive principal stress (σ_1) is contained within one pair of opposing right dihedra, and that the minimum principal stress (σ_3) is contained within the other pair.
- Lisle's method also applies a further constraint that the principal axes of stress lie in opposite pairs of a set of right dihedra that are perpendicular to the first set.
- principal stresses are mutually orthogonal.

4.2.4 Maps

Three maps were made to supplement this study:

(i) Outcrop map - a map showing the locations of the numbered stations in the field area (see Attachments). Sample numbers are coordinated with the station numbers.

(ii) Geologic map - showing boundaries of lithological units and structural data (see Attachments).

(iii) Shear zone map - illustrating the locations of the shear zones studied in this project (fig.5.15).

4.3 HISTORY OF DEFORMATION

This study is a kinematic analysis of structural features found in the SVPC for the purpose of determination of shearing direction on the Orleans Fault. Shear zones, fractures, and dikes are useful for estimating the strain and possibly the stress at the time of deformation. The possibility exists that the axes of principal stress in the plutonic complex changed through time during the Nevadan deformation. This report proposes a sequence of emplacement and deformation events to test the notion of a progressive change in orientation of the stress field through time.

4.3.1 Assumptions

It is assumed that the plutonic complex cooled steadily through time by heat transfer into the surrounding rock, without any major thermal perturbations such as sudden rapid uplift. Crystallization ages for a zircon (from an undeformed hornblende gabbro) (fig. 4.4) and a cooling age for a hornblende (from a late-stage pegmatitic gabbro from the same site) of 150$\pm$1Ma and 144$\pm$1Ma, respectively [Harper et al

(in review)], indicate a protracted period of high temperatures in the SVPC. The elevated temperatures (> ~500°C, the closure temperature for the hornblende) may be due to continued magma injection, since a small pluton such as this would otherwise have cooled to the ambient temperature of the country rock much more quickly [Harper et al, (in review)]. Subsequent to this, structural, mineralogical, and petrographic data indicate that the SVPC experienced a retrogressive cooling history from magmatic temperatures to the temperature of the country rocks (greenschist facies). It should follow that deformation would also follow a course from crystal plastic to brittle deformation. Because most of the rocks are gabbroic, this change should have been at about 400° - 500°C [Brodie and Rutter].

4.3.2 Structural and Petrographic Evidence of Cooling History

The ductile shear zones (mylonite zones) appear to be the earliest form of deformation, since they are cross-cut by both dikes (fig. 4.5) and mineral-filled fractures. Dikes cross-cut many shear zones, but are also locally plastically sheared. Brittle fractures with mineralization (epidote, prehnite, serpentine) cross-cut all ductile features and dikes and are the latest strain feature to be imposed upon the plutonic complex. Younger brittle fractures without veining are commonly seen, but only those with vein minerals are considered to be related to the emplacement and cooling of the plutonic complex during regional metamorphism.

Mineral overprinting was looked at as an indicator of decreasing temperature conditions. Amphibole composition (as evidenced by color) varies from a dark brown igneous, high-temperature hornblende to a later light green, actinolitic amphibole because of changing Ti content with temperature [Raase, 1974].

Sometimes both brown, high-temperature hornblende and light green amphibole are seen in the same rock, both having a preferred orientation, thus recording cooling. Both inside and outside the shear zones, retrogression is also evidenced by the following: sausseritization of plagioclase, and by replacement of amphibole by chlorite and plagioclase by epidote.

Recrystallization during deformation and under retrograde metamorphic conditions is indicated by the following: 1.) overprinting of igneous fabrics and high-temperature granoblastic mylonites by mylonites composed of lower temperature mineral assemblages, 2.) mylonites composed of amphibolite-greenschist facies minerals, and 3.) all ductile features cross-cut by epidote-filled fractures, . All together, these conditions suggest the following history: continued deformation while the plutonic complex was cooling, with deformation passing from plastic strain to brittle failure. This model enables the development of a time line for the history of deformation in the SVPC.

CHAPTER 5. SHEAR ZONES

5.1 DESCRIPTION

5.1.1 Field Description

Shear zones have been found in various parts of the plutonic complex, both in the interior and at the perimeter. Those studied range in width from 3.5 cm to 37 m. Some shear zones are discrete with parallel walls, while others are diffuse and anastomosing (a "marble cake" appearance) (fig. 5.1). They are recognizable in the field by gneissic layering and fine grain size. At some sites, undeformed host rock can be seen in proximity to the sheared rock and the shear sense is indicated by the fabric as it bends into the shear zone (fig. 5.2). Many rocks in shear zones appear locally overprinted by epidote, prehnite, actinolite and rarely, sulfides.

The rocks in the shear zones are characterized by the following: foliated fabrics, lineations, fine grain size, and mineral layering. Rock fabrics may provide an index to infer the amount of strain, annealing, syn-deformational metamorphism, and static retrogressive metamorphism.

5.1.2 Rock Fabrics

Fabrics of rocks found in shear zones in the plutonic complex can be grouped into four general types. These fabrics are described as seen in thin section though features can often be seen in hand sample as well. The four types are as follows:

Figure 5.1 Marble-cake appearance of some shear zone rocks. Photo at station SV 18. Coin for scale left of center.

Figure 5.2 Rock sample GE 27-6. Hornblende gabbro with dikelets and sheared fabric. Sample is about 15cm in height.

1) Type One is characterized by foam texture or granoblastic texture, whereby most of the mineral phases appear as nearly equant anhedral grains, with 120^{o} grain boundary triple junctions (fig. 3.5). Grain size generally is <0.5mm, though coarser grain size (1-2mm) is prevalent in some samples of this type. Porphyroclasts are rare; instead, augen-shaped aggregates of clinozoisite and albite appear to be pseudomorphing an earlier plagioclase phase (fig. 5.3). Mineral foliation is weak and diffuse, but where present it is defined by preferred orientation of amphibole parallel to the shear zone walls, and compositional layering of pyroxene, hornblende, and plagioclase. This fabric type poses problems in discerning shear sense due to the lack of asymmetrical features. This will be discussed later in section 5.2.2. Problems.

2) Type Two fabric has a well-developed foliation, usually defined by substantial segregation of amphibole, pyroxene, and plagioclase, and by the grain-shape orientation of amphibole grains. Overall grain size is small, about 0.1mm to 0.5mm. One or all of the following foliations may be displayed in these samples: C-foliation (shear foliation parallel with shear zone walls); S-foliations (schistose foliations forming at an angle to the C-foliation) and C' foliations (shear bands, which also form at an intermediate angle to the main foliation) (fig. 5.4). Asymmetric porphyroclasts and asymmetric aggregates are present in some rocks (fig. 5.5), though not frequent. This fabric type generally provides reliable sense of shear indicators.

3) Type Three is a fabric seen in the late-stage intrusive hornblende gabbro.

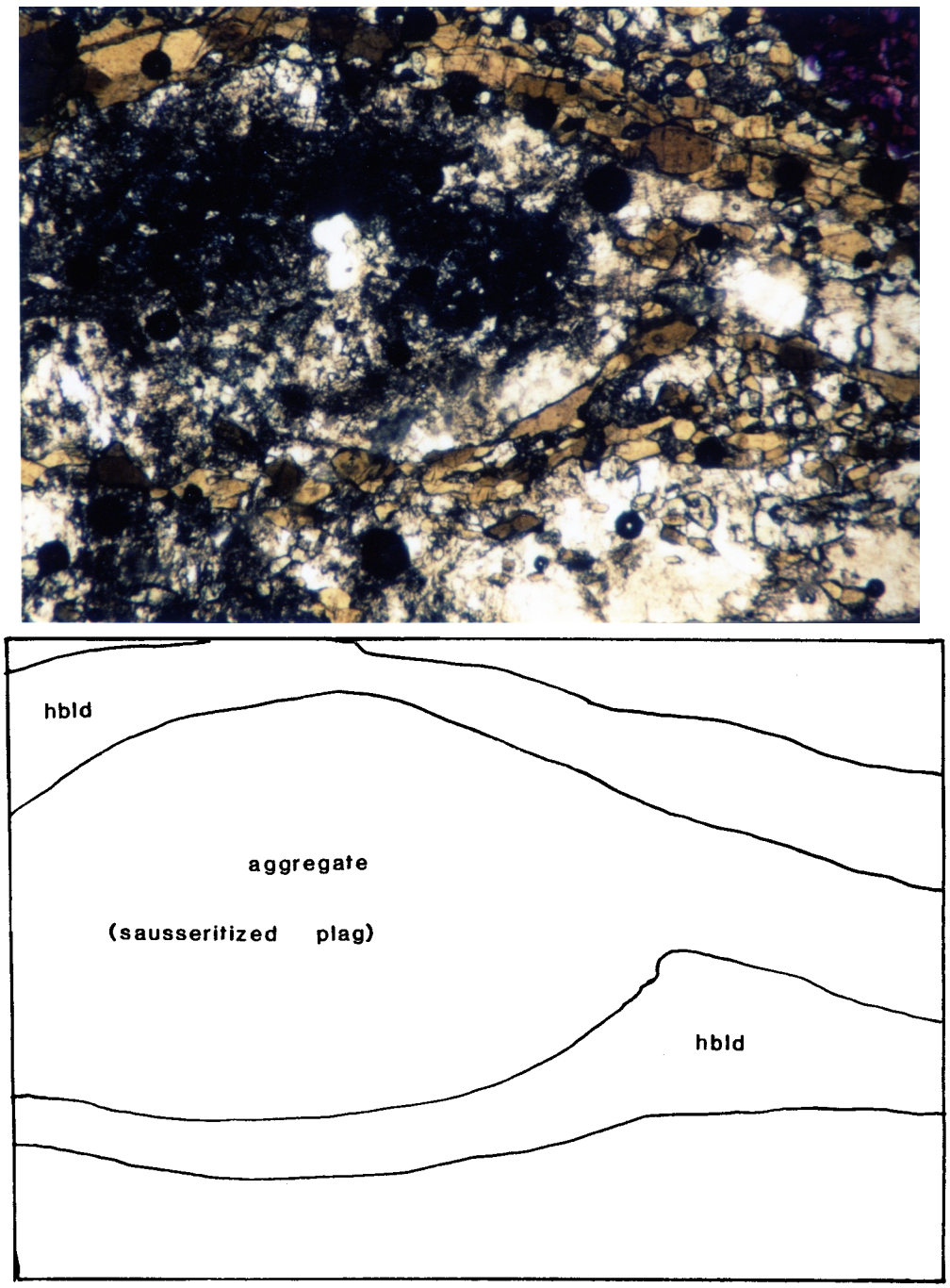

Figure 5.3 Sample CS 8b. Augen-shaped aggregate of sausseritized plagioclase grains. Brown mineral is hornblende; light minerals are plag and clinozoisite. Field of view is about 3mm long. (plane light)

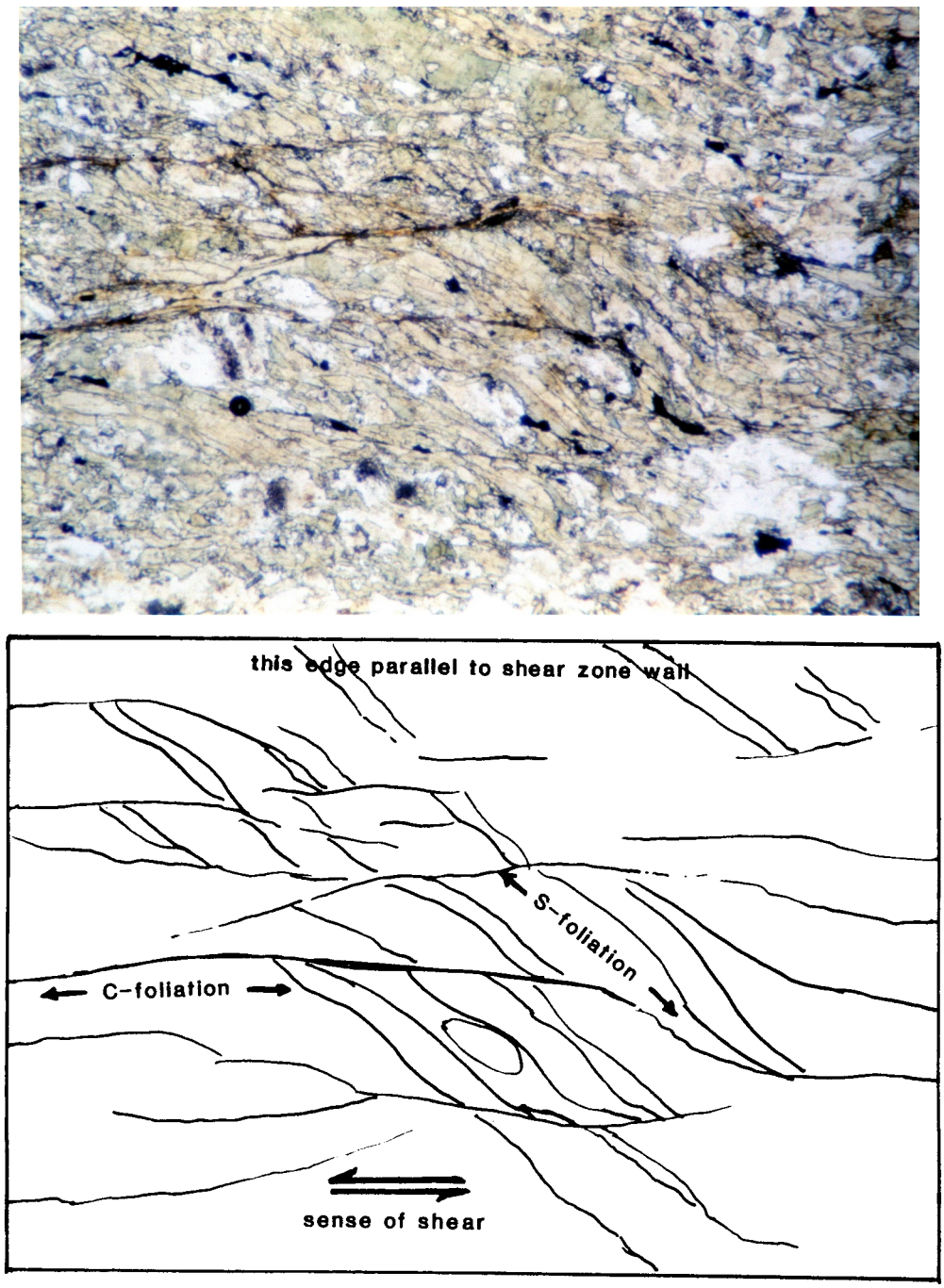

Figure 5.4 Sample WH 23-5, showing C- and S-foliation. Green hbld, chlorite, and plag. Shear zone walls are parallel with long dimension ofthe picture. Length is about 3mm. (Plane light)

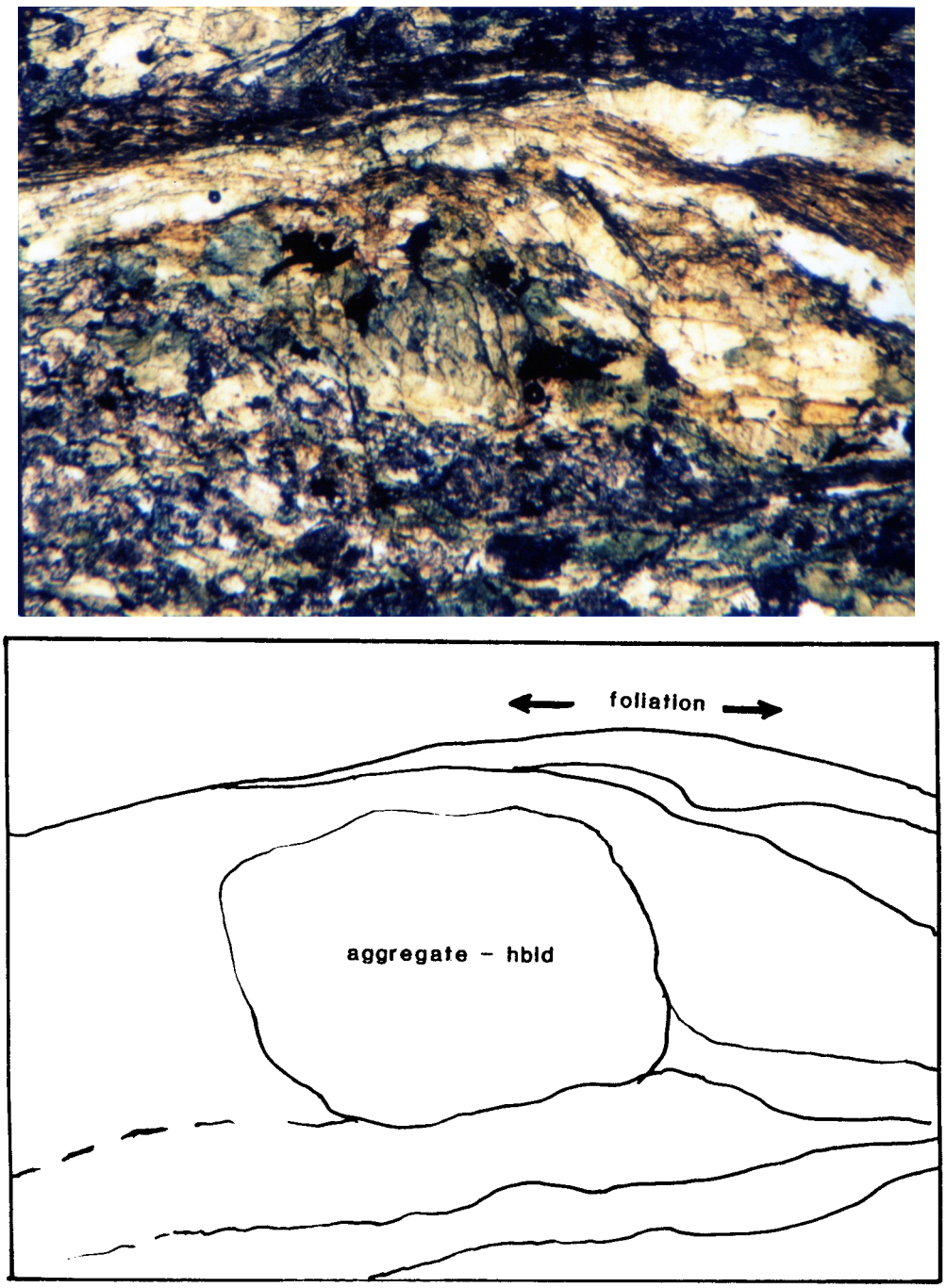

Figure 5.5 Sample WH 23-5. Foliation wrapping around an asymmetric porphyroclast/aggregate. Green hbld, chlorite, and plag. Length is about 3mm. (Plane light)

Small plastic shear zones cross-cut the original igneous fabric, creating small shear bands 2-4mm wide and easily seen in hand sample (fig. 5.2). There is a transition zone about 2cm wide at the boundary of the shear zone wall, where the igneous fabric bends into the shear zone. Elongate hornblende grains define the fabric. In thin section, plagioclase grains appear bent (fig. 5.6) and broken, and there are small, discrete zones of fine-grained (untwinned) plagioclase suggesting localization of strain with grain size reduction by recrystallization. In some places, small dikelets (about 3-5mm wide) are seen within these small shear zones (figs. 5.2). The dikelets may have either intruded the shear zone syn- or post-deformationally, or shearing may have been activated inside a preexisting dike [Passchier et al, 1990; Hollister et al, 1986; Lisle, 1989]. The display of varying amounts of deformation in the host rock does not help to answer that question; in some areas adjacent to the sheared "dikelets" little or no strain is seen, while near others, the rock fabric appears to be "bending" into the shear band.

4.) Type Four is a schistose fabric found in the deformed metamorphic aureole of the pluton. The rock is a biotite-hornfels (fig. 5.7), with abundant strained quartz-rich pebbles (fig. 5.8) which define a lineation (due to their ellipsoidal shape), and a strong foliation defined by biotite (fig. 5.9). Strained quartz-rich pebbles have asymmetric pressure shadows which give clear indication of sense of shear. Biotite foliation in the form of S-C and C-C' foliations also gives reliable sense of shear.

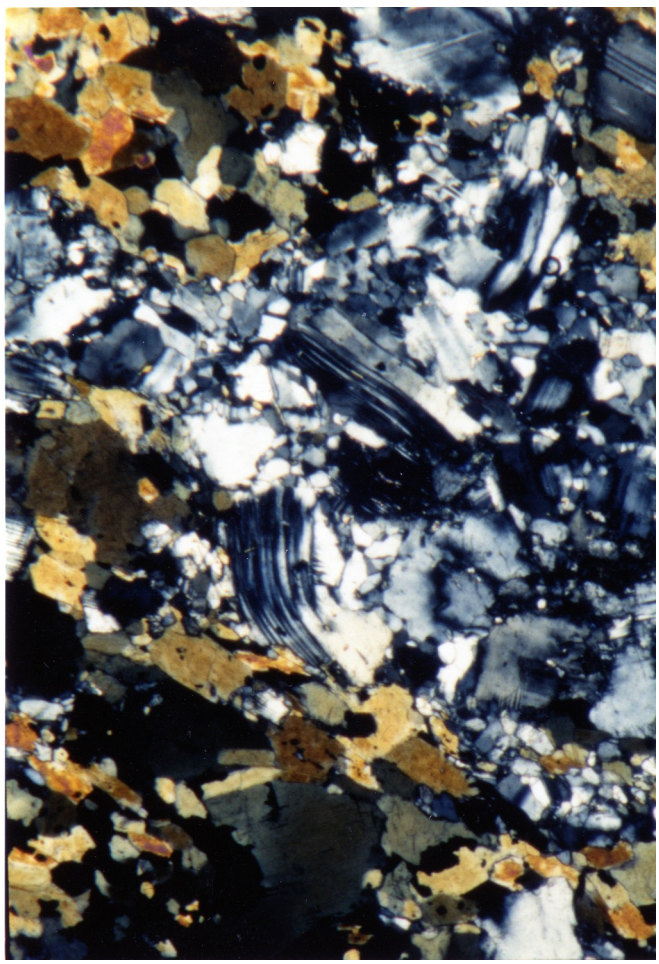

Figure 5.6 Sample GE 27-5. Bent plagioclase twins in strained rock. Hbld, plag, and opaques. (Crossed polars)

Figure 5.7 Sample CR 28-1. Strained quartz pebbles with metapelite matrix; biotite hornfels. Sample is about 24cm long and 12cm high.

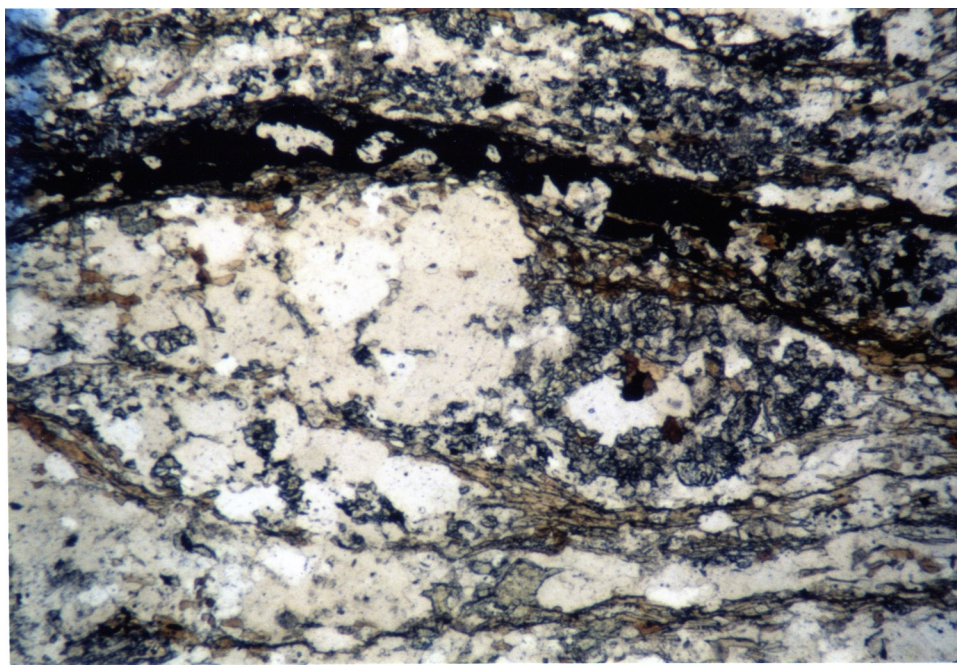

Figure 5.8 Sample CR 28-1. Strained quartz pebble with biotite, magnetite, and cummingtonite. (Plane light)

A.

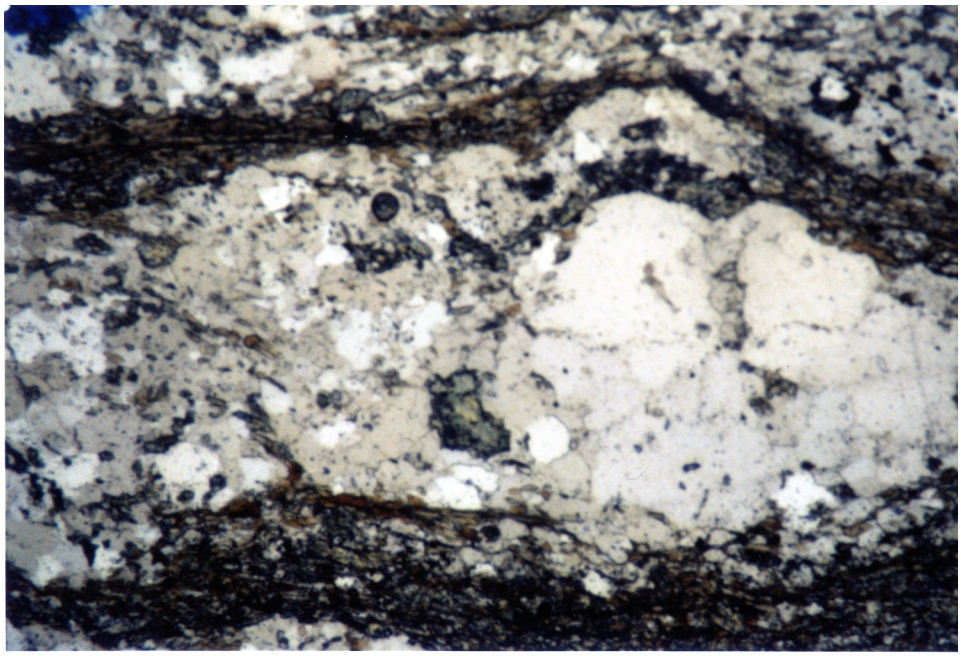

B.

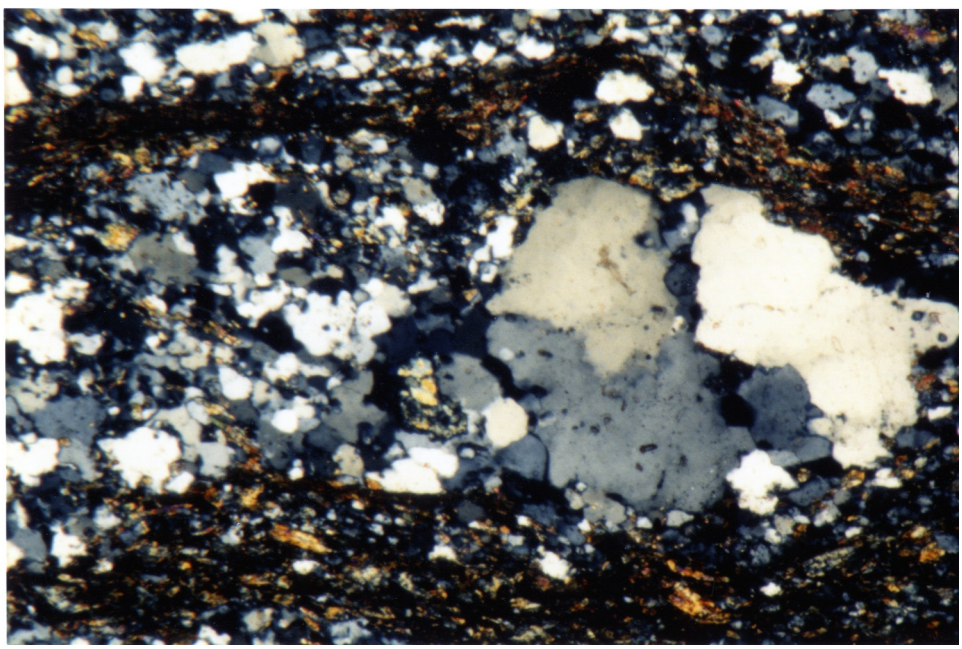

Figure 5.9 Sample CR 28-1. Biotite defines the foliaton, here outlining strained quartz pebble. A.)plane light B.)crossed polars.

5.1.3 Mineral Assemblages

The shear zone rocks studied here have included a wide variety of mineral assemblages. These assemblages and their associated metamorphic facies according to Yardley's [1989] classification are the following: primary igneous, high-grade metamorphic, retrograde metamorphic, and hornfels (contact aureole).

Primary Igneous. Some of the shear zone rocks have the original igneous minerals with igneous textures overprinted by strain fabrics [see Sec. 5.1.2 Rock Fabrics]. These primary igneous minerals include brown hornblende + calcic plagioclase $\pm$ clinopyroxene. Usually, hornblende and clinopyroxene exhibit some retrograde rims or overprinting of green amphibole. In one sample (fig. 5.10) from the late hornblende diorite, the undeformed rock and the sheared rock display the same mineral phases. Grain size reduction and bent or broken grains are sometimes the only changes seen from the original rock to the sheared rock.

High-grade Metamorphism. A large number of shear zone rocks showed evidence for high-temperature metamorphism, possibly accompanying deformation, including granulite and amphibolite facies. Samples from two different shear zones contain clinopyroxene which appears to be a newly-formed phase and contains inclusions of hornblende and plagioclase. The hornblende is brown (neoblasts), suggesting high-temperature formation according to the observations of Raase [1974], and the plagioclase is An_{55} based on Carlsbad-albite twinning [Bambauer et al, 1979] (figs. 3.4 and 3.6).

Amphibolite facies assemblages are the most common in the shear zone rocks and are indicated by the presence of brown, green, or blue amphibole plus plagioclase (ranging from bytownite to andesine) $\pm$ clinopyroxene.

Figure 5.10 Sample GE 27-5. Hornblende-diorite showing shearing in the protolith bending into the mylonite zone (from middle of sample to bottom). Hbld, plag, cpx, and opaques.

Retrograde Metamorphism. Locally in shear zones, especially in the areas of stations 16 and 23, mineral assemblages indicate greenschist facies to prehnite-pumpellyite facies conditions (fig. 5.11). A small shear zone at station 23 (about 4cm wide) shows brown hornblende almost totally replaced by green amphibole, highly saussuritized plagioclase, plus epidote, clinozoisite, and chlorite (figs. 5.4 and 5.5). In a 20 meter-wide shear zone at station 16, small sections of rock averaging 0.3m to 1m wide in surface outcrop, exhibit characteristics of static overprinting in a previously strained rock: green amphibole with crystallographic preferred orientation and former porphyroclasts appear overprinted and pseudomorphed by randomly oriented muscovite, chlorite, and clinozoisite. Other samples show these minerals (especially actinolite and chlorite) formed in a preferred orientation suggesting continued plastic deformation as the plutonic complex cooled (figs. 5.4 and 5.5).

Contact Aureole - Biotite Hornfels. Sheared rocks in the Lems Ridge Olistostrome at the western margin of the plutonic complex are biotite hornfels and are part of the contact aureole. Sample 28-1 (figs. 5.7 - 5.9) from that shear zone contains mostly strained quartz clasts, biotite, cummingtonite, and Fe-Ti oxide. Rare, colorless garnet has also been found in this area of the metamorphic aureole [Norman, 1984].

5.2 SHEAR SENSE INDICATORS

5.2.1 Description

Shear zone rocks from the SVPC were examined both in outcrop and in the

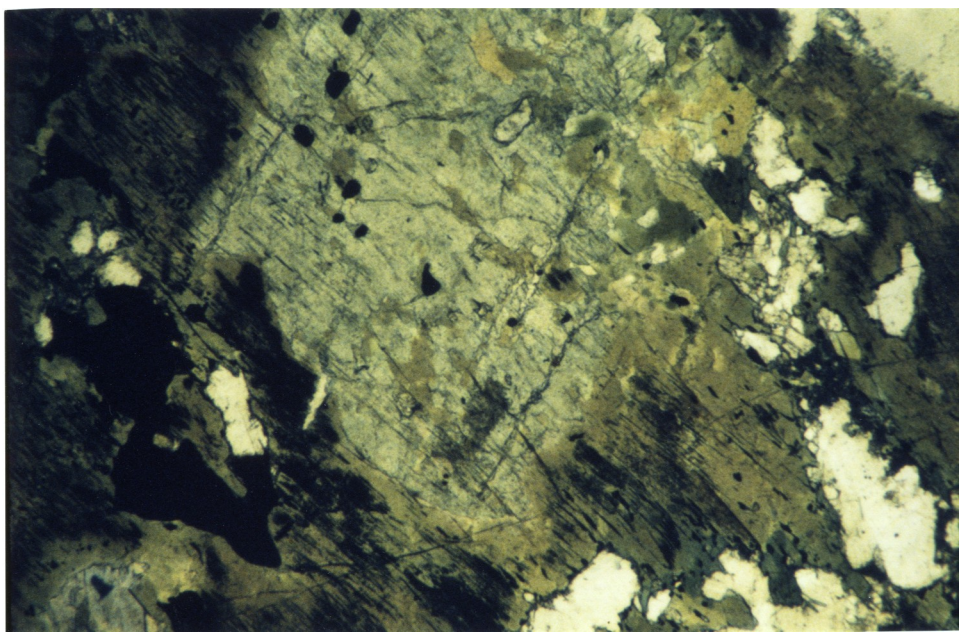

Figure 5.11 Sample GE 27-3. Cpx replaced by green amphibole + magnetite. Field of view is about 3mm long. (plane light)

laboratory for features that could be used as shear sense indicators. In sheared rocks where a lineation is present, the lineation is assumed to be parallel with the direction of maximum shearing. Rock fabrics suggest a high accumulation of strain giving features enough time to rotate into parallelism with the stretching direction. Also, strain features, such as assymetric porphyroclasts, suggest that strain was primarily simple shear. Lineations in the rocks from the SVPC are defined by aligned hornblende grains or elongate mineral aggregates. To observe shear sense indicators accurately, rocks (whether in hand specimen or thin section) were viewed as pictured in fig. 4.1. Shear sense indicators found in rocks in the SVPC are described below along with a discussion concerning their reliability:

a) Asymmetric porphyroclasts ("porphyroclast systems" of Passchier and Simpson [1986]) (fig. 5.5) are found in rocks from some shear zones in the SVPC, though their occurrence is not frequent. They are composed of various minerals: pyroxene, hornblende (usually pseudomorphing pyroxene where seen as a porphyroclast(fig. 5.11)), and plagioclase. In the shear zone within the LRO near the contact with the SVPC, asymmetrical porphyroclasts are composed of quartz clasts (fig. 5.8). Sense of shear is determined from the monoclinic asymmetry of the porphyroclast tails and from the deflection of the foliation around the porphyroclast [Simpson, 1986].

b) Asymmetric aggregates (fig. 5.3) are augen-shaped forms whose asymmetry may indicate shear direction. Two types are found: 1) lenses of host rock which have undergone less strain than the surrounding rock; and 2) multigrain lozenges of mineral aggregates (usually feldspar and

clinozoisite), believed to be pseudomorphs of porphyroclasts (probably plagioclase). Sense of shear is determined for asymmetric aggregates in the same way as for asymmetric porphyroclasts.

c) Asymmetric foliations:

(i) S-C foliations (fig. 5.4), also known as type I S-C mylonite of Lister and Snoke [1984], are evident in some of the mylonite samples from the SVPC. The S-foliation initially forms at an acute angle to the boundary of the shear zone (~45°), but rotates as strain progresses into an orientation parallel with the boundary of the shear zone. In the SVPC, the S-foliation is defined by fine-grained feldspar and amphibole (elongate or bladed). In the LRO, the S-foliation is defined by quartz and plagioclase microlithons and biotite. The C-foliation is defined by C-surfaces ("C" for cisaillement) which are zones of localized high shear strain, or shear bands. They are approximately parallel to the wall of a shear zone, and they truncate the S-foliation at fairly regular intervals [Berthe et al, 1979; Lister and Snoke, 1984]. In the SVPC , the S-foliation (amphibole or biotite grains) can be seen bending asymptotically into the shear band (C-foliation) (fig. 5.4).

(ii) C-C'foliations (fig. 5.12) were used in some samples to determine sense of shear. Simpson and Schmid [1983] and Passchier [1990] describe this fabric found in highly strained rocks as a composite foliation having two types of shear bands: a C-foliation (which is a combination of S- and C-foliations) which is approximately parallel to the shear zone walls, and a C'-foliation which is defined by shear bands that cut across the C-foliation at an angle of 20-50°, and dipping in the opposite direction than that of the S-foliation. The C'-foliation tends to develop only in advanced stages of

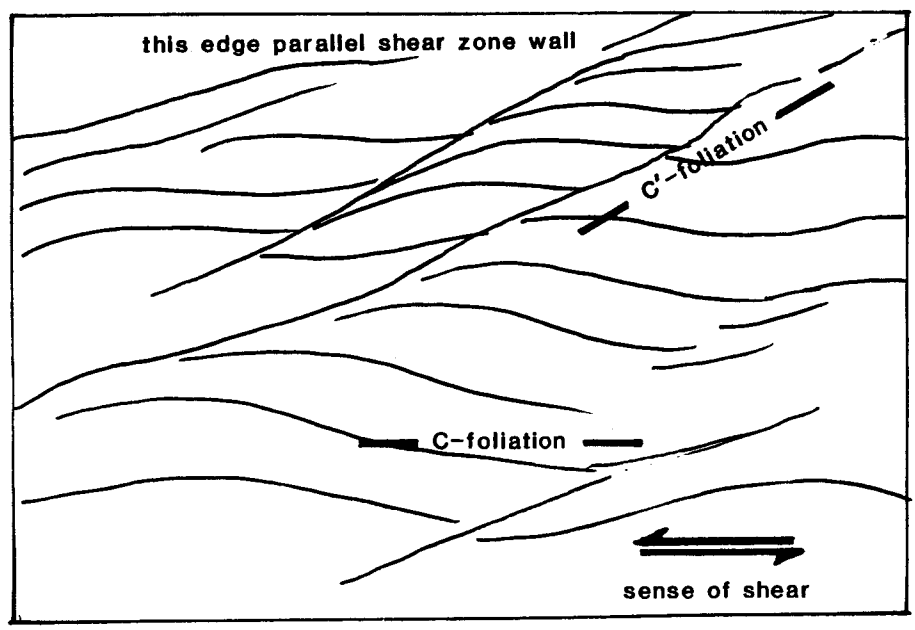

Figure 5.12 Diagram showing orientations of C-C'foliations with respect to shear zone walls and appropriate sense of shear.

strain where the S-foliation has rotated into parallelism with the C-foliation, and strain-hardening may have caused shearing to initiate on a plane oblique to the C-foliation. In the SVPC, the C-C'foliation is defined by amphiboles or phyllosilicates (biotite and/or chlorite) anastomozing around feldspar grains. In the LRO, the C-C'foliation is defined by biotite anastomozing around quartz clasts.

d) Asymmetric folds (fig. 3.3) occur in the gneissic foliation which is defined by mineral segregation (amphibole, clinopyroxene, and plagioclase) and by preferred orientation of hornblende. In some highly strained samples, all asymmetric features (e.g. S-foliation, grain-shape orientation) have rotated into the main foliation plane approximately parallel with the shear zone walls. Grain-size reduction is extensive, and few or no asymmetric porphyroclasts remain. Folds in the mineral foliation are sometimes the only indication of shear sense available. However, caution must be exercised in the use of folded mineral layering as shear criteria, because a feature such as a cross-cutting dike can become folded and rotated in a state of high shear strain, and can give the opposite sense of vergence, and therefore the wrong sense of shear (fig. 5.13).

e) Bent albite twins are used as indicators of sense of shear (fig. 5.6) . Large (1.5-2.0mm) deformed grains of twinned plagioclase (An_{73-82}) are seen in thin section in the regions adjacent to a shear zone where the rock fabric is deflected into the shear zone. Plagioclase is the predominant modal phase in this rock. The bent plagioclase grains are surrounded by other large competent grains of plagioclase, and lesser hornblende,

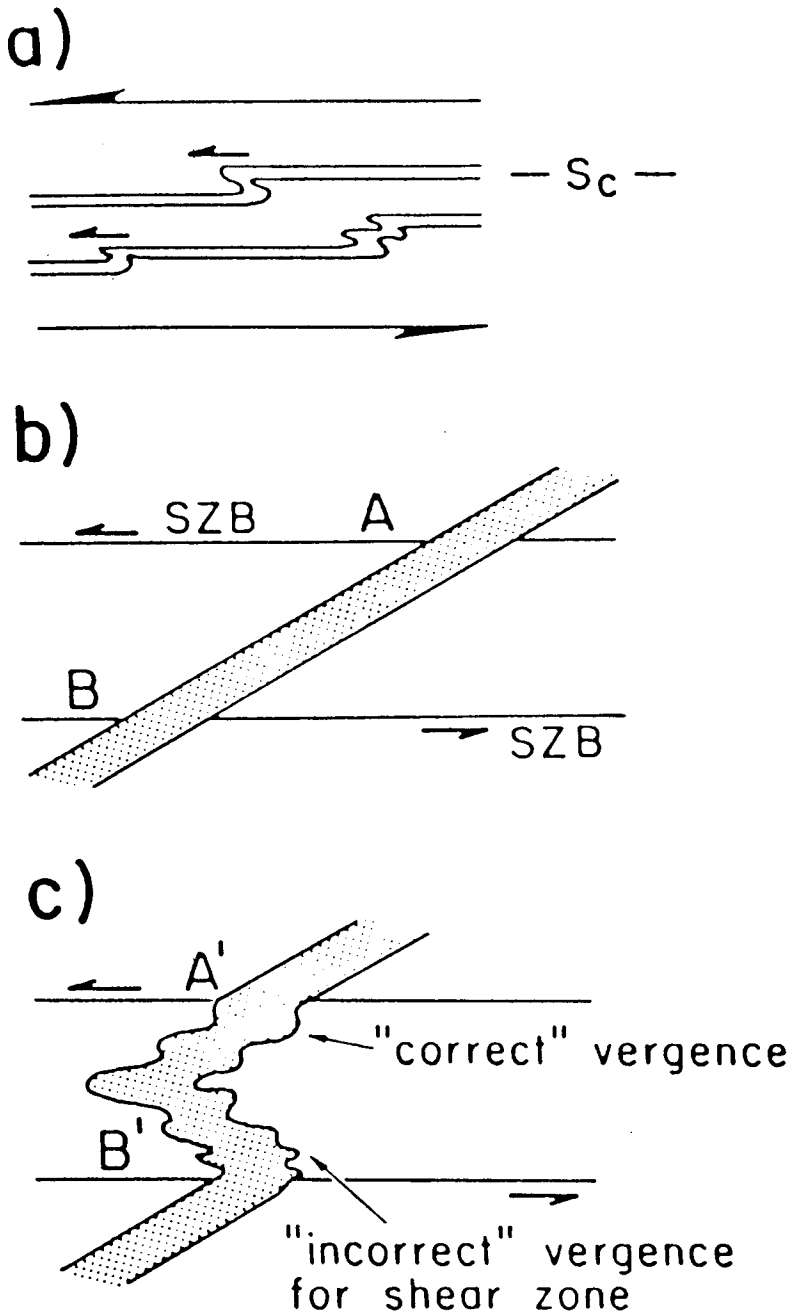

Figure 5.13 Diagram showing proper use of folded layering as sense of shear indicator. [From Simpson, 1986]

pyroxene, and smaller strain-free grains of plagioclase. At some point then, in the deformation history of this rock, the large plagioclase grains were the stress-bearing phase, and bent albite twins therefore, presumably indicate an accurate sense of shear.

f) Hornblende z-axis preferred orientation [Hall,1984] (fig. 5.14) was used as a shear sense criterion in some rocks containing brown or green hornblende. This is a statistical method; many grains must be examined in thin section and certain conditions must be met. Shear sense is indicated by the given inclination of the z-axis as pictured in fig. 5.14a. Because the orientation of the z-axis is being sought in each grain examined, and determination depends on a subtle change of pleichroism as the microscope stage is rotated (fig. 5.14b), care must be taken to count only grains displaying the {110} cleavage and specifically the (010) crystal face. To check for the proper crystallographic orientation, the cleavage should be steeply inclined to the observed face; determine this by moving the microscope stage up and down to check the dip of the cleavage. Also, if instead of the (010) face, the (110) or some other intermediate surface is being observed, then the Z-axis will be parallel with the cleavage and the key variation in pleichroism will not be seen as the stage is rotated.

5.2.2 Problems

In the SVPC, getting reliable data for sense of shear has been hampered by ambiguity in some rock fabrics, especially the granoblastic Type 1 (see sect. 5.1.2). The problem is both quantitative and qualitative: there is an insufficient quantity of

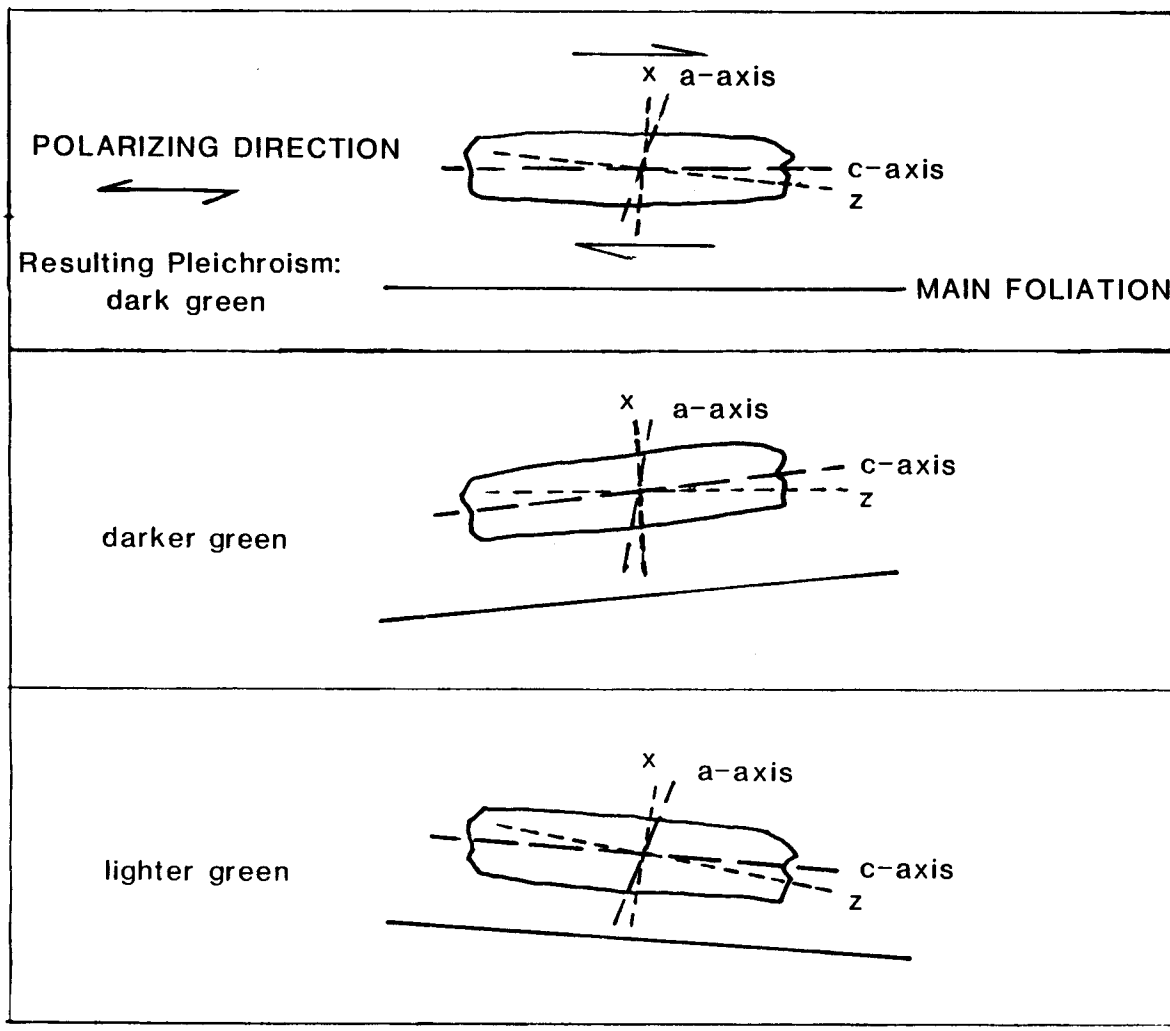

Figure 5.14 Diagram showing the Hall [1984] method of shear sense determination using the hornblende z-axis orientation. Slight rotation of the microscope stage will cause subtle changes in pleochroism which indicates the position of the z-axis. Darkest color is seen when z-axis is parallel with lower polarizing direction. [Modified from Grady, 1990]

shear sense indicators in some samples (e.g., few or no porphyroclasts), and there is insufficient asymmetry in many of the available features with which to ascertain absolute sense of shear (e.g., porphyroclasts with tails that are nearly symmetrical or are stubby and under-developed). It is believed that the two main causes for these problems in samples from the SVPC are high temperature deformation and a high accumulation of strain.

Continued deformation under high temperature conditions can produce fabrics in rocks which are markedly different from their lower-temperature relatives. Rocks that deform under the influence of stress at lower-temperature ($< \sim 600^0$) usually develop fabric asymmetries (e.g. S-C foliation, shear bands, preferred orientation) which are defined by crystallographic anisotropy (e.g. c-axis preferred orientation) or mineral grain shape (e.g. elongate or platy crystal habit). However, more elevated temperatures cause diffusion rates to be high and therefore, recovery is fast. This allows for a significant amount of strain, even at relatively low stresses, with little or no evidence of the quantity or quality of accumulated strain. The resultant fabric displays nearly equant grains with 120^0 grain boundary triple junctions and strain-free (and untwinned) crystals. High-temperature deformation can produce a fabric that does not change with continued strain, and thus the grain shapes do not accurately indicate the amount of rock strain [Tullis et al, 1982]. The presence of clinopyroxene (as a new phase) in some of these problem rocks suggests temperatures of at least lower granulite facies ($\sim 700^0$) [Yardley, 1989]. Elevated temperature levels of $>500^0$ apparently persisted for about 6 Ma in the SVPC from continued magma injection as indicated by the geochronology work of Harper et al [in review].

High accumulation of strain can also be a major factor in causing difficulties in determining sense of shear. With continued shearing, the S-foliation becomes rotated into parallelism with the C-foliation, leaving only one (combined) foliation which is subparallel with the shear zone boundary and which possesses no appreciable asymmetry, and therefore affords no indication of shear sense. Grain size reduction is another result of high strain whereby large porphyroclasts are milled down or recrystallized to smaller, strain-free grains, thereby doing away with asymmetric porphyroclasts as potential sense of shear features.

5.3 SENSE OF SHEAR - RESULTS

Rock samples and field data have been studied from five shear zones in the SVPC (fig. 5.15) in an effort to determine sense of movement in these shear zones. Table 1 (see Appendix) shows the information from the field and from each sample analyzed, listing orientations of foliation plane and lineation, sense of shear, and shear sense criteria used. A confidence level is indicated for the sense of shear determined for each sample, based on the clarity and abundance of sense of shear indicators found in the samples. They are as follows:

1.)poor

- few sense of shear indicators found (only one, two or three per thin section) and these having weak asymmetry.
- sense of shear indicators contradict each other, resulting in statistical ambiguity.

2.)weak

-few sense of shear indicators found (one or two), but with stronger

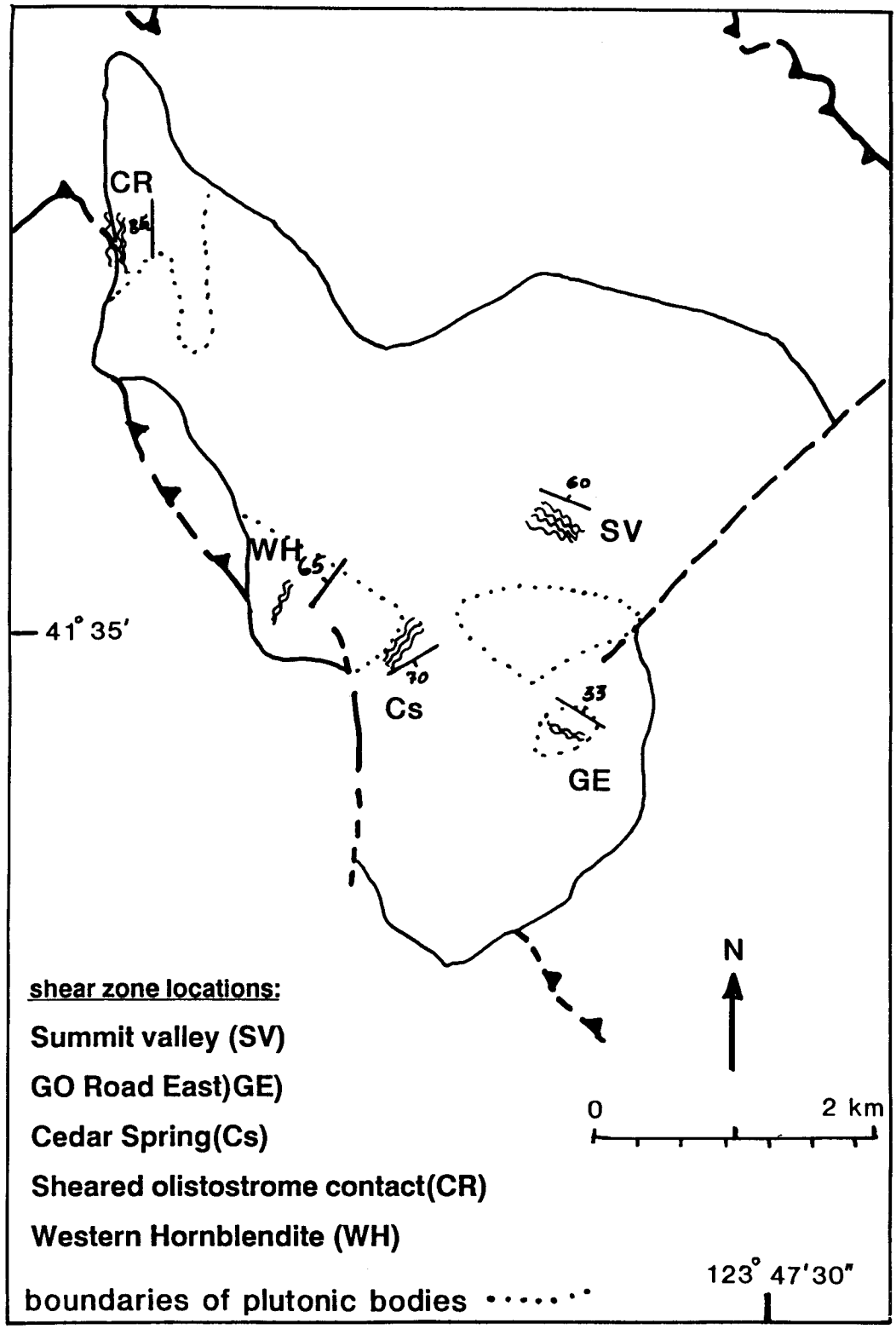

Figure 5.15 Map of Summit Valley Plutonic Complex showing locations of shear zones examined in this study, indicating strike and dip of shear zone walls in each location.

asymmetry.

- statistical ambiguity less, but still not a strong case for a definite direction.

3.)good

- few sense of shear indicators found, but with definite asymmetry.
- some contradiction among shear sense indiators found, but statcially supportive of one direction.

4.)high

- sense of shear indicators are abundant and unambiguous.

The strike and dip of the shear zone boundaries and sense of shear found in each of the five shear zones is as follows (fig. 5.15 for shear zone locations):

1.) Summit Valley (SV): (~290/60N) oblique sinistral strike-slip with a strong component of thrusting towards the west-southwest.

2.) GO-Road east (GE): (~300/33N) low-angle thrust fault towards the northwest.

3.) Western hornblendite (WH): (36/65W) oblique sinistral strike-slip with component of thrust towards the south.

4.) Cedar Springs (CS): (~59/70SE) oblique sinistral strike-slip fault.

5.) Olistostrome contact (CR): (~360/85W) reverse fault, with thrusting towards the northeast.

Orientations of foliation planes, lineations, plus shear sense data were plotted on a Schmidt Equal Area Net (lower hemisphere projection), using the slip linear plot method [pg.259, Marshak and Mitra, 1988] which illustrates the direction and sense of offset, and allows the paleostress field for the deformation to be inferred (see Chap.4.2.1).

Of the five shear zones examined, there is great variation of shearing direction. However, within each shear zone, data are fairly consistent. It may be possible to explain the variation and to determine the most regional shear direction by considering boundaries in the pluton. When deformation is imposed upon a pluton composed of rocks of varying competencies, mechanical behavior may vary locally to accommodate these different properties. Norman [1984] observes that intrusional-contact relationships within the plutonic complex are often sheared, as well as the contacts with the country rocks.

The Western hornblendite (WH) shear zone may have been an intrusive contact between the hornblendite unit (an early intrusional unit) and harzburgite of the Rattlesnake Creek terrain (RCT) of the upper plate. A large (> 10 m^2) fractured block of the harzburgite is present near this small shear zone, but the contact relationship is unclear due to late brittle faulting locally disrupting the units.

The Cedar Spring (CS) shear zone may be a contact between dioritic (later intrusional unit) and the older harzburgite of the upper plate (RCT). Again, the contact relationship in the area is unclear due to late brittle faulting.

The Olistostrome Contact (CR) shear zone is a high-angle thrust fault. The plutonic material has moved down with respect to the country rock (LRO).

The Summit Valley (SV) shear zone is broad in extent and is located in the SVPC in the topographical "saddle" just north of the summit. It is within a large intrusive body of hornblende gabbro that does not locally abut any other plutonic or country rock unit. This shear zone may therefore, be a more reliable indicator of the regional crustal movement direction.

The GO Road East (GE) shear zone is also located in the interior of an intrusive unit away from any contact or boundary. It is located within a leucocratic pyroxene gabbro that is probably one of the later intrusions in the SVPC. The data from this shear zone may also be more representative of the regional deformation.

5.4 PALEOSTRESS FIELD - RESULTS

5.4.1 Equal-area Projection Plots with Slip Linears

The stereonet projection plot (fig. 5.16) of shear zone data from the SVPC shows most of the arrows (slip linears) point towards an area in the western hemisphere of the stereonet projection labeled "σ_1", and away from an area in the eastern hemisphere labeled "σ_3", though several arrows do not fit the pattern. This pattern is a good indication that most of the shear zones were created by the same stress field. High concentrations of high-angle intersections in the M-plane plot (fig. 5.17) are considered along with the slip linear plot to find possible locations of principal stress axes, according to Aleksandrowski [1985]. Locations of possible σ_1, σ_2, and σ_3 axes are indicated on the M-plane plot (fig. 5.17). σ_1 corresponds with the pole to cleavage in the LRO (fig. 5.16). Studies show that slatey cleavage generally forms approximately perpendicular to σ_1 [Suppe, 1985].

There is another pattern in the plot that may have value for interpretation of the direction of deformation. The orientations from the Summit Valley (SV) shear zone (fig.5.16, open circles) and those from the GO Road East (GE) (filled circles) are consistently pointing in a westerly direction, but show a variation in pole

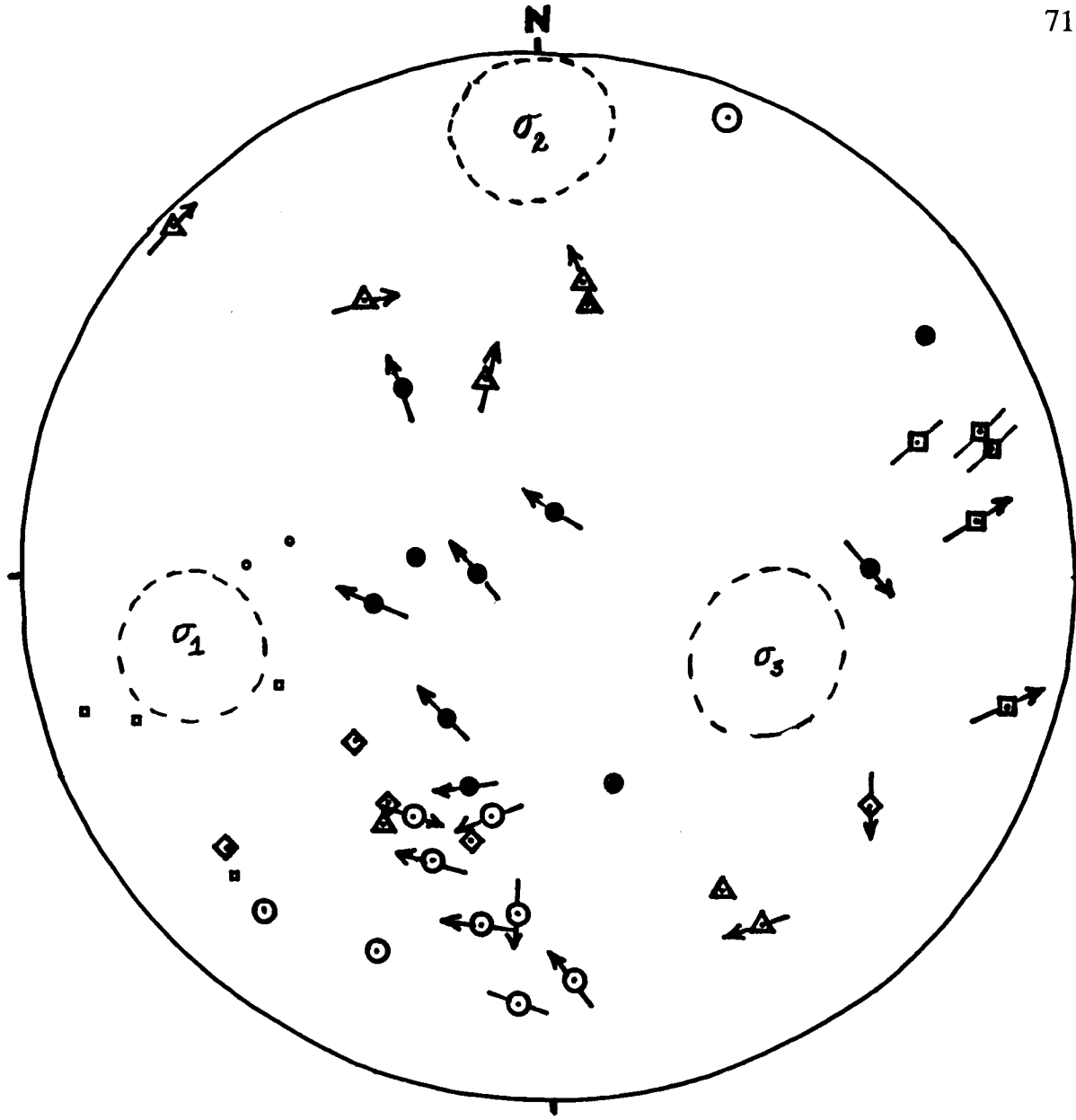

Summit Valley (SV) ⊙

GO Road East (GE) ●

Cedar Spring (CS) ▲

Sheared olistostrome contact (CR) ▣

Western Hornblendite (WH) ◈

Figure 5.16 Stereographic projection of shear zone data from SVPC, using slip linears (see text). Also shown are local foliations, and estimated paleostress axes. Small open circles and squares are cleavage from LRO (see fig. 4.4)

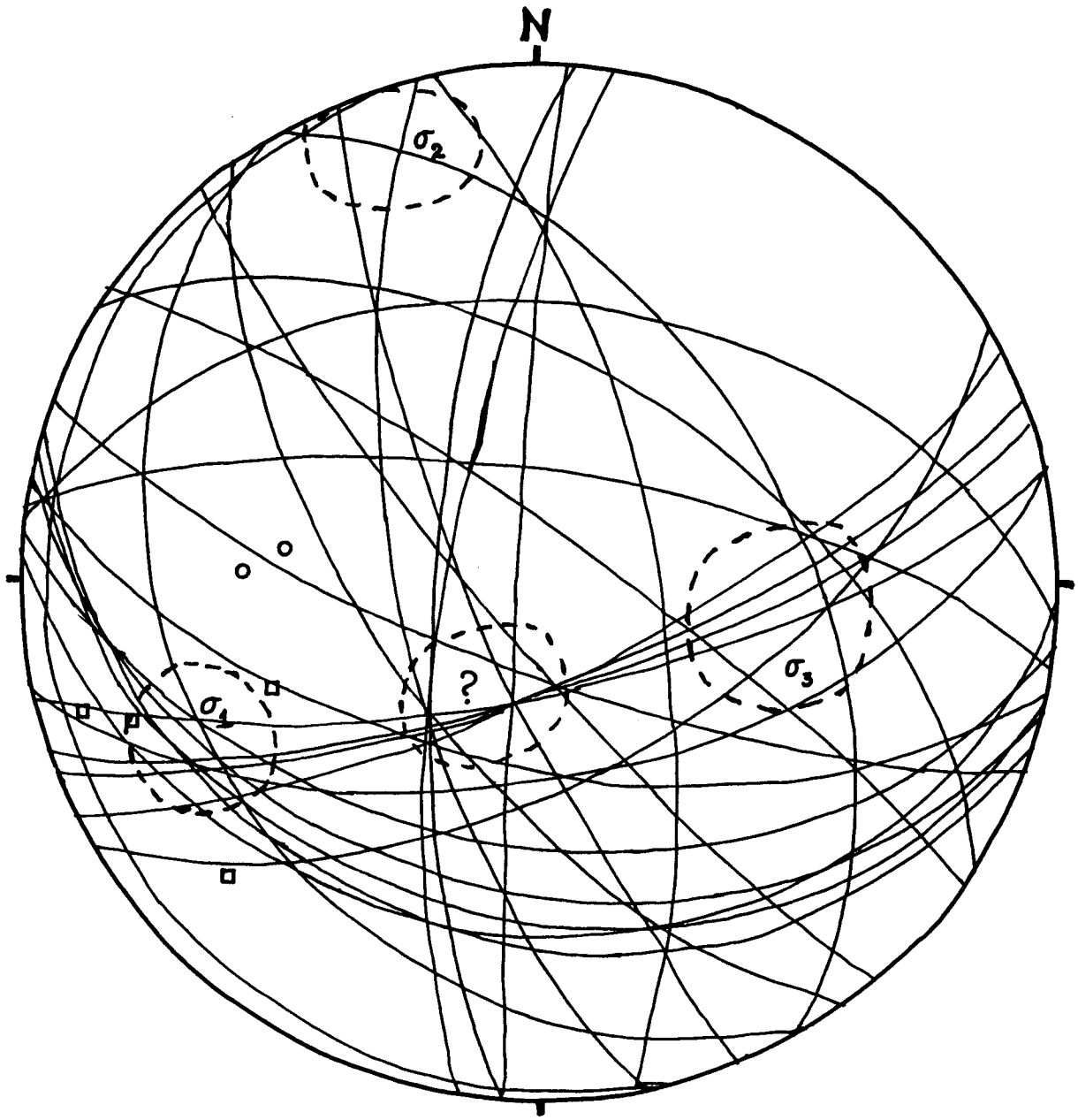

Figure 5.17 Plot of M-planes of shear zone fault data, with areas of high concentrations of high-angle intersections shown. These are possible axes of principal stresses.

orientation along a great circle which is oriented approximately north-south. There is also a variation in the direction in which the slip linears point from west to northwest. This variation in direction suggests two possibilities: first, that σ_1 and σ_2 varied with time, perhaps switching with each other: and second, that there was a progressive change in shearing direction with time from the direction indicated by the higher temperature SV shear zone rocks (fig. 5.16, open circles) to the lower temperature GE shear zone rocks (filled circles).

5.4.2. Rotation of Data to Paleohorizontal

The structural data from shear zones in the SVPC was rotated on a stereonet projection (as described thoroughly in Chap.4.2.2) to remove dip from post-emplacement folding.

The geometry of faulting after rotation of the data is in a configuration suggesting predominantly normal faulting. Most slip linears (direction of movement of hanging wall) are pointing towards the middle of the plot (fig. 5.18) indicating downward movement of the hanging wall. Overall, the movement of material in the upper plate is still from east to west as indicated by the abundance of slip linears pointing westward, but the fault kinematics are changed from reverse faulting to normal faulting. Discussion of this will be included in Chap.8.

5.4.3 Stress Analyses

Two computer programs were used with structural data from shear zones to get estimates for the orientations of principal stresses in the paleostress field in the SVPC. The work of Reches [1987] and Bott [1959] was the basis of one of the

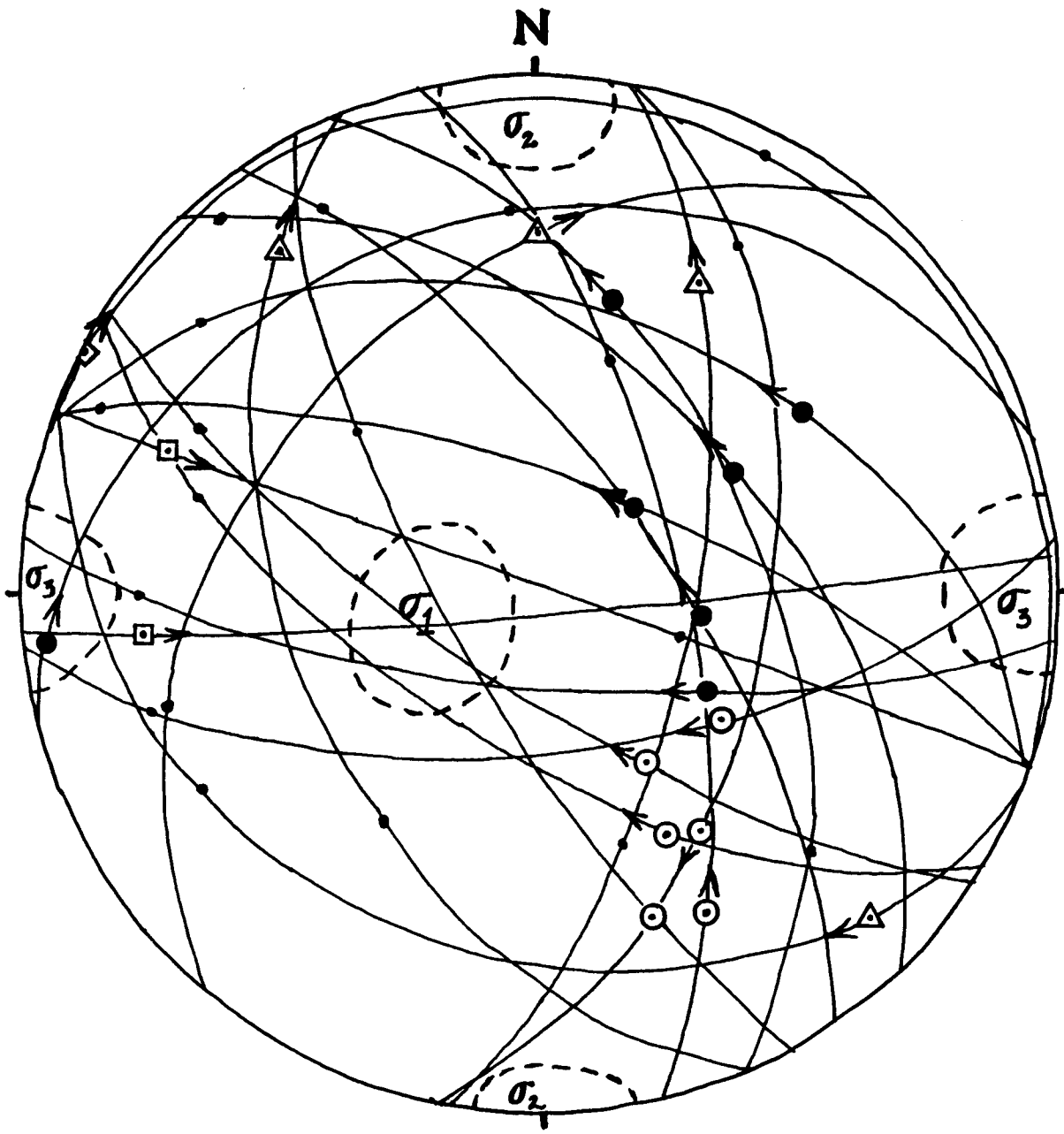

Figure 5.18 Stereographic projection of rotated shear zone data from SVPC also showing M-planes. (Foliations and stress axes are also rotated.)

programs which provides the user with best fit estimates of the orientation of the axes of principal stresses and values for the magnitudes of stresses from the given fault data. The other, called ROMSA, was written by Lisle [1988] and outputs the orientation of a probable σ_3 from input σ_1 values, comparing both to the fault data set. Please see Chap. 4.2.3 for a more thorough description of these analysis methods.

Results. The orientations of axes of principal stresses recorded from both the Reches and the Lisle stress analysis methods were plotted on an equal area stereogram (fig. 5.19). These orientations were then rotated to take out dip due to late folding and return to the paleohorizontal (see Chap.4.2.2).

The final (rotated) σ_1 orientations derived from the two analysis methods are about 50^0 away from each other (fig. 5.19), with the Lisle σ_1 nearly vertical and the Reches σ_1 trending 50^0 and plunging 35^0 to the northeast. The Lisle orientation for σ_3 is nearly horizontal trending 250^0 and the Reches σ_3 is plunging 43^0 towards 275^0. In fact, the σ_1 orientation for one set is about 50^0 away from the σ_3 orientation for the other set. However, σ_2 orientations from both methods are fairly coincident (within 20^0 of each other), nearly horizontal, and trending at about 160^0.

Reches' method calculates the overall stress ratio of the fault set where

$$\text{Stress Ratio (Phi)} = (\text{sigma 2} - \text{sigma 3}) / (\text{sigma 1} - \text{sigma 3}).$$

The data set for shear zones in the SVPC showed a stress ratio that was generally $>.44$ (with the highest value being .75). This intermediate value for the stress ratio indicates that the principal stresses during shearing were equally different in

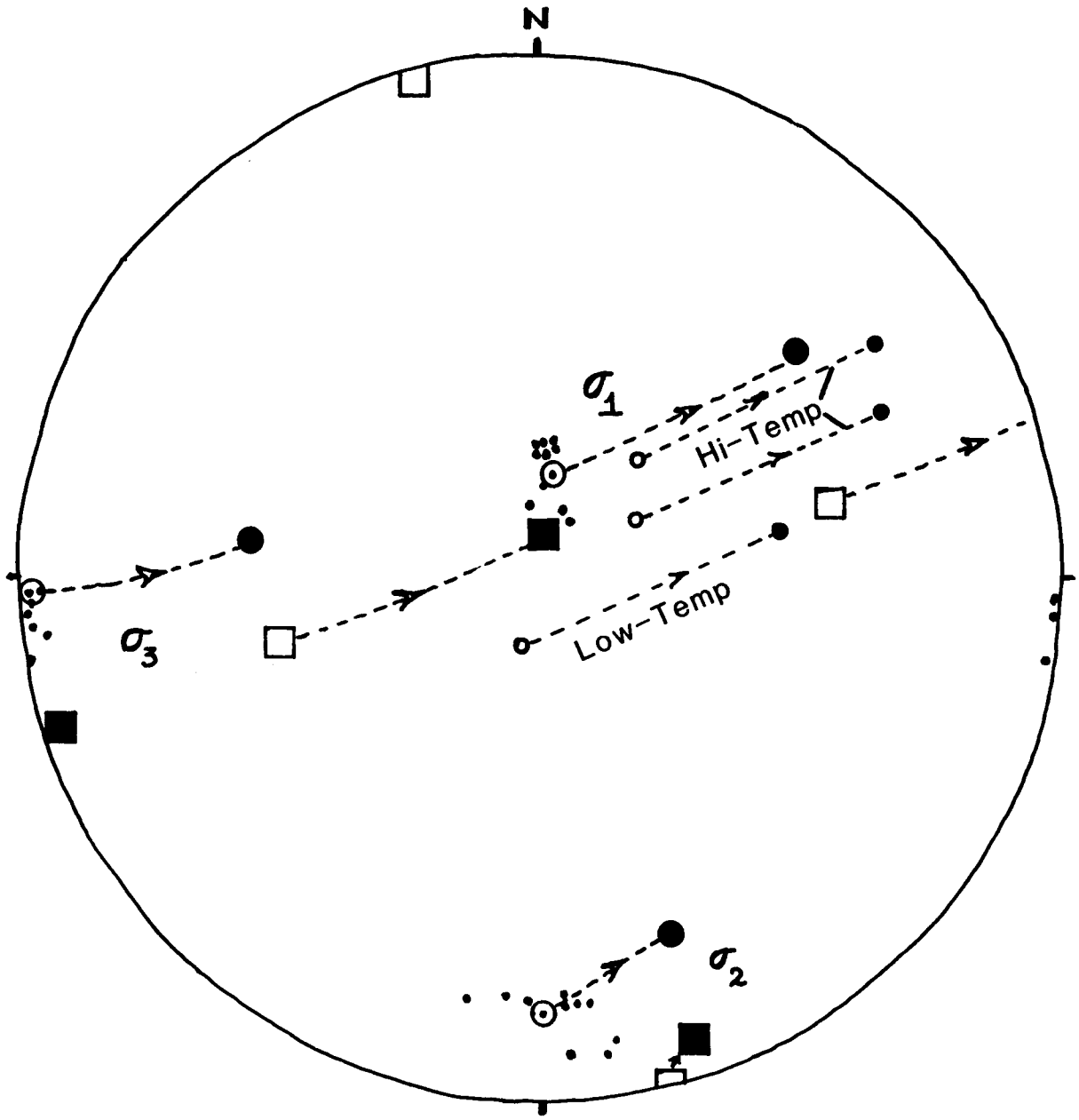

Figure 5.19 Paleostress Analysis of shear zone data. Circles are data from Reches' method; squares are from Lisle's method (ROMSA). Rotation paths for paleohorizontal shown with dotted lines. Hi-temp and low-temp shear zones also shown.

magnitude from each other; no two principal stresses were similar in value to each other.

High-temperature and Low-temperature Zones. To see what Reches' method would reveal about a possible change in shearing direction as the plutonic complex cooled (see Chap.4.3 History of Deformation), shear zone data was separated into two groups: those samples which exhibited high-temperature mineral assemblages during shearing and those with lower-temperature assemblages during shearing. (A minimum of five data are required in each input file for Reches' method.) These data files were run through the analysis program separately and the results were plotted along with the other stress analysis data (fig. 5.19; only the σ_1 axes were plotted. The σ_2 and $\sigma_3$axes are in the same locations as those from the other data). It is interesting to note that the positions of theσ_1 axes are different from each other, about 350 apart. The stress ratios (Phi) are very different also, with the high-temperature shear zones reflecting a mid-level value averaging 0.45, and the low-temperature shear zones having high values for Phi, approximately 0.89 (a mid-level value for Phi indicates that the principal stresses are about equally different in value from each other, while a higher value indicates that σ_1 and $\sigma_2$are very similar to each other in magnitude. Similar values for any two principal stress axes might suggest the possibility of a changing tectonic regime. However, it could be a local phenomenon, or an inter-seismic stress variation. It is also difficult to say defensibly that the difference in position of the twoσ_1 axes has any significance; the two groups of shear zones might still have been caused by the same stress field at the same time.

CHAPTER 6. DIKES

6.1 INTRODUCTION

Dikes are sheet-like intrusions which are discordant with layering or foliation in the country rock. Dikes occupy fractures that are generally assumed to be oriented approximately perpendicular to to the direction of the σ_3 axis [e.g., Suppe, 1985] except where they intrude previously existing planes of weakness. With this assumption, dikes can be used to infer σ_3. Coupled with data from fracture sets, it may be possible to infer the principal axes of stress in the ambient stress field at the time of formation of contemporaneous dikes and fractures in the SVPC. Dike cusps, steps, and segments (fig. 6.1) have been shown to be useful kinematic indicators with their long dimension parallel to the direction of propogation, which is also approximately parallel with the σ_2 axis [Pollard, 1988].

Dike orientations in the SVPC were recorded for the purpose of determining the stress field at the time of intrusion. Dike orientations were also collected at two outcrops outside the plutonic complex to the west: in the adjacent Lems Ridge Olistostrome (LRO) and along the olistostrome-pluton contact. These dikes are believed to be part of the same dike swarm which permeates the SVPC and all the surrounding country rock, in both the lower and the upper plate [Norman, 1984; Ohr, 1987]. Spectacular roadcut outcrops of these dikes in the LRO (fig. 6.2) afforded collection of a sizeable data set, with cross-cutting relationships exposed, as well as a variety of accessory features (cusps, steps, etc.).

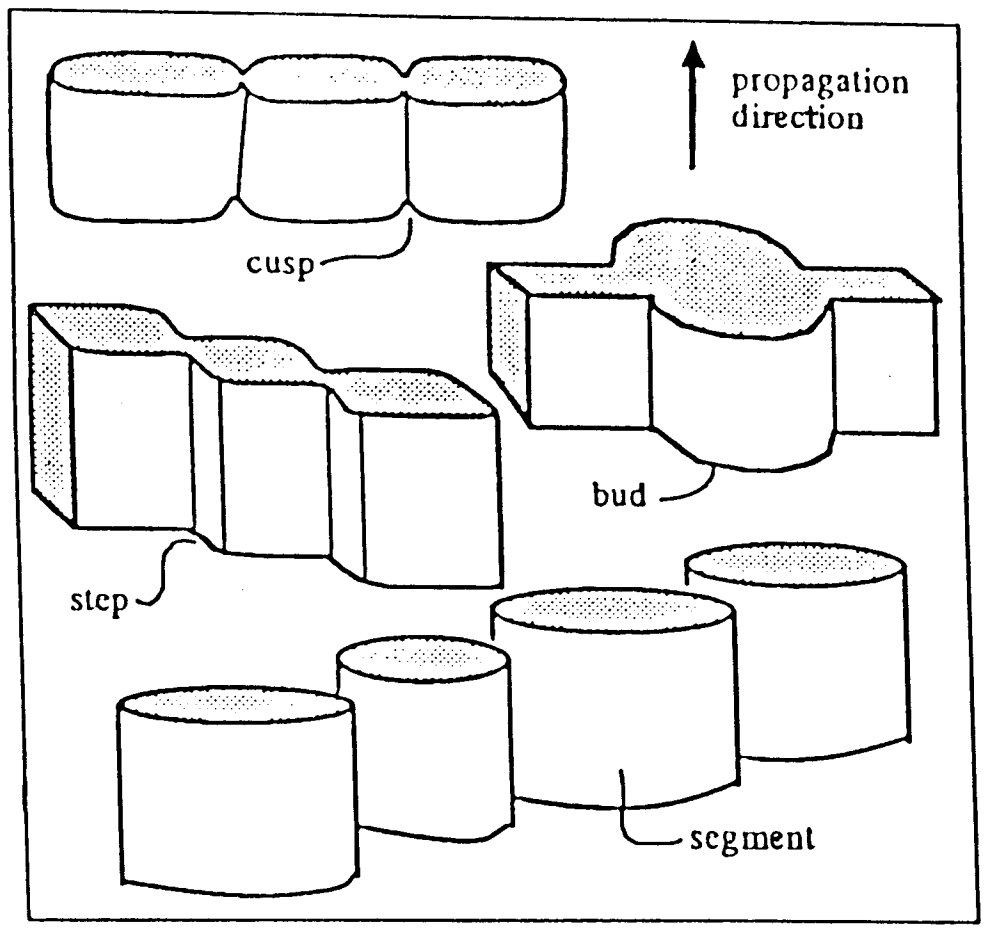

Figure 6.1 Schematic illustration of the common small-scale structures found along outcrops of mafic dikes, insluding cusps, steps, buds, and echelon segments. The principal propagation direction is indicated. [From Pollard, 1988]

Figure 6.2 Outcrop of dikes in the LRO along the GO Road.

6.2 DESCRIPTION.

Most commonly seen in the SVPC are fine-grained microdiorite dikes. Hornblende-plagioclase pegmatites and quartz-bearing pegmatites are also seen, but only the microdiorites were considered in this study for their kinematic value; the microdiorites are generally flat-walled and ubiquitous, whereas the pegmatites tend to be asymmetric and are less commonly seen in outcrop.

The microdiorite dikes range in width from 6cm to 60cm. They contain hornblende, plagioclase, and a trace of apatite and opaques. They are in general, more altered than the plutonic rocks, with plagioclase altered to sericite and clinozoisite, and hornblende exhibiting incipient alteration to chlorite and actinolite. However, in most cases, igneous textures are preserved [Norman, 1984]. Lineations and foliations are sometimes present, though determination of the origin (magmatic flow or shearing) is not always possible. Plastic shearing is suggested by one dike set seen in outcrop along the GO Road (fig. 6.3) in which an oblique foliation visible in one dike might have been created by the same stress field that caused the offset of the other dike.

6.3 CROSS-CUTTING RELATIONSHIPS.

The microdiorites were the last intrusive pulse in the SVPC and are found cross-cutting all types of rocks in the plutonic complex, including other dikes [Norman, 1984]. Cross-cutting relationships were noted in the field where dike orientations were measured so that the data could be analysed for a change in the stress field with time (see fig. 6.5).

Figure 6.3 Mafic dike in the SVPC cross-cut by a younger dike. Sheared offset of older dike is sympathetic with oblique foliation in younger dike.

Figure 6.3 Mafic dike in the SVPC cross-cut by a younger dike. Sheared offset of older dike is sympathetic with oblique foliation in younger dike.

6.4 METHODS.

Strikes and dips of dike walls were measured in three areas: 1) inside the SVPC, 2) at the plutonic contact between the SVPC and the Lems Ridge Olistostrome, and 3) in the adjacent Lems Ridge Olistostrome. The trend and plunge of the long dimension of cusps, steps, and segments were measured, at the Lems Ridge Olistostrome localities. Poles to the dike planes were plotted on Schmidt equal area lower hemisphere projection, and cusps, steps, and segments were plotted as linear features. A technique which provides a more accurate indicator of the true extension direction uses displaced offsets on opposite walls of a dike [Bussell, 1989]. This method requires meticulous geometric construction, good three-dimensional exposure, and care in choosing useable offsets. Ideally, in a unchanging stress field and if the dikes were intruded perpendicular to σ_3 , then all the poles-to-dikes should cluster about one point (σ_3); and cusps, steps, corrugations, and segments would cluster about another point, 90^0 away (σ_2).

6.5 RESULTS.

The orientation of the extension direction is plotted on an equal area net the same as a lineation. Cross-cutting relationships and relative ages are indicated where observed in the field. There are three major patterns apparent in the stereographic projection plots of dikes within and around the SVPC (fig. 6.4): (1) in the SVPC plot, there is a distribution of the poles-to-dikes along a great circle, (2) the LRO plot shows poles-to-dikes varying along a different great circle, and (3) the cusps and steps (σ_2) are varying between two orientations.

The equal area (Schmidt net) projection plot for dikes within the SVPC and at the

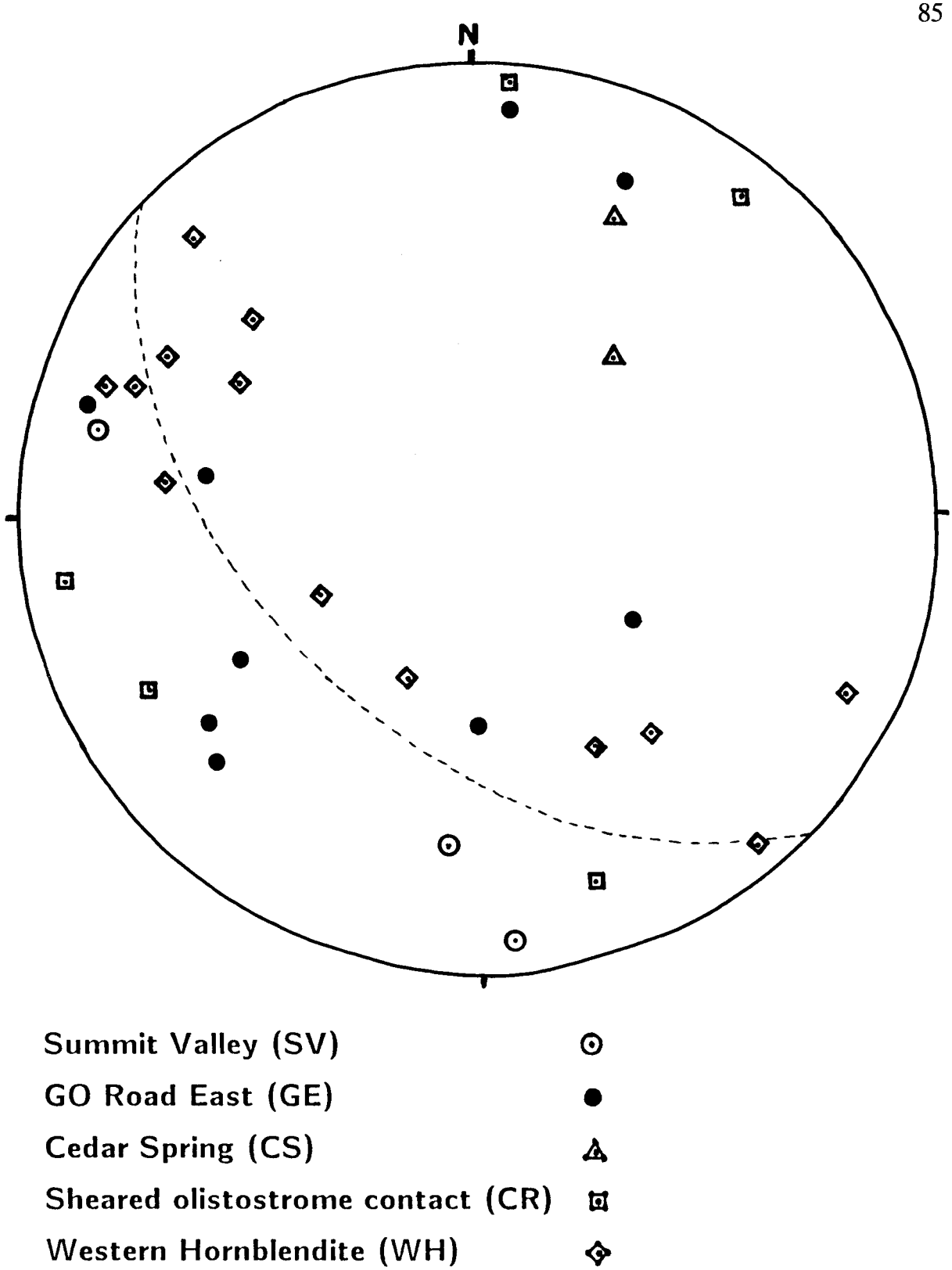

Figure 6.4 Stereographic projection of dikes within the SVPC.

pluton-olistostrome contact shows poles-to-dikes clustering loosely along a great circle striking 314^0 and dipping about 50^0 to the southwest (see trace of great circle, fig. 6.4). There is a small cluster of poles-to-dikes trending about 25^0 and plunging 25^0 NNE. The dikes in the LRO (fig. 6.5) are generally steeply dipping and strike consistently WNW; their poles-to-dikes trend Southwest varying from shallow to steeply plunging, with some poles plotting near the primitive circle in the NNE (see trace of great circle, fig. 6.5). The linear features (cusps,steps,etc.) are divided between two areas: one set trends WNW at about 280^0 and spread across the net along the 90^0 (vertical) great circle, and the other set plot in the same area as the poles-to-dikes near the primitive circle in the NNE. The dilation (extension) direction of dikes in the LRO (fig. 6.5) [R.J. Alexander, unpublished field data] are grouped around a point which trends toward the Southwest and plunges moderately steeply (about 60^0). The cross-cutting relationships and relative ages of dikes show no definite sequential pattern; there are almost equal numbers of older and younger dikes in each of the two clusters of poles-to-dikes (see fig. 6.5, "O" and "Y" for "older" and "younger").

6.5.1 Paleostress Field

The best approximation of σ_3 from the dike data comes from the true extension directions which plot inside the cluster of poles-to-dikes from both the SVPC and the LRO (fig. 6.5). σ_2 is thought to be parallel with the direction of propogation and with the long dimension of cusps, nodes, and bends [Pollard, 1988]. These features (those from both this study and from Alexander, unpublished field data) plot in two locations which are similar to the poles-to-dikes (see circles with dot and circles with "S", fig.6.5). The concentration of these features in the NNE seems to

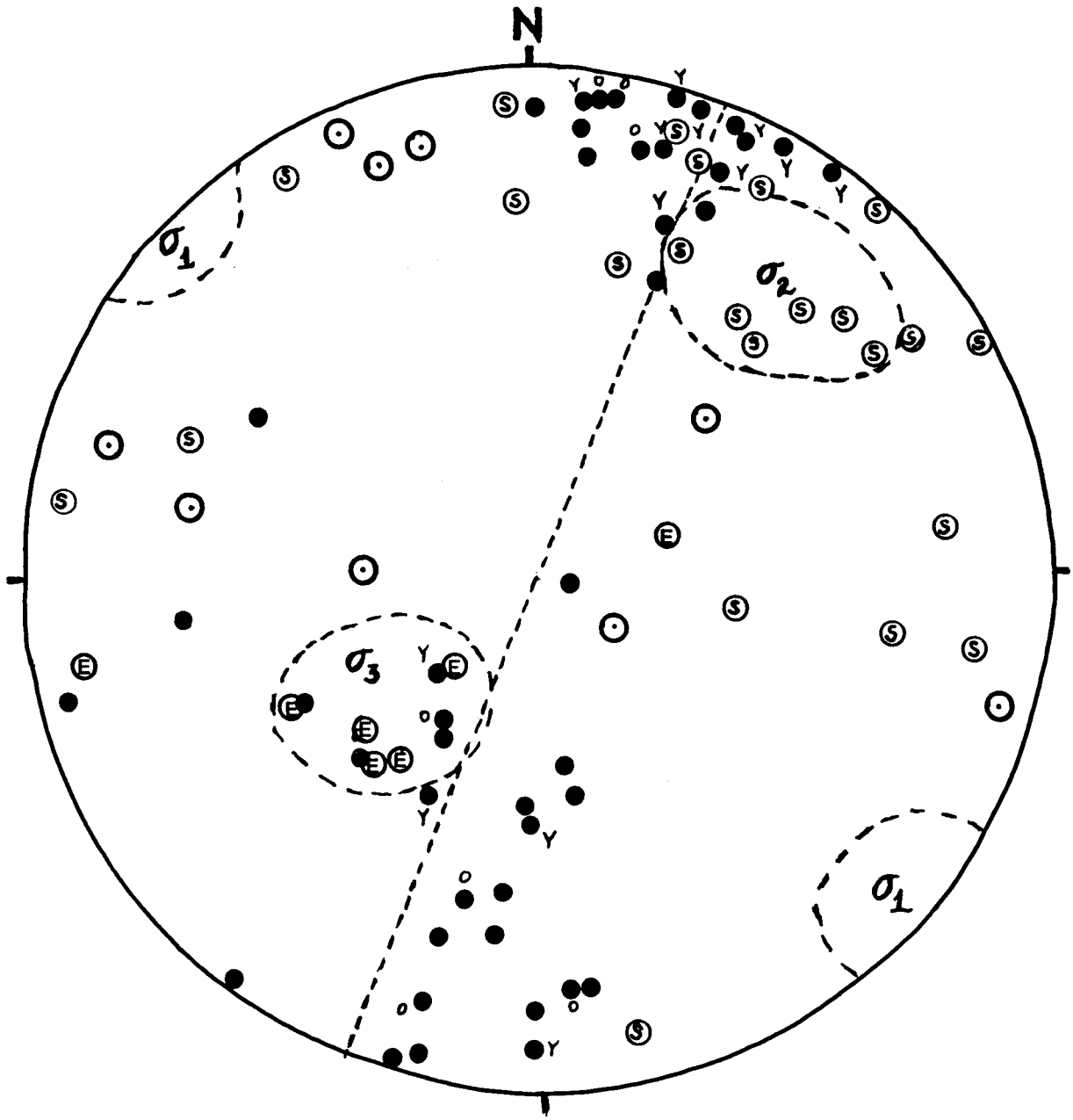

Figure 6.5 Stereographic projection of dikes in the LRO. (Circles with "E" inside are true extension direction and circles with "S" are steps [from R.J.Alexander, unpublished field data]).

be a good indication of σ_2 , but there is the suggestion that σ_2 and σ_3 may have been flipping positions with each other. Fig. 6.6 shows the proposed stress field from the dike data rotated to paleohorizontal (see Chap. 4.2.2 for explanation). The paleostress field information from the dikes is compared to that from the shear zones and veins in Chap.8 - Discussion.

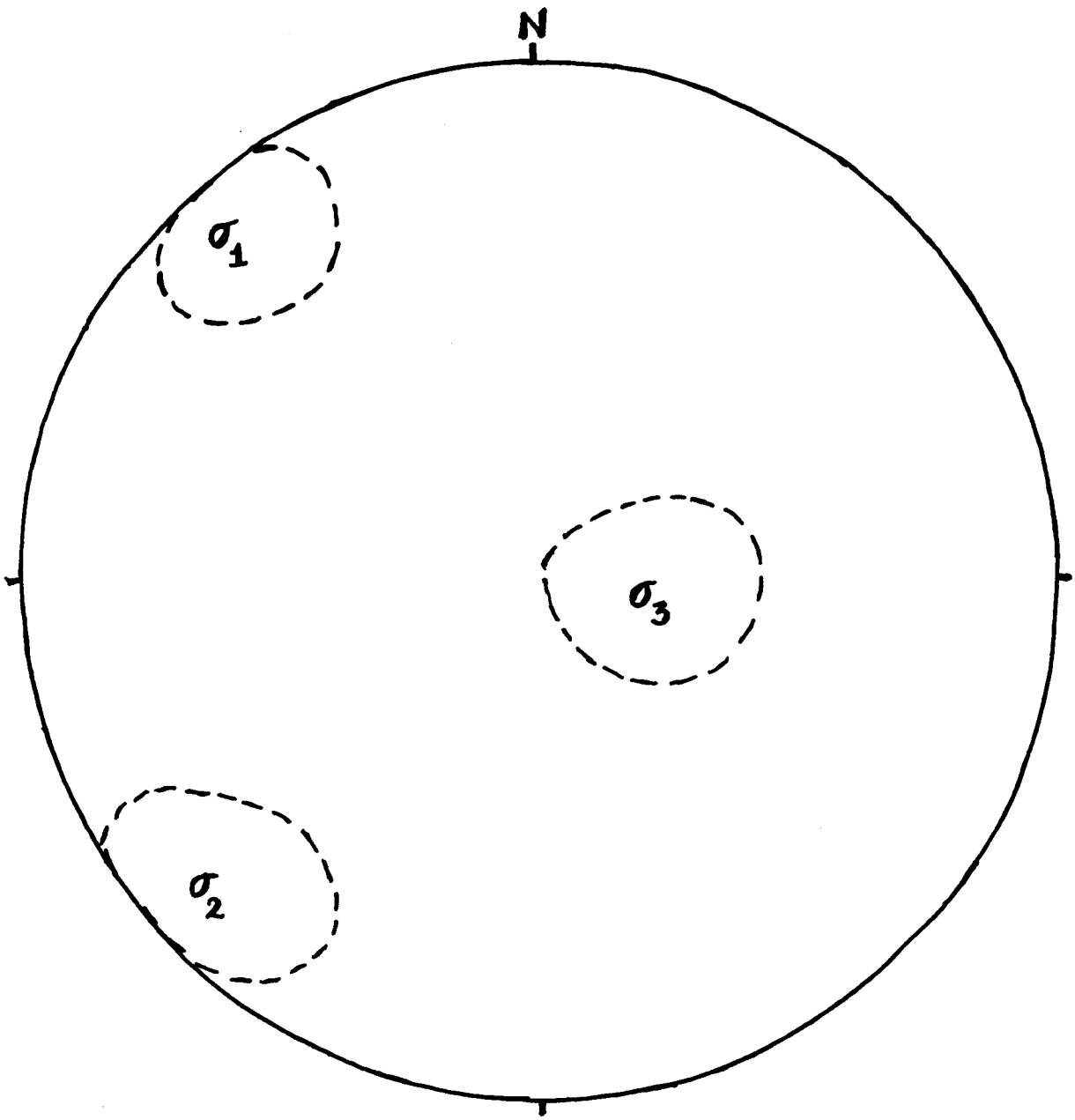

Figure 6.6 Orientation of stress field from dike data after rotation to paleohorizontal.

CHAPTER 7. VEINS

7.1 INTRODUCTION

Fractures are useful in determining the geologic stress field at the time of deformation. Fractures (including joints and small faults) are a record of small strains, and using stereonet plots [see Chap.4.2.1; Marshak and Mitra, 1988], the axes of principal stresses can often be inferred. The fractures studied in the SVPC were only those which had been filled by veins of epidote, prehnite, or serpentine. It is assumed that they were precipitated from circulating hydrothermal fluids during cooling of the SVPC, in order to constrain the investigation to fractures which occurred as close to the emplacement of the plutonic complex as possible.

Veins are considered to have formed late in the cooling history of the plutonic complex, when relatively low temperature deformation ($<400^0$) was dominant; they cross-cut other structures including shear zones and dikes. If there was a change in the stress field through time, it might manifest as a change in the strain recorded by the earlier ductile shear zones as compared to the brittle fractures.

7.2 DESCRIPTION

The fractures considered in this study were usually filled with minerals distinct from those in the host rock: a white mineral (usually prehnite, figs. 7.1 and 7.2) and epidote, except in the case of serpentine fibers found on the serpentinized harzburgite country rock (fig. 7.3). The thickness of most veins measured is about 2-5mm. Many veins that were observed have slip fibers and steps; assuming that the

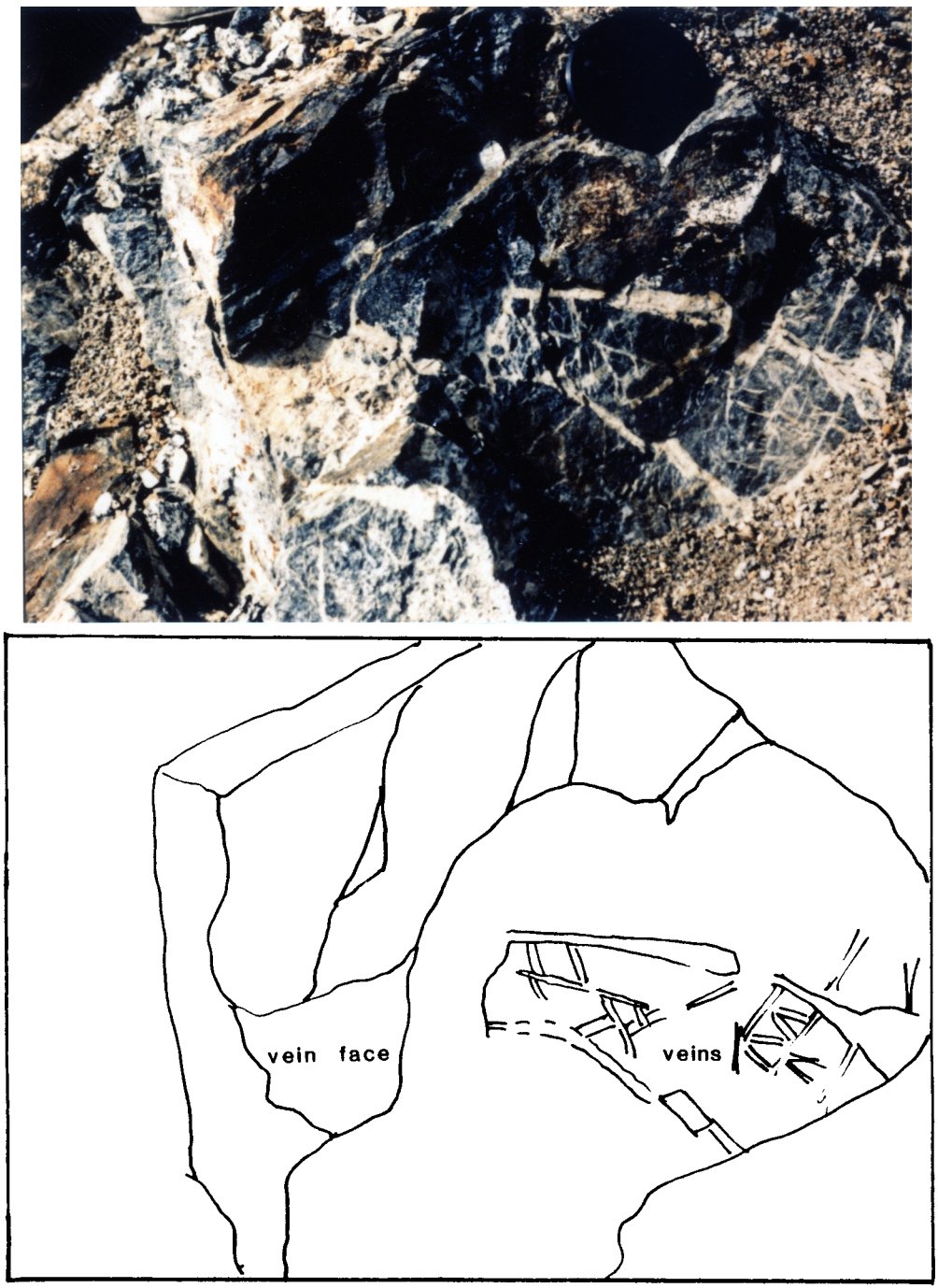

Figure 7.1 Fractured rock with white veins, probably filled with prehnite. Cartoon below is for clarification of photo. (Long edge of view is about 0.6m long)

Figure 7.2 Micrograph of prehnite vein with crossed-polars. (Field of view is about 1.5mm long.

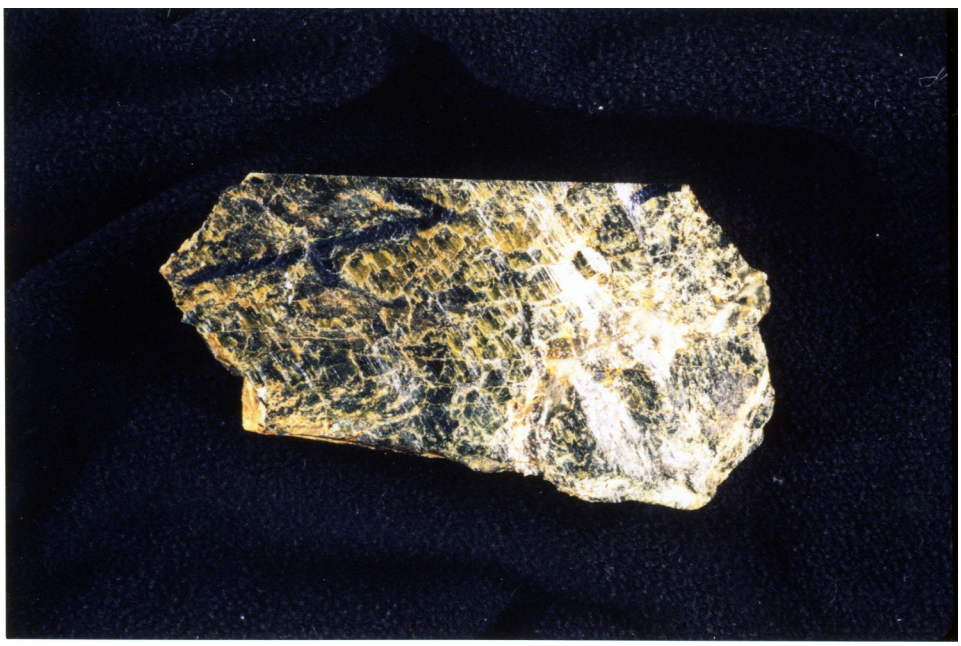

Figure 7.3 Rock sample with serpentine fibrous slickensides. Long dimension of rock is 110mm.

steps and fibers were created by crack-seal accumulation of minerals from migrating fluids during increments of strain, they should provide the direction and sense of slip [Petit,1987].

7.3 METHODS.

Orientations of veins were measured in the field. Where present, slickenstriae orientations and sense of shear were recorded.

Data was plotted using the Schmidt equal area net (lower hemisphere projection). Where sense of shear was known, an arrow is drawn through the pole-to-plane showing the direction of movement of the hanging wall of the fault, according to the slip linear plot method described by Marshak and Mitra [1988, p.259]. Where only relative slip direction is known, only a line is drawn through the pole-to-plane. [For a more detailed explaination of the technique, see Chap. 4.2.1] In the ideal case, the plotted data from a fault set that was created in the same stress field will have all the slip linears pointing towards one area (σ_1), and away from another area (σ_3).

7.4 RESULTS.

7.4.1 Equal-area Projection Plots with Slip Vectors

Several different equal area projections were made for the vein data from the SVPC with different groupings of the data, in an attempt to discern definable patterns for interpretation of the results. Data were grouped by vein mineral type, and then by location, but since no distinct patterns emerged from the plots, all of the veins are shown together in fig. 7.4. A separate plot was made for all veins which displayed

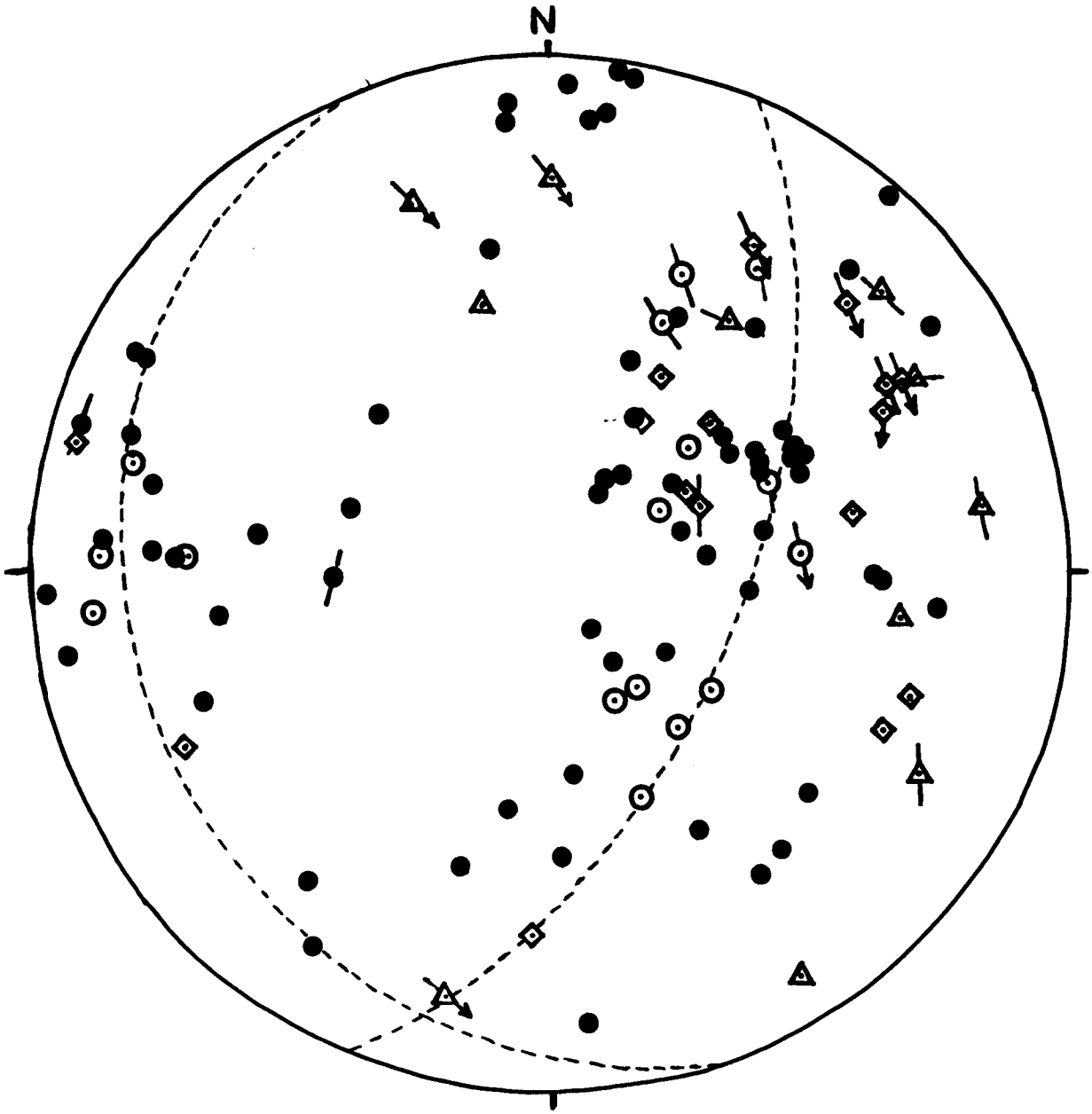

Figure 7.4 Stereographic projection of veins in the SVPC. Veins are plotted as pole-to-plane with slip linear arrow (see text).

slickenstriae which indicated sense of slip, using the slip linear method and M-planes for use in determination of the paleostress field (fig. 7.5).

In the vein plot (fig. 7.4), two major clusters are exhibited in the data, but there is a great deal of scatter. Poles-to-planes are distributed around two great circles: one striking 23^0 and dipping about 60^0 to the east, and the other, striking 340^0 and dipping about 20^0 to the west (see traces of great circles on fig. 7.4). These two great circles are about 90^0 apart.

The plot of slip linears and M-planes (fig. 7.5) shows a grouping of pole-to-veins clustered in the northeast quadrant of the stereographic projection. Slip linears are pointing in various directions without any discernable pattern. There is not enough data to give a definitive indication of the principal axes of stress.

7.4.2 Rotation of Data to Paleohorizontal

Vein orientations were rotated back to paleohorizontal (see Chap.4.2.2) to remove dip from late regional folding. In general, the poles-to-veins plot near the primitive circle, with slip linears parallel to the primitive circle indicating strike-slip faults with vertical to sub vertical fault planes. The small data set presents a scant pattern from which to deduce the stress field axes with the slip linear method, but a stress field orientation has been attempted here nevertheless. The new configuration of the vein data (fig. 7.6) suggests a σ_1 that is almost vertical, σ_3 that is nearly horizontal and trends approximately 165^0. σ_2 must be 90^0 from the other two axes; it is almost horizontal and trends approximately 75^0.

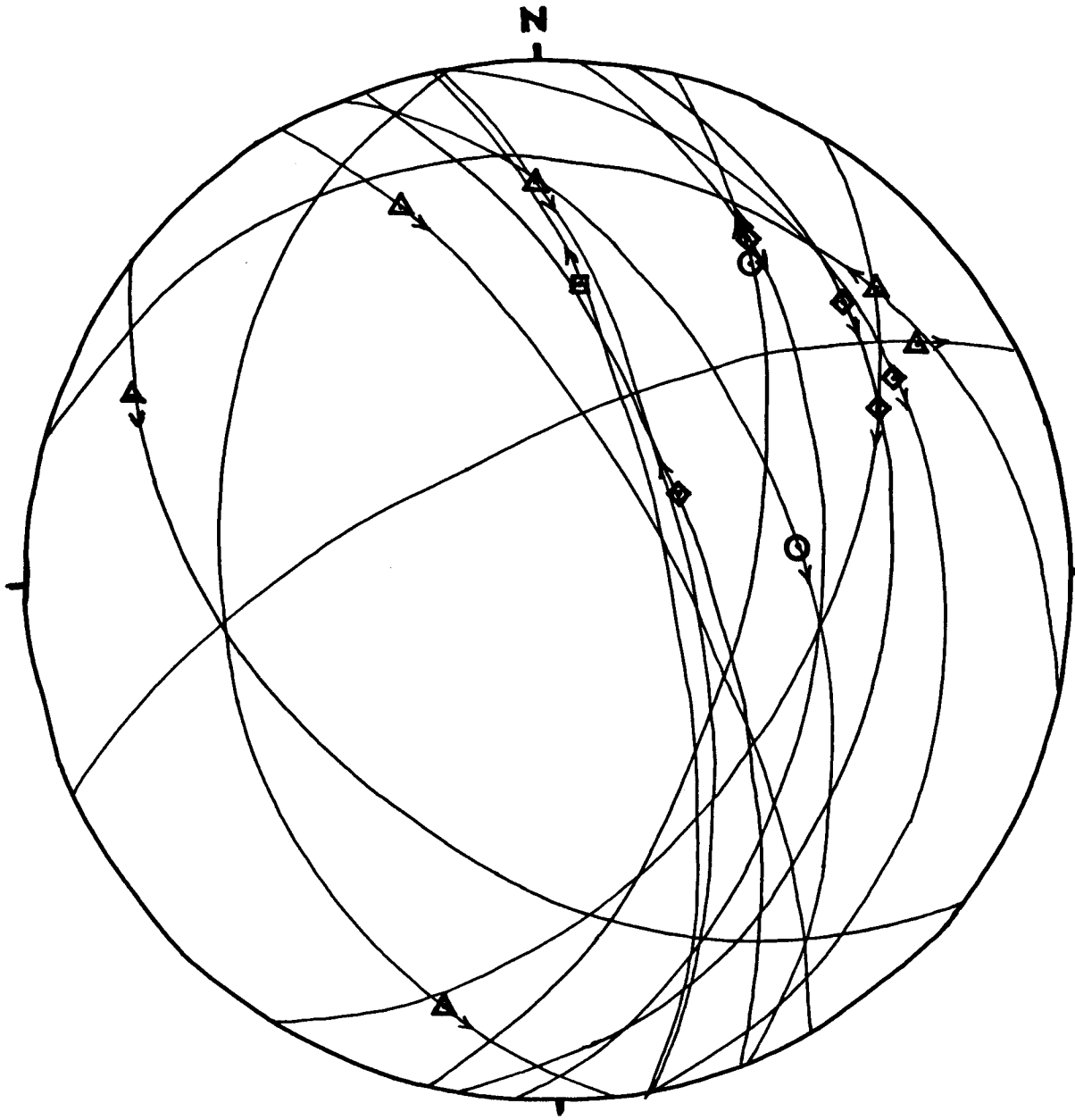

Figure 7.5 Stereographic projection of veins with slickenstriae and known slip direction. The M-plane is also shown.

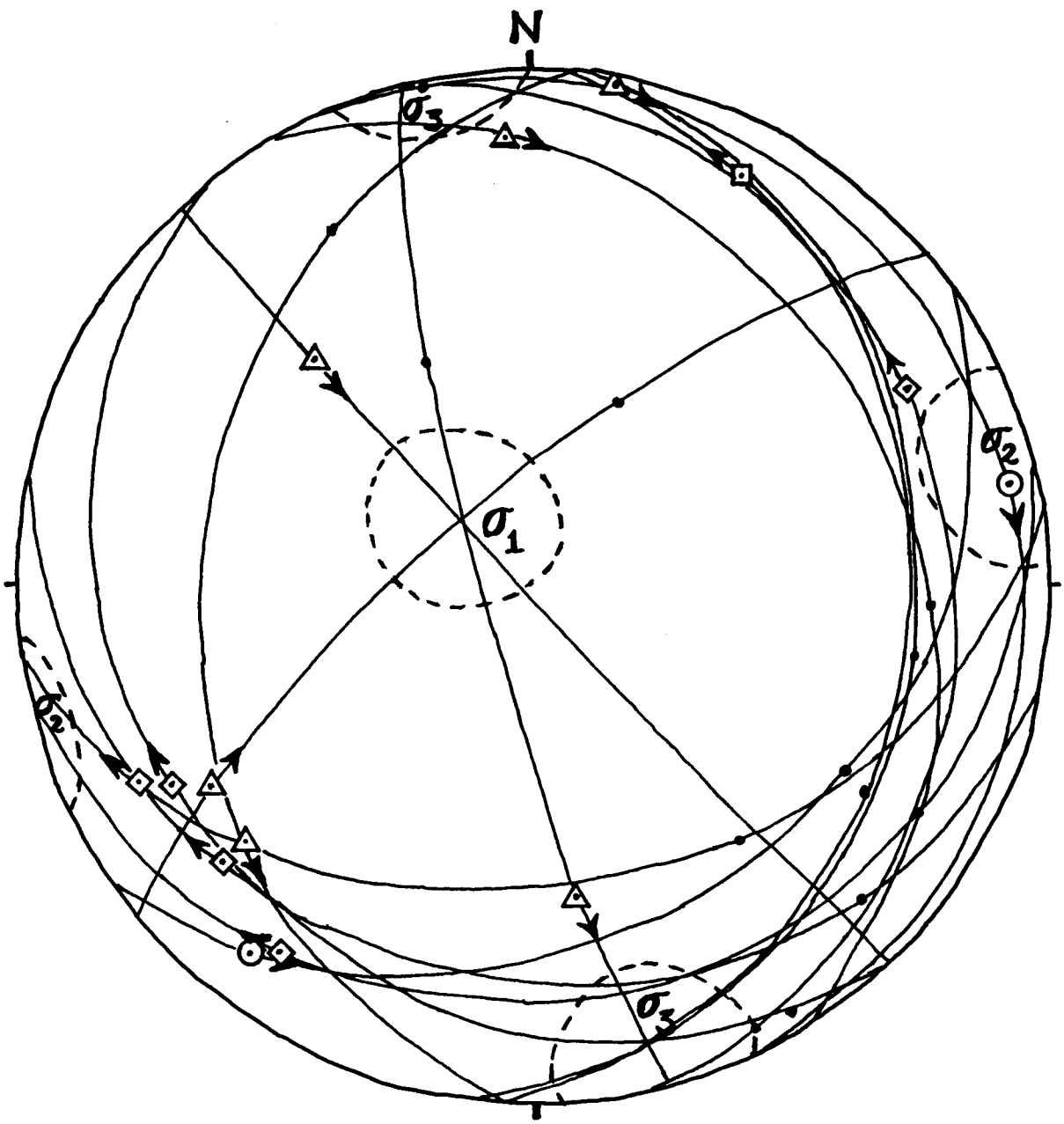

Figure 7.6 Stereographic projection of vein data after rotation to paleohorizontal.

7.4.3 Veins: Stress Analyses

To try to determine the axes of principal stresses at the time of deformation, two computer programs were employed to analyze the vein orientation information, using only the vein data which indicated sense of shear. The method described by Reches [1987] & Bott [1959] determines the "best fit" stress field for the imput data and evaluates the magnitude of stresses. The Lisle [1988] method evaluates possible σ_3 orientations from a range of input σ_1 orientations and calculates the percentage of probability of a good match of each σ_1 with the given fault set. (See Chap.4.2.3 for more thorough description.)

Results. The orientations of axes of principal stresses recorded from both the Reches & Bott and the Lisle stress analysis methods were plotted on an equal area lower hemisphere stereonet projection (fig. 7.7). These orientations were then rotated to take out dip due to late folding and return to the paleohorizontal (see above: Rotation of Data to Paleohorizontal).

The orientations for the axes of principal stresses determined by the two computer analyses are fairly coincident, all pairs being within 20^0 of each other. The positions of the axes are similar to those from the shear zone data (fig. 5.20), except that the positions of σ_2 and σ_3 are switched in the two cases.

The value for the stress ratio (Phi)

Stress Ratio (Phi) = (sigma 2 - sigma 3) / (sigma 1 - sigma 3)

is <0.42, actually averaging 0.22. The low value of this ratio indicates that the magnitudes of the principal stresses σ_2 and σ_3 are close in value. This is seen in tectonic domains where the style of faulting changes because the values of σ_2 and

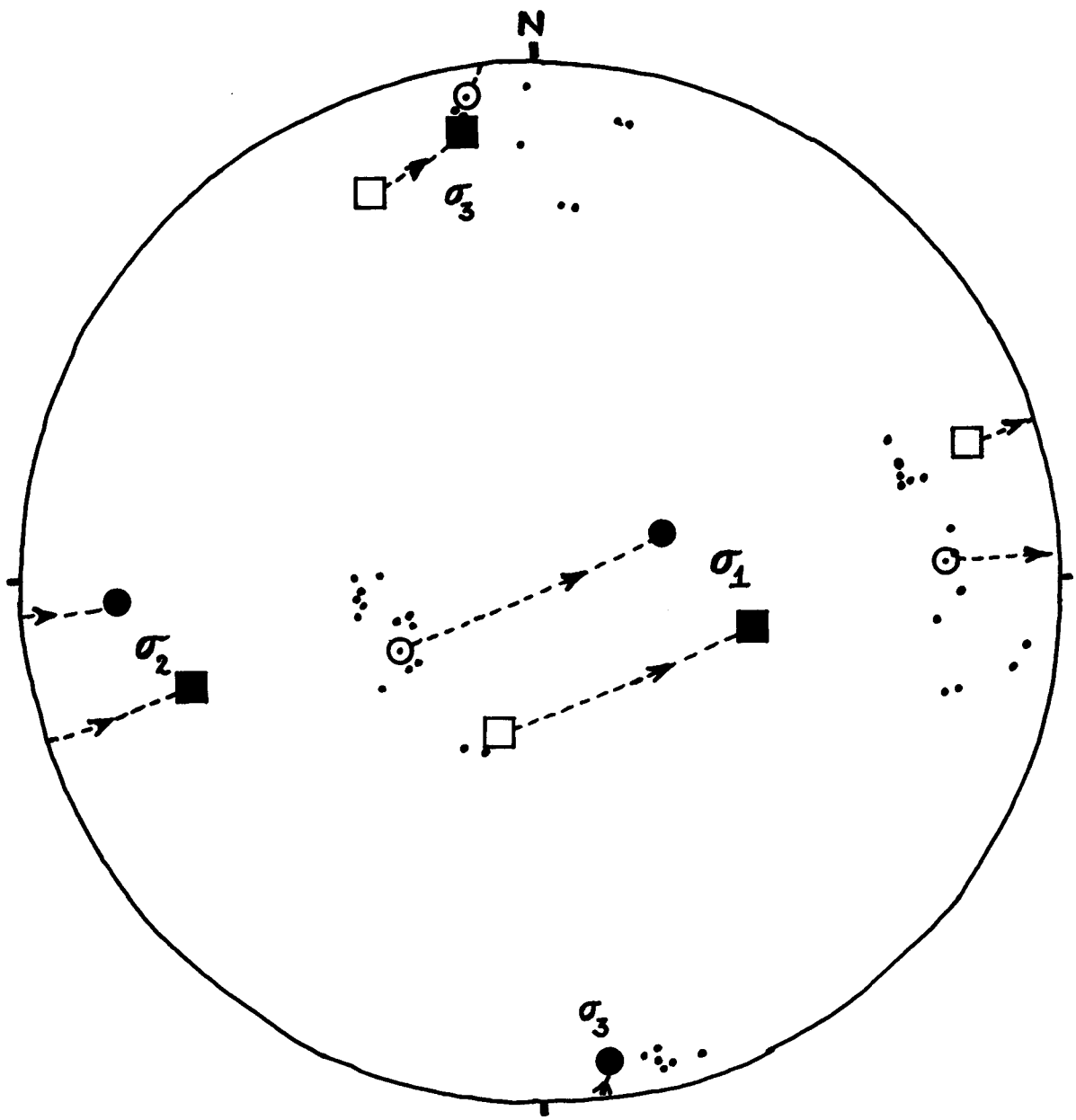

Figure 7.7 Paleostress Analysis of vein data. Circles are data from Reches' method; squares are from Lisle's method (ROMSA). Rotation paths for paleohorizontal shown with dotted lines.

σ_3 are so similar compared to σ_1, and σ_2 and σ_3 appear to change places with each other. This phenomenon and its relationship to the SVPC will be discussed more in Chapter 8.

CHAPTER 8. DISCUSSION

8.1 SHEAR ZONES

Graphical and mathematical analyses of the shear zone data support the stress field configuration seen in fig. 8.1 (all ROTATED to proposed paleohorozontal). σ_1 is subvertical for the graphical method and Lisle's method. However, Reches' method of stress analysis puts σ_1 50^0 away from the other data. The data are closer together for the σ_2 orientation, but for σ_3, again the Reches' orientation is almost 50^0 away from the others.

The Reches method is based in part on the Coulomb failure criterion:

$$\text{Shear Stress} > \text{Cohesion} + \text{Friction} * (\text{Normal Stress} - PH_2O).$$

The application of the Reches method to shear zones may be limited due to the fact that the values for these parameters are very different from brittle faults to ductile shear zones. For example, the value of the coefficient of friction in ductile deformation is probably extremely low, especially in the case of high-temperature ductile deformation; ductile shearing can take place on a variety of planes, with a minimal amount of shear stress. Lisle's method does not rely on values of coefficient of friction or stresses, but rather a more simple graphical construct (Chap.4.2.3) similar to a fault plane solution. Support for this argument may be seen in the data for brittle faults with mineralized veins (fig. 7.7) where the data points for the two methods plot much more close to each other.

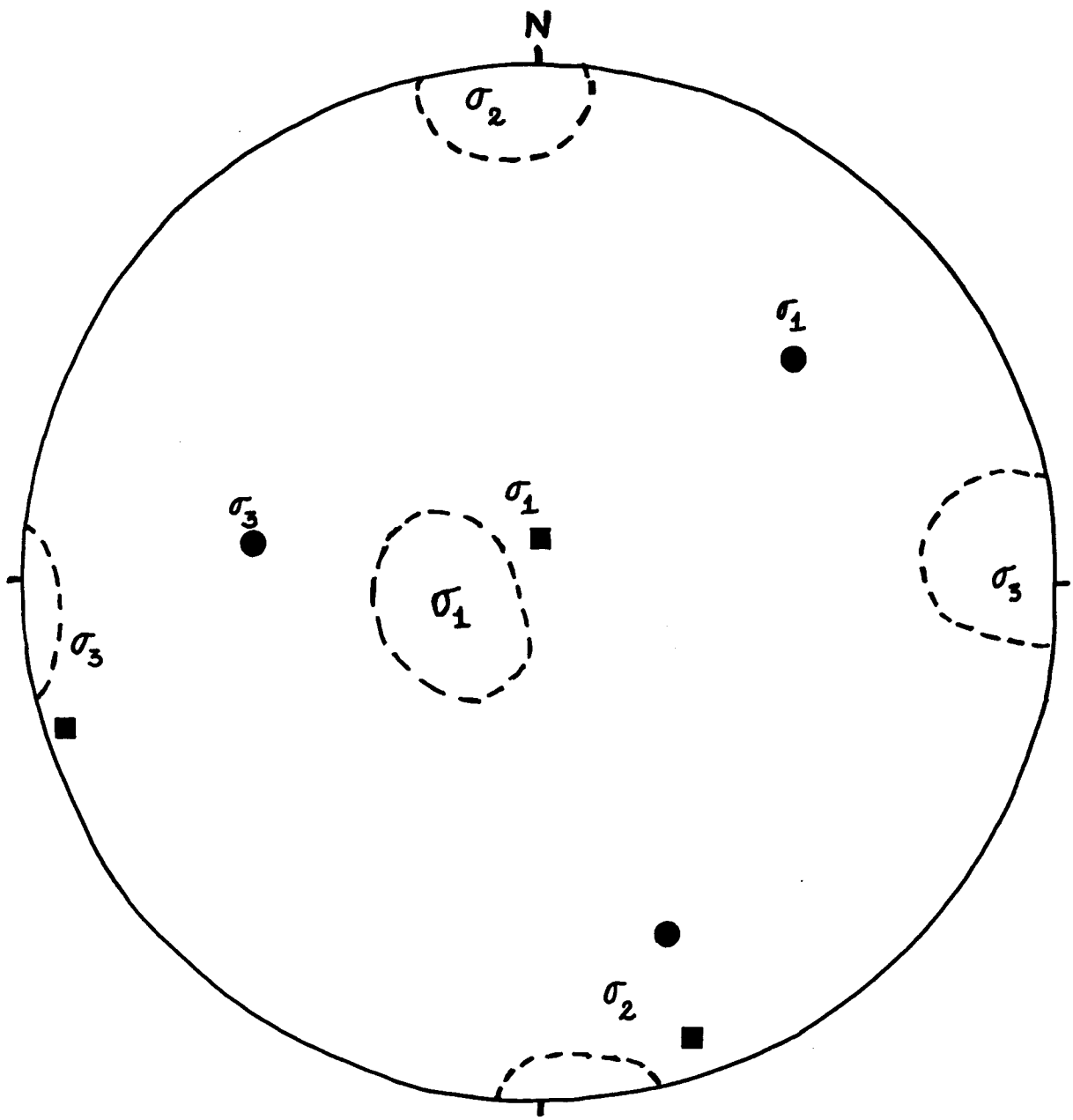

Figure 8.1 Stress field configuration from shear zone data. Areas marked by broken line are data from graphical methods. Circles and squares are data from mathematical methods, Reches' and Lisle's methods respectively.

Change in Stress Field. An attempt to establish whether or not there was a change with time of the shearing direction would require that the relative ages of the shear zones in the SVPC be determined. According to the assumptions mentioned in Chap.4.3 regarding the history of deformation, determining a decline in temperature at the formation of the different shear zone rocks should give the time sequence of formation of those rocks. Of the five shear zones studied, two (CS and SV) fall into the high-temperature field (amphibolite-granulite facies), one shear zone (CR) was deformed while being contact metamorphosed and is a biotite hornfels assemblage, another (WH) displays greenschist facies conditions, and finally, samples from the fifth (GE) indicate deformation near brittle conditions. Rocks in the GE have not experienced the upper amphibolite/granulite facies conditions that the SV and CS area rocks exhibit, and may have been intruded or deformed later in the cooling history of the plutonic complex. There are no neoblasts of clinopyroxene in any of the GE rocks, as there are in many of the SV and CS rocks. Porphyroclasts of clinopyroxene in the GE samples have been replaced by actinolitic hornblende, and lower temperature blue-green amphibole represents about 10% of the amphibole phase present in the samples studied. The undeformed country rocks from the GE area appear to have retained their original igneous fabric except where deformed in and near the shear zone. Igneous grain size is large (1-3.5mm) compared to most rocks from the SV and CS area; porphyroclasts are present in shear zone rocks in the GE area, whereas most SV and CS rocks are granoblastic and fine-grained. If the GE rocks are the younger of the two areas, then the northwesterly shearing was the latest in the plutonic complex having progressed from a more westerly direction of older rocks. This speculation certainly needs more support. For it is possible that the high-temperature area and the low-temperature area were deformed under the same stress field but sheared on different (predisposed ?) planes of failure. The

data from the dikes and the fractures are also evaluated (below) for possible change in stress field.

8.2 DIKES

The paleostress field from the dike data is shown in fig. 8.2. The arrangement of the axes is indicative of a convergent, compressive tectonic regime, with reverse faulting and a plate motion vector bearing NW-SE.

Change in Stress Field. The failure of the poles-to-dikes to concentrate in one area of the plot suggests that there is a changing stress field. Moreover, the presence of two different patterns in the poles-to-dikes positions makes a simple explanation of any progressive change in the stress field challenging; the plots show variations in orientations of poles-to-dikes along two completely different great circles (figs. 6.4 and 6.5). The SVPC poles-to-dikes vary along a great circle striking 314^0 and dipping about 50^0 to the southwest (see trace of great circle, fig. 6.4). The poles-to-dikes in the LRO vary along a great circle trending NNE and dipping 90^0 (fig.6.5). Also, there are two separate clusters of cusps, steps, and segments (significators of σ_2), suggesting a change in the σ_2 axis position.

It appears as if the axes of principal stresses are changing with each other as follows: σ_2 with σ_3 varying along the great circle traced between them by the poles-to-dikes (fig.6.5); and σ_1 and σ_3, varying along the great circle traced between them by poles-to-dikes (fig.6.4).

A major change in the orientation of the axes of principal stresses could occur in a compressive domain where plate convergence is causing reverse faulting, stacking of

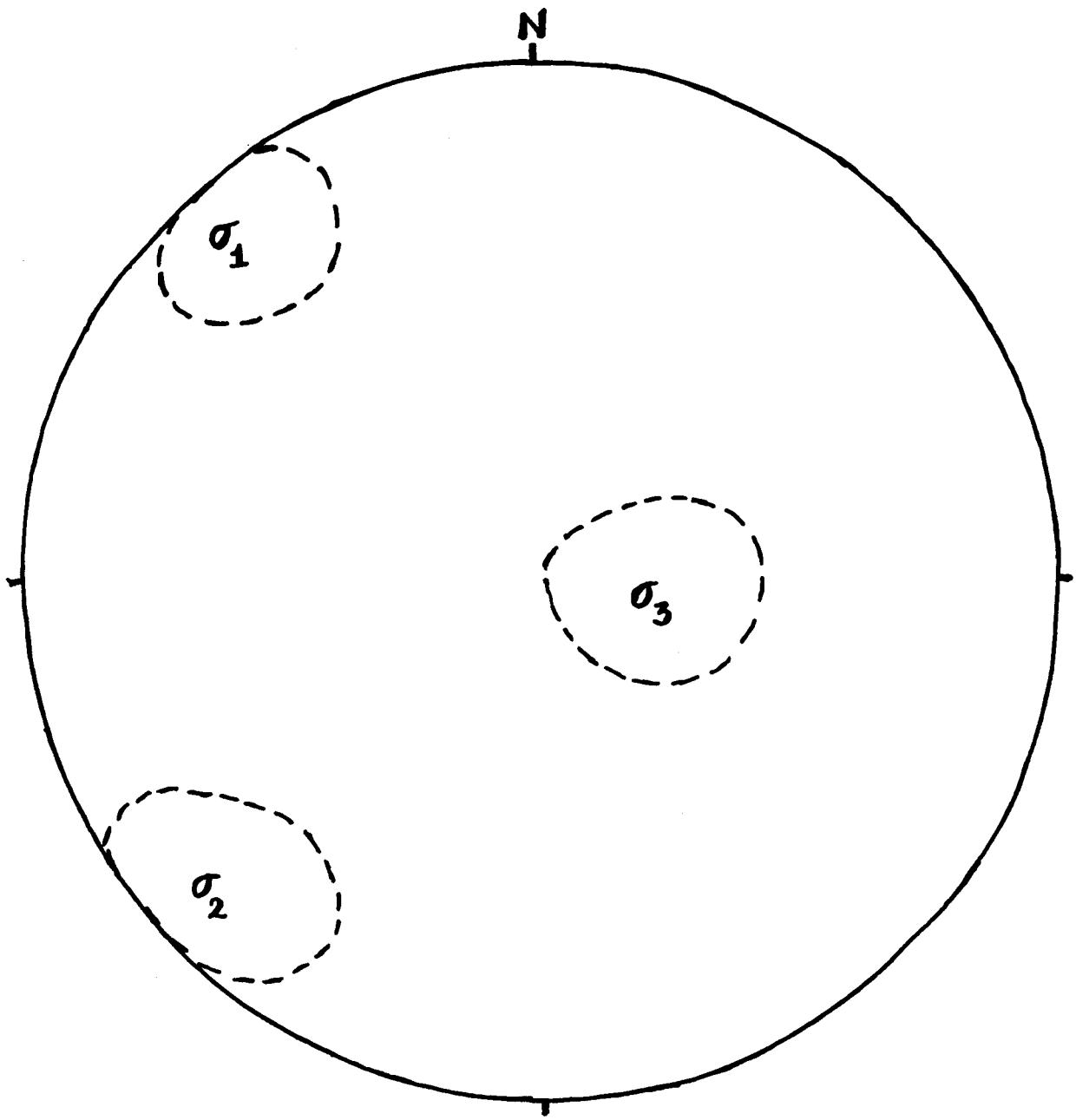

Figure 8.2 Orientation of stress field from dike data after rotation to paleohorizontal.

crustal wedges, and downwarping of the underthrust plate. Early on and at shallow crustal levels, a given point in the underthrust plate would experience the following stress field (fig. 8.3): the orientation of σ_1 would be horizontal, $\sigma_2$would also be horizontal (the confining pressure), and σ_3 would be vertical. As underthrusting proceeded, that point in the underthrust plate would encounter the change in the axis of maximum compressive stress from horizontal to vertical, as the pressure due to the overlying crust increased.

The second pattern seen in the stereographic projection plots is the distribution of poles-to-dikes along a great circle (fig.6.4). Such an arrangement of data suggests the possibility that there was a progressive rotation of the axes of principal stresses. This could occur if there was a change in the direction of plate motion at this convergent plate margin.

Either mechanisms would be feasible in the tectonic domain of the SVPC. Unfortunately, relative timing relationships were not clearly indicated. If anything, cross-cutting relationships suggest that the axes of principal stresses were flipping repeatedly through time.

8.3 VEINS

Stereonet projection plots of vein data gave marginal assistance in deducing the paleostress field in the SVPC. The poles-to-vein plot (fig. 7.4) showed data widely scattered, and the slip linear plot (fig. 7.5) of veins with known slip direction displayed an unclear pattern. The plot of rotated (to paleohorizontal) vein data (fig. 7.6) indicates primarily strike-sip faults with vertical to sub vertical fault planes, and a tentative stress field is indicated on the plot. Mathematical techniques of stress

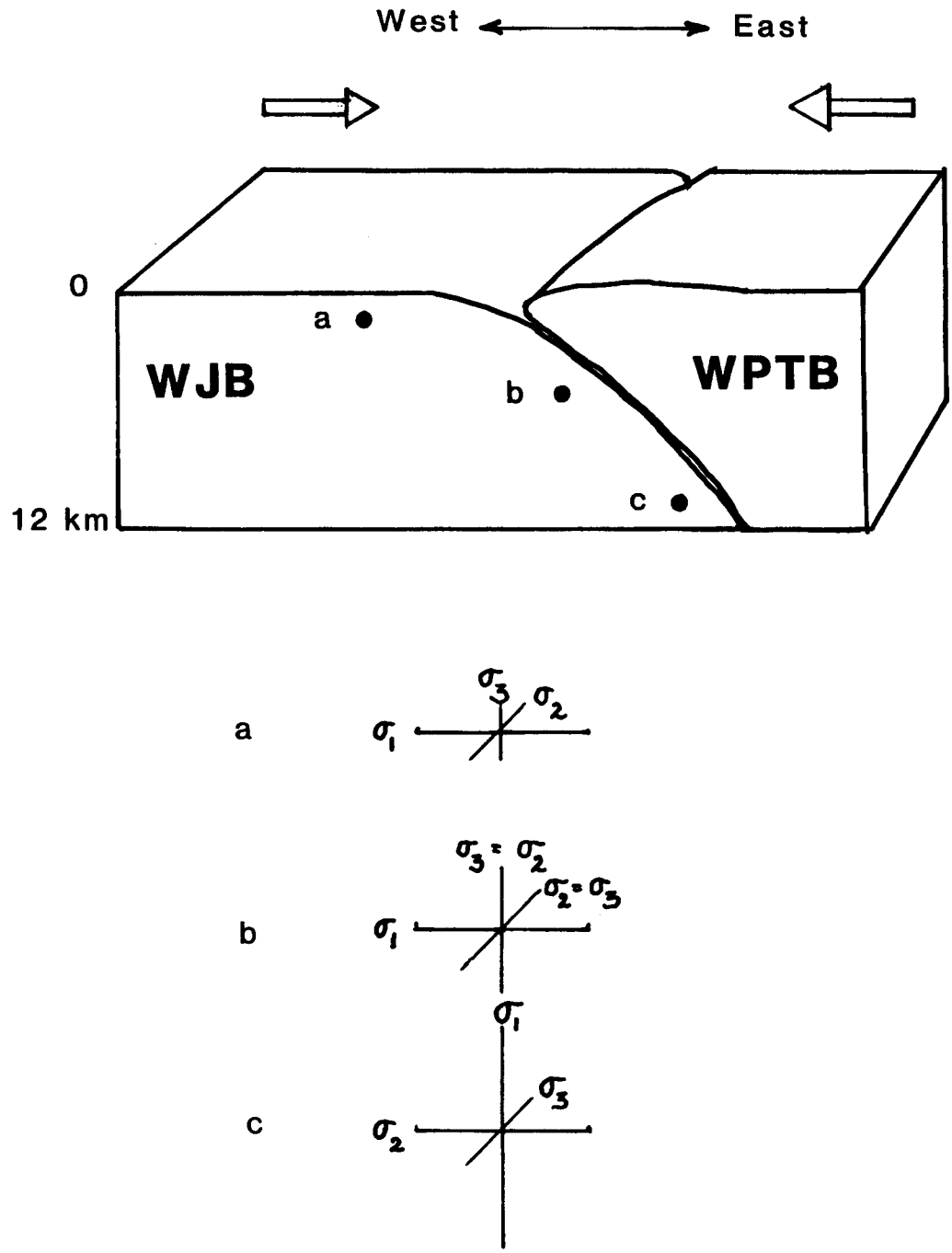

Figure 8.3 Schematic diagram of the changing stress field within an element of a crustal segment as it is buried by underthrusting. For the sake of simplicity, the horizontal east-west trending axis is held constant in magnitude while the other two axes change.

inversion yielded more definitive results (fig. 7.7). Results from these various techniques are plotted together in fig. 8.4 to show the overall paleostress field from the vein data.

Change in Stress Field. The stereonet projection plot of (rotated) vein data in the SVPC (fig. 7.6) indicates that most faults are strike slip with subvertical fault planes. The plot also shows poles-to-veins plotting in a wide spread of positions around the primitive circle; this means that some faults (veins) are oriented 90^0 to each other. This suggests the possibility that the two minor stress axes, σ_2 and σ_3, which are both nearly horizontal (fig. 7.6), are changing orientation with each other, or appearing to do so because the values of stresses at those axes are equal or almost equal. The value of the stress ratio (Phi) (see Chap.7.4.3) is low for the vein data, also indicating that the magnitudes of stress of the σ_2 and σ_3 axes are very similar.

Hancock [1987] describes a fault domain in which extension faults, joints, or hybrid faults can form at 90^0 to each other. In this model, the stress field remains dynamically constant, but minor changes occur as a result of local responses to elastic strain release or distance from a neutral surface. σ_2 and σ_3 are most likely equal or almost equal in value. Hancock suggests that the ideal domain in which to see this kind of fault array is one in which the intermediate and minimum stress axes are horizontal, and the fractures are extensional and all nearly vertical. The fractures from the SVPC are not purely extensional, but manifest a component of shearing shown by slickenstriae; these may be what Hancock [1987] calls "hybrid" faults which can also be seen in the same domain. Also, only one of the sets is nearly vertical. However, there is a strong possibility that the σ_2 and σ_3 axes may

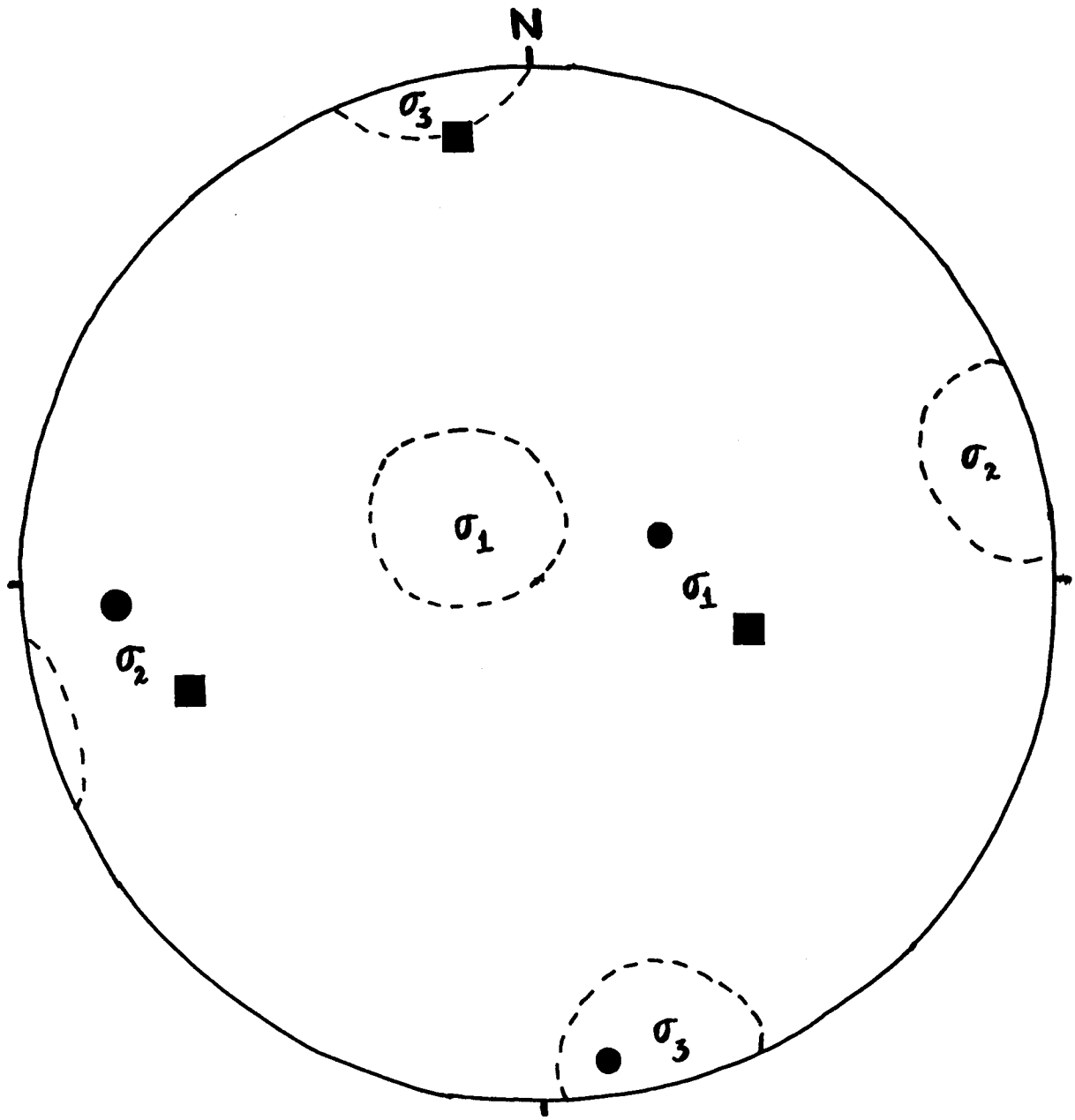

Figure 8.4 Stress field configuration from vein data after rotation to paleohorizontal. Areas marked by broken line are data from graphical methods. Circles and squares are data from mathematical methods, Reches' and Lisle's methods respectively.

be "switching", due to regional changes in the stress field from underthrusting of the two terranes penetrated by the SVPC. Initially, the tectonic domain was convergent with σ_1 horizontal, but as underthrusting continued and rocks were buried to deeper levels, σ_1 theoretically should eventually switch to a vertical position (fig. 8.3). Also, with the confining effect of tectonic burial in an orogenic setting, σ_3 would most likely be similar in value to σ_2. A similar effect is seen in the kinematics of the dike data from the SVPC; the σ_3 axis appears to be switching between two positions that are about 90^0 away from each other [see Chap.6].

8.4 CONCLUSIONS

Petrographic work, stereographic projection plot analysis, and mathematical stress analyses support the following conclusions about the deformation in the Summit Valley Plutonic Complex and possible along the Orleans fault:

1.) Paleostress Field. The shear zone data and vein data concur on the configuration of the principal stress axes at the time of deformation of the SVPC, with the exception of the positions of the σ_2 and σ_3 axes which are flipped with each other (fig. 8.5) and may have progressively changed through time from the time of ductile shearing until brittle fracturing. The dike data has indicated a different configuration for the paleostress field than that for the shear zones and veins (fig. 8.2). There was a great deal of scatter in the dike data in the stereographic projection plot (figs. 6.4 and 6.5) with indications that stress axes were shifting with each other (see above, 8.2). Unfortunately, the dike data was not suitable in format to input into the mathematical stress analyses used for the shear zones and

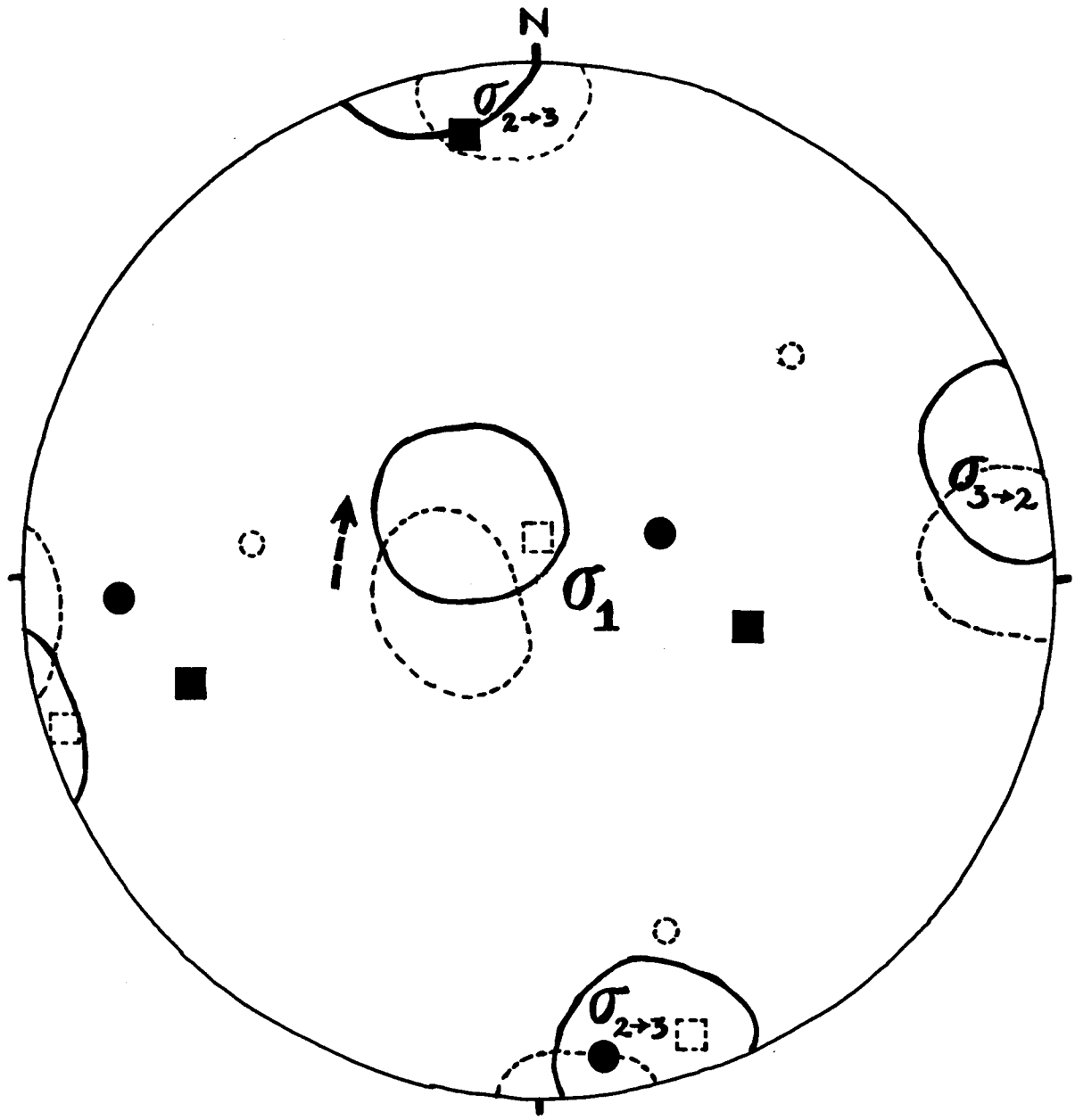

Figure 8.5 Combined shear zone and vein data for paleostress field configuration. Areas marked by broken line are data from shear zones (graphical methods); areas marked by solid line are vein data. Circles and squares are data from mathematical methods, Reches' and Lisle's methods respectively.

veins. The similarity of positions of the axes from the dike data compared to the others is curious (eg. the concurrence of σ_3 in the dike data with σ_1 in the shear zones and veins), but problematic.

2.) Direction of transport. Sense of shear data from ductile shear zones indicate that the overall direction of movement of material in the hanging wall in the plutonic complex was to the northwest, as shown by the slip-linear plots of data from the various shear zones. There is a suggestion of change of direction of transport indicated by the change in orientation of the slip linear arrows from West to NW. The same change is hinted at in the combined plots of stress field axes from the shear zones and veins (fig. 8.5); there is a slight offset of the σ_1 axis from the shear zones data to the veins data (see dotted arrow, fig.8.5), an offset which exhibits the same rotation sense as that seen in the variation of the slip linear arrows in the shear zone plots which would be from west to northwest. Harper [unpublished data] has seen the same rotation in direction of movement in the deformed Galice Fm just to the northwest of the SVPC.

3.) Fault Orientation. The paleostress field orientation discussed in item 1 (above) is not the expected configuration for a convergent, compressive tectonic domain (ie. the Nevadan Orogeny). Two explainations are put forth for the seemingly anomalous behaviour in the SVPC; 1.) burial of the crustal wedges containing the SVPC caused shifting of the values of the principal stresses (see above, 8.2 Dikes and 8.4 Veins) (fig. 8.3); and, 2.) that during the time of deformation that is recorded in the shear zones, dikes, and veins in the SVPC, normal faulting was occuring according to the

model put forth by Platt [1986]. If the SVPC was located in the crust far enough back from the leading edge of the thrust wedge, it might experience extensional normal faulting in response to thickening of the wedge from compression and underplating. Because the known orientation of the Orleans Fault in the study area is approximately horizontal [Norman,1984], the high angle that the σ_1 axis makes with the Orleans Fault suggests that the original geometry of the fault was as is, but that the stress field changed to arrive at the configuration seen in this study, an hypothesis that would support the burial model of stress field change.

8.5 FUTURE WORK

Areas in which further study could directly benefit this body of kinematic information are listed below:

1.) It may be possible to observe cross-cutting relationships of veins in the field to detect any change in mineralogy of vein fill that could be correlated with a change in orientation of a vein set.

2.) More thorough sampling of different areas in individual shear zones could provide a more complete picture of the conditions dominating the shearing (e.g. high or low temperature conditions, early or late episode according to cross-cutting relationships) to establish a more thorough deformation history for the purpose of demonstrating a progressive change in the geometry of deformation.

3.) More thorough mapping at the wall rock boundaries of the plutonic complex where the margin is sheared and faulted might furnish valuable information about movement on the Orleans Fault. This is made difficult by heavy underbrush (esp. manzanita bushes) and rough terrain.

4.) Dikes within the SVPC could be examined more closely for information that would enhance the kinematic data already available. Cross-cutting relationships of dikes with each other and with shear zones should be noted. Careful inspection of dike walls will show the presence of cusps and bends which are valuable in determining the principal axes of stress. Also, sheared dikes should be noted as a valuable piece of information about the stress field.

5.) A paleomagnetic study in or adjacent to the study area would help to constrain the paleohorizontal (or plate rotation) for the plutonic complex.

REFERENCES

Aleksandrowski, P., 1985, Graphical determination of principal stress directions for slickenside lineation populations: an attempt to modify Arthaud's method: Journal of Structural Geology, v.7, p.73-82.

Bambauer, H.U., Taborszky,F., Trochim,H.D., 1979, Optical Determination of Rock-Forming Minerals: E.Schweizerbart'sche Verlagsbuchhandlung, Stuttgart, 188 p.

Bard, J.P., 1986, Microtextures of Igneous and Metamorphic Rocks: Reidel, Dordrecht, Holland, 264 p.

Berthe, D., Choukroune, P., and Jegouzo, P., 1979, Orthogneiss, mylonite and non coaxial deformation of granites: the example of the South Armorican Shear Zone: Journal of Structural Geology, v.1, no.1, p.31-42.

Bird, D.K., Schiffman, P., Elders, W.A., Williams, A.E., McDowell, S.D., 1984, Calc-silicate mineralization in active geothermal systems: Economic Geology, v.79, p.671-695.

Bott, M.H.P., 1959, The mechanics of oblique slip faulting: Geology, v.46,p.109-117.

Brodie, K.H., Rutter,E.H., 1985, On the Relationship between Deformation and Metamorphism, with Special Reference to the Behavior of Basic Rocks: in, Metamorphic Reactions, Kinetics, Textures, and Deformation,Ed. A.B.Thompson and D.C.Rubie, New York, p.138-179.

Burchfiel, B.C., and Davis,G.A., 1981, Triassic and Jurassic tectonic evolution of the Klamath Mountains-Sierra Nevada geologic terrane: in Ernst, W.G., ed., The Geotectonic Development of California: Englewood Cliffs, New Jersey, Prentice-Hall, p.50-70.

Bussell, M.A., 1989, A simple method for the determination of the dilation direction of intrusive sheets: Journal of Structural Geology, vol.11, p. 679-687.

Davis, G.H., 1984, Structural Geology of Rocks and Regions; John Wiley & Sons, Inc., New York, 492 p.

Dick, H.J.B., 1976, The origin and emplacement of the Josephine Peridotite of southwestern Oregon (Ph.D. thesis):New Haven, Yale University, 409p.

Dick, H.J.B., 1977, Partial melting in the Josephine Peridotite: The effect on mineral composition and its consequences for geothermometry and geobarometry: American Journal of Science, v.277, p.801-832.

Emerman, S.H. and R.Marrett, 1990, Why Dikes?: Geology, v.18, p.231-233.

Garcia, M.O., 1979, Petrology of the Rogue and Galice Formations, Klamath Mountains, Oregon: identification of a Jurassic island arc sequence: Journal of Geology, v.86, p.29-41.

Garcia, M.O., 1982, Petrology of the Rogue River island-arc complex, southwest Oregon: American Journal of Science, v.282, p.783-807.

Gorman, C.M.III, 1985, Geology, Geochemistry, and Geochronology of the Rattlesnake Creek Terrane, West-Central Klamath Mountains, California: M.S.thesis, University of Utah, Salt Lake City, Utah, 111p.

Grady, K., 1990, Geology and structure of the rocks associated with the basal (Madstone) thrust of the Josephine ophiolite in southwestern Oregon: Evidence for a metamorphic sole: M.S.thesis, State University of New York, Albany, New York, 161p.

Gray, G.G. and S.W.Petersen, 1982, Northward continuation of the Rattlesnake Creek terrane, north central Klamath Mountains, California: Geological Society of America Abstracts with Programs, v.14, p.167.

Gray, G.G., 1986, Native terranes of the central Klamath Mountains, California: Tectonics, v.5, p.1043-1054.

Groshong, R.H.,Jr., 1988, Low-temperature deformation mechanisms and their interpretation: G.S.A. Bulletin, v.100, p.1329-1360.

Hall, P.C., 1984, Some aspects of deformation fabrics along the highland/lowland boundary, northwest Adirondaks, New York state: (M.S.Thesis) Albany, State University of New York, 124 p.

Hancock, P.L., Al-Kadhi, A., Barka, A.A., Bevan, T.G., 1987, Aspects of analysing brittle structures: Annales Tectonicae, v.1, p.5-19.

Hardcastle, K.C. 1989, Possible paleostress tensor configurations derived from fault-slip data in eastern Vermont and western New Hampshire: Tectonics, v.8, p.265-284.

Hardcastle, K.C. and Hills, L.S., 1991, BRUTE3 and SELECT: QuickBASIC-4 programs for determination of stress tensor configurations and separation of heterogeneous populations of fault-slip data: Computers & Geosciences, v.17, p.23-43.

Harper, G.D., 1980a, Structure and petrology of the Josephine ophiolite and overlying metasedimentary rocks, northwestern California [PhD. thesis]: Berkeley, California, University of California, 259p.

Harper, G.D., 1980b, The Josephine ophiolite - the remains of a Late Jurassic marginal basin in northwestern California: Geology, v.8, p.333-337.

Harper, G.D., 1984, The Josephine ophiolite, Geological Society of America Bulletin, v.95, p.1009-1026.

Harper, G.D., Norman, E.A., and Jones, D.L., 1983, The Lems Ridge olistostrome - sediment fill of an ancient fracture zone: Geological Society of America Abstracts with Programs, v.15, p.427.

Harper, G.D., Saleeby,J.B., and Norman, E.A., 1985, Geometry and tectonic setting of sea-floor spreading for the Josephine ophiolite, and implications for Jurassic accretionary events along the Californian margin: in, Howell, D.G., ed., Tectonostratigraphic Terranes of the Circum-Pacific Region: Circum-Pacific Council for Energy and Mineral Resources, Earth Science Series No.1, Houston, p.239-257.

Harper, G.D., and Wright, J.E., 1984, Middle to late Jurassic tectonic evolution of the Klamath Mountains, California-Oregon: Tectonics, v.3, p.759-772.

Harper, G.D., Saleeby,J.B., and Heizler,M., 1991, Isotopic Age of the Generation, Translation, and Emplacement of the Josephine Ophiolite, Klamath Mountains, Oregon-California: (in review).

Hershey, O.H., 1911, Del Norte County (California) geology: Mineral and Science Press, v.102, p.468.

Hollister, L.S. and Crawford, M.L., 1986, Melt-enhanced deformation: A major tectonic process: Geology, v.14, p.558-561.

Irwin, W.P., 1960, Geologic reconnaissance of the northern Coast Ranges and Klamath Mountains, California, with a summary of the mineral resources: California Division of Mines and Geology Bulletin 179, p.19-38.

Irwin, W.P., 1966, Geology of the Klamath Mountains Province, in Bailey,E.H., ed., Geology of northern California: California Division of Mines and Geology Bulletin 190, p.19-38.

Irwin, W.P., 1972, Terranes of the Western Paleozoic and Triassic belt in the southern Klamath Mountains, California: U.S.Geological Survey Professional Paper 800-C, p.103-111.

Irwin, W.P., 1981, Tectonic accretion of the Klamath Mountains, in Ernst, W.G., ed., The Geotectonic Development of California: Englewood Cliffs, New Jersey, Prentice-Hall, p.29-49.

Jachens, R.C., Barnes,C.G., Donato,M.M., 1986, Subsurface configuration of the Orleans fault: Implications for deformation in the western Klamath Mountains, California: Geological Society of America Bulletin, V.97,p.388-395.

Krantz, R.W., 1988, Multiple fault sets and three-dimensional strain: theory and application: Journal of Structural Geology, v.10, p.225-237.

Krantz, R.W., 1989, Orthorhombic fault patterns: the odd axis model and slip vector orientations: Tectonics, v.8, p.483-495.

Kretz, R., 1991, The dilation direction of intrusive sheets: Journal of Structural Geology, v.13, p.97-99.

Lisle, R.J., 1989, Paleostress analysis from sheared dike sets: G.S.A. Bulletin, v.101, p.968-972.

Lisle, R.J., 1988, ROMSA: A BASIC program for paleostress analysis using fault-striation data; Computers & Geosciences, v.14, p.255-259.

Lisle, R.J., 1987, Principal stress orientations from faults: an additional constraint: Annales Tectonicae, v.1, p.155-158.

Lister, G.S., and A.W.Snoke, 1984, S-C Mylonites: Journal of Structural Geology, v.6, p.617-638.

Marshak, S.and Mitra,G., 1988, Basic Methods of Structural Geology: S. Marshak and G. Mitra, ed., Prentice Hall,New Jersey, 446p.

Miller, R.B., 1988, Fluid flow, metasomatism and amphibole deformation in an imbricated ophiolite, North Cascades, Washington: Journal of Structural Geology v.10, p.283-296.

Norman, E.A.S., 1984, The Structure and Petrology of the Summit Valley Area, Klamath Mountains, California: M.S.thesis, University of Utah, Salt Lake City, Utah, 148 p.

Norman, E.A., Gorman,C.M., Harper,G.D.,and Wagner,D., 1983, Northern Extension of the Rattlesnake Creek terrane: Geological Society of America Abstracts with Programs, v.15, p.314-315.

Ohr, Matthias, 1987, Geology, Geochemistry, and Geochronology of the Lems Ridge Olistostrome, Klamath Mountains, California: M.S.thesis, State Yniversity of New York at Albany, Albany, New York, 247 p.

Passchier, C.W., 1990, Shear bands in rocks: from Crustal Dynamics Pathways and Records, 80th Annual Meeting of the Geologische Vereinigung e.V. Abstracts with Program, Ruhr-Universitat Bochum,FRG, p.17.

Passchier, C.W., Myers,J.S., and Krner,A., 1990, Field Geology of High-Grade Gneiss Terrains: Springer-Verlag, Berlin, Heidelberg, 150 p.

Passchier, C.W. and C. Simpson, 1986, Porphyroclast systems as kinematic indicators: Journal of Structural Geology, v.8, p.831-843.

Paterson, S.R., Tobisch, O.T., Vernon, R.H., 1989, Criteria for establishing the relative timing of pluton emplacement and regional deformation: Penrose Conference report, Geology, v.17, p.475-476.

Paterson, S.R., Vernon, R.H., Tobisch, O.T., 1989, A review of criteria for the identification of magmatic and tectonic foliations in granitoids: Journal of Structural Geology, v.11, p.349-363.

Petit, J.P., 1987, Criteria for the sense of movement on fault surfaces in brittle rocks: Journal of Structural Geology, v.9, p.597-608.

Platt, J.P., 1986, Dynamics of orogenic wedges and the uplift of high-pressure metamorphic rocks: Geol. Soc. of Amer. Bul., v.97, p.1037-1053.

Platt, J.P. and R.L.M.Vissers, 1980, Extensional structures in anisotropic rocks: Journal of Structural Geology, v.2, p.397-410.

Pollard, D.D., 1988, Elementary fracture mechanics applied to the structural interpretation of dykes: in: Halls, H.C. and Fahrig, W.F., eds., Mafic Dyke Swarms, Geol.Surv. Canada Spec. Paper 34, p.5-24.

Prior, D.J., R.J.Knipe, M.P.Bates, N.T.Grant, R.D.Law, G.E.Lloyd, A.Welbon, S.M.Agar, K.H.Brodie, R.H.Maddock, E.H.Rutter, S.H.White, T.H.Bell, C.C.Ferguson, J.Wheeler, 1987, Orientation of specimens: Essential data for all fields of geology: Geology, v.15, p.829-831.

Raase, P., 1974, Al and Ti contents of hornblende, indicators of pressure and temperature of regional metamorphism: Contr. Mineral. and Petrol., v.45, p.231-236.

Reches, Z., 1987, Determination of the tectonic stress tensor from slip along faults that obey the Coulomb Yield condition; Tectonics, v.6, p.849-861.

Saleeby, J.B., 1984, Pb/U zircon ages from the Rogue River area, western Jurassic belt, Klamath Nountains, Oregon: Geol. Soc. Am. Abs. Prog., v.16,p.331.

Schmid, S.M., 1982, Microfabric studies as indicators of deformation mechanisms and flow laws operative in mountain building: in, Mountain Building Processes, ed. K.J.Hsu, Academic Press, p. 95-110.

Simpson, C., 1986, Determination of Movement Sense in Mylonites: Journal of Geological Education, v.34, p.246-261.

Snoke, A.W., 1972, Petrology and structure of the Preston Peak area, Del Norte and Siskyou Counties, California [PhD. thesis]: Stanford, Califonia, Stanford University, 274p.

Snoke, A.W., 1977, A thrust plate of ophiolitic rocks in the Preston Peak area, Klamath Mountains, California: Geological Society of America Bulletin, v.88, p.1641-1659.

Stierman, D.J., 1984, Geophysical and geological evidence for fracturing, water circulation and chemical alteration in granitic rocks adjacent to major strike-slip faults: Journal of Geophysical Research, v.89, p.5849-5857.

Strand, T.G., 1963, Geologic map of Calofornia, Weed Sheet: Calofornia Division of Mines and Geology.

Suppe, J., 1985, Principles of Structural Geology: Prentice-Hall, Inc., Englewood Cliffs, NewJersey, 537 p.

Tullis, J., Snoke, A.W., and Todd, V.R., (conveners), 1982, Significance and petrogenesis of mylonitic rocks: Penrose Conference Report, Geology, v.10, p.227-230.

Turner, F.J., 1981, Metamorphic petrology: Mineralogical, field, and tectonic aspects: McGraw-Hill, New York, 524 p.

Vernon, R.H., Paterson, S.R., Geary, E.E., 1989, Evidence for syntectonic intrusion of plutons in the Bear Mountains fault zone, California: Geology, v.17, p.723-726.

Wells, F.G., Cater, F.W., and Rynearson, G.A., 1946, Chromite deposits of Del Norte County, California: California Division of Mines Bulletin 134, p.1-76.

Wright, J.E., 1982, Permo-Triassic accretionary subduction complex, southwestern Klamath Mountains, Northern California: Journal of Geophysical Research, v.87, p.3805-3818.

Wright, J.E., and M.R.Fahan, 1988, An expanded view of Jurassic orogenesis in the western United States Cordillera: Middle Jurassic (pre-Nevadan) regional metamorphism and thrust faulting within an active arc environment, Klamath Mountains, California: Geological Society of America Bulletin, v.100, p.859-876.

Wright, J.E., and Wyld,S.J., 1986, Significance of xenocrystic Precambrian zircon contained within the southern continuation of the Josephine ophiolite: Devils Elbow ophiolite remnant, Klamath Mountains, northern California: Geology, v.14, p.671-674.

Yardley, B.W.D., 1989, An Introduction to Metamorphic Petrology: Wiley & Sons, New York, 248 p.

APPENDIX I

Table I

Shear Zone Orientations Spreadsheet (SVPC_SZ.CAL)

confidence scale: POOR, WEAK, GOOD, HIGH
t-o-b = top over bottom

Sample #	Foliation Plane Strike/dip	Mineral Lineation	Sense-of-shear/criteria used	Confidence
Stop 8 (CS) Cedar Spring				
Sample 8a	59/68 NW	plunge:22 SW	Oblique sinistral str-slip, E to N, W to S / shear band and folded foliation	GOOD
Sample 8b	57/59 SE	trend:67 plunge:26 E	Oblique sinistral str-slip, top-down-over-bottom to East / S-C foliation., asymm.porph.	GOOD
Stop 16 (CS) Cedar Spring				
Sample 16-3	74/32 S	trend: 22 plunge:31 S pitch: 54 S	Oblique sinistral str-slip, t-o-b to N / S-C foln(biotite) and preferred orient. hbld	WEAK
Sample 16-4	44/87 E	plunge: 5 S	Oblique sinistral str-slip	WEAK
Stop 17 (BS) Bear Trail				
Sample 17-2	98/47 S	trend: 332 plunge:42 S pitch: 58 S	t-o-b to NW / S-C foliation	HIGH
Stop 18 (SV) Summit Valley				
Sample 18-2	94/71 NW	trend: 104 plunge:17 W	(indeterminate)	

Shear Zones (cont.)

Stop 19 (SV) Summit Valley				
Sample 19-1	281/58 N	plunge: 3 E	t-o-b to West / asymm.porph. and Peter Hall technique	WEAK
Sample 19-2	292/50 N	plunge: 3 E	t-o-b to West /asymm. tails on aggregates	HIGH
Stop 20 (SV) Summit Valley				
Sample 20-1	299/41 NNE	trend: 103 plunge: 7 E	t-o-b to East / S-C foln and pressure shadows	LOW
Stop 21 (SV) Summit Valley				
Sample 21-1	283/39 N	trend: 72 plunge:21 E	t-o-b to West / asymm.porph and S-C foliation	GOOD
Sample 21-2	87/67 N	trend:320 plunge:52 NW	t-o-b to West / folded folds	GOOD
(shearing dike in previous sample)				
	14/73 E	trend: 68 plunge:60 E		
Stop 22 (SV) Summit Valley				
Sample 22-1	95/56 N	trend: 0 plunge:58 NW	top-up-over-bottom to SW / asymmetric porphyroclasts	WEAK
Stop 23 (WH) Western Hornblendite				
Sample 23-5	36/65 W	trend:13 plunge:35 NW	top-up-over-bottom to South /S-C and C-C'foln., asymm.porph.	HIGH
Stop 27 (GE) GO Road East				
(field	72/37 NW		t-o-b to WEST / asymm.fabric	HIGH
measurements)	290/36 N	trend:88 plunge:34 SE	t-o-b to NW / asymm.fabric	HIGH

		Shear Zones (cont.)		
(field meas.)	280/11 S	trend: 304 plunge:11 E	t-o-b to NW / asymm.fabric	HIGH
Sample 27-5	351/27 NE	trend:307 plunge:25 E	t-o-b to SW / asymm.porph.	HIGH
Sample 27-6 has two sheared dikelets and a sheared fabric:				
(white dikelet:)				
	0/10 E	trend: 320 plunge:12 SE	t-o-b to NW / asymm.fabric	GOOD
(black dikelet:)				
	305/27 E	trend: 320	t-o-b to NW / asymm.fabric	GOOD
(shearing in top of same rock)				
		trend: 357		GOOD
Sample 27-7	359/52 W	trend: 323 plunge:27 NW pitch: 32 NW	top-up-over-bottom to SE /S-C foln. and asymm.porph.	GOOD
Sample 27-8	53/37 SE	trend: 344 plunge:34 SE	t-o-b to NW / asymm.fabric	GOOD
Stop 28 (CR) Creek				
Sample 28-1	353/72 SW	trend: 218 plunge:64 SW	top-up-over-bottom to East / press.shadows and S-C foln.	HIGH
Sample 28-2	17/81 NW	plunge:61 SW	t-o-b to East / S-C foliations and asymm.porph.	HIGH

Table II

----------Foliation Orientations----------

(SVPCFOLN.CAL)

Location	Strike/dip	Lineation
Stop 4 (CS)	100/44 SE	
Stop 5 (CS)	61/59 NW 123/48 NE	
Stop 17 (BS)	98/47 S	trend: 332 plunge:42 S pitch: 58 S
Stop 18 (SV)	112/84 S 310/73 NNE	
Stop 19 (SV)	114/68 NNW	plunge: 3 E
Stop 23 (WH)	319/40 N 286/44 N 304/44 N 304/44 N 320/69 NE	(These orientations were all taken from Harzburgite country rock)
Stop 27 (GE)	328/75 SW 8/20 E	
Stop 28 (CR)	345/78 SW 341/65 SW 343/77 SW	(local lineation...) trend:67 plunge:53 SW
Stop 29 (GE)	42/67 E 28/68 E	plunge:53 NE
Stop - Lem's Ridge Olistostrome	2/47 E 7/40 E	

Table III

DIKE ORIENTATIONS (SVPCDIKE.CAL)

Stop 12 (CS)	Stop 23 West Hbldte	Stop 27 GoRd East
266/82 N	46/76 SE	17/77 E
	42/55 SE	317/67 NE
	22/69 SE	
Stop 21	335/31 NE	(cross-cut dike)
	7/58 E	(older)
14/73 E	30/50 SE	275/80 SE
(trend/plunge)	28/65 SE	(cross-cutting)
68/60 E	20/75 SE	33/33 W
	25/78 W	
	295/31 N	330/50 NE
Stop 22	52/51 NW	294/70 S
	63/47 NW	323/63 NE
95/61 NW	50/83 NW	90/38 N
	56/75 NW	9/50 NE
		0/10 E
		trend:320
		305/27 E

Stop 28 OlistromeContact	Stop Z44(Harper) LR Olistrome
95/85 S	276/53 N
72/63 NW	(dike w/ bend)
332/70 NE	296/67 S
	90/75 N
(conjugate set)	
310/80 SW	284/87 N
351/80 NE	83/71 N
	277/76 S
(boudinned sill)	(node previous dike)
(boudin axis)	(trend/plunge)
43/15NW	271/63 W
	278/70 S
	30/51 S

----------DIKE ORIENTATIONS---(cont.)----------

Stop Z53(Harper) LR Olistrome	Stop Z53 (cont)	Stop Z53 (cont)
273/38 N	(dike w/ bend)	277/82 S
80/37 N	287/90 E	307/90 V
	81/31 NE	299/86 S
(dike w/bend)		288/75 S
330/43 NE	280/83 S	285/74 S
345/84 NE	(dike w/ bend)	296/40 N
	285/63 N	315/22 N
(w/ corrugations)	277/61 NE	85/71 N
(trend/plunge)	271/83 N	285/76 N
337/7	272/41 N	300/30 N
340/17	313/41 NE	
	295/75 SW	
91/80 S	283/56 N	
15/6 W	291/62 SW	
295/85 SW	293/52 SW	
278/83 S	302/28 N	
290/87 S	296/84 S	
63/90 V		
34/78 E		

Table IV

FRACTURE ORIENTATIONS (SVPCFRCT.CAL)

STOP #/ SAMPLE #	FRACTURE PLANE	LINEATIONS SLICKENSTR.	SENSE OF OFFSET	VEIN FILL MINERAL
Stop 5				
	306/50 SW	trend 295 plunge 9		epidote
	(same plane)	trend 299 plunge 16		epidote
	352/73 SW	pitch 2 N		epidote
	284/74 NE	pitch 35 W	rev.flt.	epidote
	332/69 SW	pitch 68 NW		epidote
	320/73 SW	pitch 12 N	dextral (?)	epidote
	337/58 SW	pitch 32 N		quartz
	340/61 SW	pitch 44 N		?
	329/73 SW	pitch 68 N	rev.l.lat	?
	25/75 SE	pitch 44 SW	dextral (?)	(gouges)
	75/62 SE			talc
Stop 14				
	10/73 SW			?
	145/25 NNE			?
Stop 15				
	98/86 SE			?
Stop 16				
	29/70 W	plunge:43 NW		serpentine
16-1	70/65 SE	pitch:70 SE	t-o-b to SE	serpentine
	90/65 SE	pitch: 65 SE	t-o-b to SE	serpentine
	124/74 N			?
	137/80 NE			?
	187/58 SW			serpentine
	76/44 SE			white vein
	58/81 NW			white vein
	115/74 N			?
	71/43 SE			?
Stop 17				
17-2	98/47 S	trend:332 plunge:42 S pitch: 58 S	t-o-b to NW (slickenside steps)	white vein
Stop 18				
18-1	248/39 NNW			white vein
	36/32 NW			white vein
	50/32 NW			white vein
	52/23 NW			white vein
	62/23 NW			white vein
	318/30 SW			white vein
	2/60 ENE			white vein
	355/77 NE			white vein
	3/75 NE			white vein
	15/71 NE			white vein

STOP #/ SAMPLE #	FRACTURE PLANE	LINEATIONS SLICKENSTR.	SENSE OF OFFSET	VEIN FILL MINERAL
Stop 19				
	16/73 NE			?
	8/82 NE			?
	61/75 SE			?
	28/85 E			?
	59/78 SE			?
Stop 20				
	157/38 SW	trend: 350		serpentine
	113/44 SW	trend: 143		serpentine
	113/53 SW	trend: 152		serpentine
20-1	355/40 W	trend: 340 plunge: 3 N	t(W)-o-b(E) to South	serpentine
20-1	304/61 S	plunge:45 E	t-o-b to NW	serpentine
	304/42 NE			?
	327/60 NE			?
Stop 21				
21-1	330/20 SW			white min
Stop 23				
	334/61 SW	trend: 355	t-o-b to S	white min
	331/63 SW	trend: 335		white min
	302/64 SW	trend: 322	t-o-b to SE	white min
	318/67 SW	plunge: 25 SE	t-o-b to SE	white min
	331/66 SW	pitch: 7 SE	t-o-b to SE	white min
	335/26 SW	trend: 0 S		serpentine
	314/67 SW			?
	328/65 SW			?
	309/77 SW			?
	311/87 SW			?
	347/36 NE			?
	294/51 NE			?
	321/50 NE			?
	311/52 NE			?
	317/38 NE		(dike offset by vein) t-o-b to NW	
	31/37 SW			?
	10/54 SW	pitch:33 NW		?
	288/20 SE	pitch:20 SW		?
	32/21 SE			?
	49/73 NW			?
	85/9 NW			?
23-4	25/60 NW			serp.+talc
23-4	19/62 NW			serp.+talc
	334/67 NE			epidote
	15/83 NE			epidote
	92/61 NW			epidote
	329/25 SW	pitch:10 S	t-o-b to NW	serpentine
Stop 26				
	7/47 E			epidote or
	18/73 E			white min
	28/77 SE			"

STOP #/ SAMPLE #	FRACTURE PLANE	LINEATIONS SLICKENSTR.	SENSE OF OFFSET	VEIN FILL MINERAL
	2/61 E			"
	4/75 E			"
	357/87 NE			"
	350/83 NE			"
	12/66 NE			"
	3/65 NE			"
	352/54 NE			"
	302/17 SW			"
	355/25 SW			"
	327/35 SW			"
	325/24 SW			"
	307/19 SW			"
	6/32 SW			"
	350/35 SW			"
	323/35 SW			"
	335/43 SW			"
	329/44 SW			"
	85/76 SE			"
	60/49 NW			"
	41/56 NW			"
	302/75 NE			"
Stop 27				
	339/60 NE			"
	28/78 NE			"
	308/65 NE			"
	310/52 SW			"
	297/46 SW			"
	334/43 SW			"
	344/22 SW			"
	80/53 SE			"
	291/36 S			"
	97/78 S			"
	275/77 SE			"
	83/33 NW			"
	87/47 NW			"
	281/39 N			"
	287/50 NW			"
	300/15 SW			"
	327/77 SW			"
	334/43 SW			"
	43/36 SE			"
	280/87 SE			"
	278/88 S			"
	265/80 SE			"
	272/84 SE			"
	52/12 NW			"
	34/23 NW			"
	55/18 NW			"
	315/71 SW			"
	317/35 SW			white min

STOP #/ SAMPLE #	FRACTURE PLANE	LINEATIONS SLICKENSTR.	SENSE OF OFFSET	VEIN FILL MINERAL
	300/36 SW			white min
	85/77 N			white min
	349/50 SW			white min
	5/64 SW			white min
	18/33 E			white min
	333/38 SW			epidote
	358/34 SE	trend:20		epidote
		plunge:9		epidote
	16/84 E	plunge:8 N		epidote
	312/89 S			epidote
	50/60 W			epidote
	338/43 SW			epidote
	55/61 NW			epidote
	314/62 SW			?
	309/69 SW			?
	96/86 S			?
	86/86 SE			?
	307/63 NE			?
	280/90 V			?
	1/53 W			epdte+white
	331/38 SW			epdte+white
	299/28 S			epdte+white
Stop 28				
	85/69 S			quartz

APPENDIX II

EXPLANATION OF LITHOLOGIC UNITS (FROM NORMAN, 1984)

QUATERNARY

Qls — Landslide

UPPER JURASSIC OR CRETACIOUS

JKig — Hornblende-gabbro to diorite stock (JKig). Medium grained with complex cross-cutting relationships; generally fresh with localized hydrothermal alteration and veining; dark grey to light grey depending on hornblende and pyroxene content.

JKih — Hornblendite (JKih) with lesser gabbro and clinopyroxenite cut by coarse-grained hornblende-plagioclase dikes; black on fresh surface, weathers dark red brown. Often shows tectonic disruption; may contain blocks of serpentinite.

Jkip — Olivine clinopyroxenite to wehrlite (JKip). Dull black on fresh surface, weathers reddish tan to brown.

UPPER JURASSIC

Jg — Galice Formation - metagraywacke and slate (Jg). Medium-grey metagraywacke, fine to coarse sandstone with rare pebble conglomerate; grains are flattened giving a foliated appearance. Slate is dark gray, light gray on weathered surface. Sequence varies from dominantly slate to massive metagraywacke to thin rhythmic bedding of metagraywacke and salte.

Jlr — Lems Ridge Olistostrome (Jlr). Black pebbly mudstone and/or pale green tuffaceous matrix with boulders up to 15 meters of metagabbro, chert, greenstone, and limestone. Pebbles also include argillite, sandstone, vesicular volcanics, and mica schist. Mudstone matrix is frequently foliated. Converted to hornfels near pluton; cut by mafic dikes. Chert bed at base.

TRIASSIC TO LOWER JURASSIC

Hz — Harzburgite Tectonite (Hz). Dull dark green to black on fresh surface and reddish-tan to white on weathered surface. Largely serpentinized; locally sheared. Minor dunite, pyroxenite, and lherzolite.